

ISTANBUL TECHNICAL UNIVERSITY ★ GRADUATE SCHOOL

**CARBONDIOXIDE CAPTURING FROM INDUSTRIAL FLUE GAS VIA
CALCIUM CARBONATE INDUCING MICROORGANISMS**



Ph.D. THESIS

Mert KOLUKISAOĞLU

Department of Environmental Engineering

Environmental Biotechnology Programme

MARCH 2025

ISTANBUL TECHNICAL UNIVERSITY ★ GRADUATE SCHOOL

**CARBONDIOXIDE CAPTURING FROM INDUSTRIAL FLUE GAS VIA
CALCIUM CARBONATE INDUCING MICROORGANISMS**



Ph.D. THESIS

**Mert KOLUKISAOĞLU
(501182801)**

Department of Environmental Engineering

Environmental Biotechnology Programme

Thesis Advisor: Prof. Mahmut ALTINBAŞ

MARCH 2025

İSTANBUL TEKNİK ÜNİVERSİTESİ ★ LİSANSÜSTÜ EĞİTİM ENSTİTÜSÜ

**KALSIYUM KARBONAT OLUŞUMUNU TETİKLEYEN
MİKROORGANİZMALAR İLE KARBONDİOKSİT YAKALAMA**

DOKTORA TEZİ

**Mert KOLUKISAOĞLU
(501182801)**

Çevre Mühendisliği Anabilim Dalı

Çevre Biyoteknolojisi Programı

Tez Danışmanı: Prof. Dr. Mahmut Altınbaş

MART 2025



Mert KOLUKISAOĞLU, a Ph.D. student of ITU Graduate School student ID 501182801, successfully defended the thesis/dissertation entitled “CARBON DIOXIDE CAPTURING FROM INDUSTRIAL FLUE GAS VIA CALCIUM CARBONATE INDUCING MICROORGANISMS”, which he prepared after fulfilling the requirements specified in the associated legislations, before the jury whose signatures are below.

Thesis Advisor : **Prof. Mahmut ALTINBAŞ**
Istanbul Technical University

Jury Members : **Assoc. Prof. Ebru KOCA AKKAYA**
Yıldız Technical University

Prof. Süleyman ÖVEZ
Istanbul Technical University

Prof. Mustafa Evren ERŞAHİN
Istanbul Technical University

Prof. Bestami ÖZKAYA
Istinye University

Date of Submission : 06 January 2025
Date of Defense : 19 March 2025



To my family,



FOREWORD

First, I would like to express my gratitude to Prof. Ibrahim Demir, who encouraged me to start the doctoral program and mentored me in this regard. I was able to benefit from his wisdom throughout my doctoral studies, as well as during my master's degree, until that sad day. I remember him with respect and longing.

I also express my gratitude to my dear thesis advisor Prof. Mahmut Altınbaş. He has always been giving credit to my plans for my thesis studies and guided me to develop them. His contributions to this thesis study are immense, I thank him very much. In addition, Dr. Ece Polat as my mentor has always been helpful in improving ideas and applying them in the laboratory. She has always participated and contributed without any regrets on weekday evenings and weekends when I was able to do the experiments in the laboratory during my free time from work. I thank her deeply from my heart. In addition, I would like to thank all my managers and all colleagues at Tüpraş who encouraged me to continue my Ph.D. studies in my free time from work. Also this project was funded by İTÜ BAP organization with the project ID of MDK-2021-43272.

I was able to complete all my doctoral studies by stealing most of our time from my wife and son. I would like to thank my dear wife Nuray for her patience, tolerance, helpfulness and interest throughout all these studies. Without her encouragement and constant help, I wouldn't have been able to complete my studies. I will tell lots of stories to our son Kerem about those moments soon, hopefully. I would also like to thank my mother Özlem, my father Cengiz and my brother Emre Kolukısaoglu, who have contributed a lot to my life.

Lastly, it was a journey of self-discovery for me as well. A quotation from Rumi says, "As you start to walk the way, the way appears". I realized myself in that way with perseverance during my Ph.D. studies. There were no quick wins. After a comprehensive planning session, there was only a routine of lab work. I can assure you there are tons of reasons why you cannot attend lab nor read an article that day, but if you continue without any hesitation, you will have a chance to complete such a tough and long journey.

January 2025

Mert KOLUKİSAOĞLU

TABLE OF CONTENTS

	<u>Page</u>
FOREWORD.....	ix
TABLE OF CONTENTS.....	xi
ABBREVIATIONS	xv
LIST OF TABLES	xvii
LIST OF FIGURES	xix
SUMMARY	xxiii
ÖZET	xxvii
1. INTRODUCTION.....	1
1.1 Significance of the Thesis	1
1.2 Purpose and Scope of the Thesis.....	2
2. LITERATURE REVIEW.....	5
2.1 An Overview of Conventional Carbon Capture.....	5
2.2 Carbon Capture via Microalgae	6
2.2.1 Open raceway ponds.....	7
2.2.2 Vertical column photobioreactors (VC-PBRs).....	8
2.2.3 Horizontal tubular photobioreactors (HT-PBRs).....	9
2.2.4 Flat panel photobioreactors (FP-PBRs).....	9
2.2.5 Other innovative photobioreactors	10
2.2.6 Comparison of the closed photobioreactors	11
2.3 Importance of carbonic anhydrase (CA) enzyme.....	12
2.4 Coculture Applications	12
2.5 Effects of Flue Gas Input	13
2.6 Calcite Recovery by Precipitation.....	14
3. MATERIAL AND METHODS.....	17
3.1 Experiments with Algae Species.....	17
3.1.1 Growth conditions	18
3.1.2 Biomass, total chlorophyll and carotenoid	19
3.1.3 Biochemical structure	20
3.1.4 Amino acid extraction and measurements	21
3.1.5 Fatty acid methyl ester (FAME) measurement.....	22
3.1.6 Carbonic anhydrase activity measurement	22

3.1.7 Statistical analysis	24
3.2 Coculture Experiments with Algae and Bacteria	24
3.2.1 Algal growth, total chlorophyll and carotenoid analysis	26
3.2.2 EPS analysis.....	27
3.2.3 Enzyme activity analysis.....	28
3.2.4 Microbial community analysis via qPCR method	28
3.2.5 Calcium ion analysis	29
3.2.6 Alkalinity analysis by measuring carbonate and bicarbonate ions	29
3.2.7 XRD and SEM Analysis	30
3.3 Design of Pilot Scale Experiment	30
3.3.1 Open raceway.....	30
3.3.1.1 Light intensity, pH, aquatic temperature and growth	31
3.3.1.2 Total chlorophyll and carotenoid.....	31
3.3.1.3 Suspended solids and volatile suspended solids	32
3.3.1.4 CA enzyme activity	32
3.3.1.5 Dominance of Algae in Coculture via qPCR.....	32
3.3.2 Bubble column photobioreactor.....	33
3.3.2.1 Total chlorophyll and carotenoid.....	34
3.3.2.2 Suspended solids and volatile suspended solids	34
3.3.2.3 CA enzyme activity	35
4. RESULTS AND DISCUSSION.....	37
4.1 Assessment of Alkaline pH Effects on Algae Species	37
4.1.1 Growth, chlorophyll, and carotenoid production	37
4.1.2 Biochemical Contents	41
4.1.3 Amino acids contents	43
4.1.4 Fatty Acid Methyl Ester Contents.....	46
4.1.5 Carbonic anhydrase enzyme activity	48
4.2 Principal Component Analysis to Evaluate the Results	50
4.3 Analytic Hierarchy Process Method to Determine Algae Species	54
4.4 Coculture Experiments with Algae and Bacteria	55
4.4.1 Growth, total chlorophyll and carotenoid	56
4.4.2 EPS analysis result.....	58
4.4.3 CA enzyme activity results	61
4.4.4 qPCR analysis results.....	64
4.4.5 Calcium ion content	65

4.4.6 Carbonate and bicarbonate ions content	67
4.4.7 XRD and SEM analysis.....	68
4.5 Open Raceway Ponds	71
4.5.1 Light intensity, pH, aquatic temperature and growth	71
4.5.2 Total chlorophyll and carotenoid.....	73
4.5.3 Suspended solids and volatile suspended solids.....	75
4.5.4 CaCO ₃ mass balance.....	75
4.5.5 CA enzyme activity	77
4.5.6 EPS analysis	78
4.5.7 Carbonate and bicarbonate ions content	79
4.6 Closed Photobioreactor Outcomes.....	80
4.6.1 Growth, suspended solids and volatile suspended solids	80
4.6.2 Total chlorophyll and carotenoid.....	80
4.6.3 Suspended solids and volatile suspended solids.....	82
4.6.4 CaCO ₃ mass balance.....	83
4.6.5 CA enzyme activity	84
4.6.6 EPS analysis	85
4.6.7 Carbonate and bicarbonate ions content	86
5. CONCLUSIONS AND RECOMMENDATIONS.....	87
REFERENCES.....	91
APPENDICES	101
CURRICULUM VITAE.....	105



ABBREVIATIONS

AHP	: Analytic Hierarchy Process
CA	: Carbonic Anhydrase
CBAM	: Carbon Border Adjustment Mechanism
CCS	: Carbon Capture & Storage
EDS	: Energy Dispersive X-ray Spectrometer
EPS	: Extracellular Polymeric Substance
ESP	: Electro-Static Precipitator
ETS	: Emission Trading System
EU	: European Union
FAME	: Fatty Acid Methyl Ester
FP-PBRs	: Flat Panel Photobioreactors
HT-PBRs	: Horizontal Tubular Photobioreactors
IVR	: Inoculation Volume Ratio
MPBRs	: Membrane Photobioreactors
NSCR	: Non-Selective Catalytic Reduction
OD	: Optical Density
PBR	: Photobioreactor
qPCR	: quantitative Polymerase Chain Reaction
SCR	: Selective Catalytic Reduction
SEM	: Scanning Electron Microscope
SS	: Suspended Solids
S/V	: Surface/Volume
UNFCCC	: United Nations Framework Convention on Climate Change
VC-PBRs	: Vertical Column Photobioreactors
VSS	: Volatile Suspended Solids
XRD	: X-Ray Diffraction



LIST OF TABLES

	<u>Page</u>
Table 2.1 : Comparison between closed type photobioreactors (Qin et al., 2019) ..	11
Table 3.1 : Growth durations and studied culture media.	17
Table 3.2 : The primers used for sequencing the strains.....	18
Table 4.1 : The pH levels at which the highest growth was observed, combined with correspondent biomass and incubation time.....	39
Table 4.2 : Total chlorophyll and total carotenoids amount with total carotenoids to total chlorophyll ratio of strains in different pH conditions ($\mu\text{g}/\text{mg}$)....	40
Table 4.3 : Carbonic Anhydrase enzyme activity per biomass in different pH conditions (mU/mg biomass).....	50
Table 4.4 : Selection of microalgae species for carbon capture using the AHP method.	55
Table 4.5 : Band assignments for FTIR of EPS.	60
Table 4.6 : Mass balance in raceway pond - Spirulina monoculture.	76
Table 4.7 : Mass balance in raceway pond - Coculture.	76
Table 4.8 : Mass balance in BPR - Monoculture.	83
Table 4.9 : Mass balance in BPR - Coculture.	84
Table 5.1 : Selection of the most feasible CCS technology for industrial applications using the AHP method.....	89



LIST OF FIGURES

	<u>Page</u>
Figure 2.1 : Most common CCUS methods in use (Global CCS Institute, 2023).	5
Figure 2.2 : Open raceway ponds with paddle wheels operated in outdoor mode from UK. Different sizes of the ponds for preparing inoculum cultures (Koller, 2015).	8
Figure 2.3 : Tubular PBR setup (Torzillo & Zitelli, 2015).	9
Figure 2.4 : Flat panel photobioreactor setup (Lindblad et al., 2019).	10
Figure 2.5 : MBPR flow diagram (Theepharaksapan et al., 2023).	10
Figure 3.1 : Evolutionary relationship of the strains.....	18
Figure 3.2 : 8th day of incubation - <i>Spirulina</i> sp.	19
Figure 3.3 : Suspended solid measurement of coccus culture from Lake Salda.....	20
Figure 3.4 : Calibration equation for Nitrophenol standard.....	23
Figure 3.5 : Day zero of the coculture setup - first attempt	25
Figure 3.6 : Day zero of the coculture setup - second attempt.....	26
Figure 3.7 : Optical density peak points of (a) <i>A. platensis</i> and (b) <i>B. pasteurii</i>	26
Figure 3.8 : Open Raceway Setup. 1. Coculture media, 2. Monoculture media.....	31
Figure 3.9 : Bubble column PBR, monoculture, day 0.....	34
Figure 4.1 : Growth durations of different species such as: (a) <i>Chlamydomonas reinhardtii</i> , (b) <i>Arthrosphaera platensis</i> , (c) <i>Chlorella vulgaris</i> , (d) Filamentous-type cyanobacteria from Salda Lake, (e) Coccus-type cyanobacteria from Lake Salda.	38
Figure 4.2 : The protein-lipid and carbohydrate contents of the cultures: (a) <i>Chlamydomonas reinhardtii</i> , (b) <i>Arthrosphaera platensis</i> , (c) <i>Chlorella vulgaris</i> , (d) Filamentous-type cyanobacteria from Salda Lake, (e) Coccus-type cyanobacteria from Lake Salda.	43
Figure 4.3 : Heat map of the amino acid measurements.....	45
Figure 4.4 : SFA, MUFA and PUFA contents of the cultures changing with pHs: (a) <i>Chlamydomonas reinhardtii</i> , (b) <i>Arthrosphaera platensis</i> , (c) <i>Chlorella vulgaris</i> , (d) Filamentous-type cyanobacteria from Salda Lake, (e) Coccus-type cyanobacteria from Lake Salda.	47
Figure 4.5 : C16-C18 contents of the FAMEs (a) <i>C. reinhardtii</i> , (b) <i>S. platensis</i> (c) <i>C. vulgaris</i> , (d) Coccus-type cyanobacteria, (e) Filamentous-type cyanobacteria.	48
Figure 4.6 : Principal component analysis (PCA). Sample projection of <i>Chlamydomonas reinhardtii</i> , <i>Arthrosphaera platensis</i> (<i>Spirulina</i>), <i>Chlorella vulgaris</i> , Filamentous-type cyanobacteria from Salda Lake (Salda filamentous), Coccus-type cyanobacteria from Salda Lake (Salda coccus).	51

Figure 4.7 : 3D PCA plot of (a) <i>Chlamydomonas reinhardtii</i> , (b) <i>Arthrosphaera platensis</i> (<i>Spirulina</i>), (c) <i>Chlorella vulgaris</i> , (d) Filamentous-type cyanobacteria from Salda Lake (Salda filamentous), (e) Coccus-type cyanobacteria from Salda Lake (Salda coccus) and (f) overall data.....	53
Figure 4.8 : Hierarchy of the Criteria.....	54
Figure 4.9 : Coculture experiment set (first attempt with failure end). (1) Picture from day 0, (2) Picture from day 1, (3) Picture from Day 2, (4) Picture from Day 3.....	55
Figure 4.10 : Coculture experiment setup (second attempt) - photos from the 12th day.....	56
Figure 4.11 : Algae TSS correlation graphic by OD680 nm.....	56
Figure 4.12 : Bacteria TSS correlation graphic by OD600 nm.....	57
Figure 4.13 : Coculture suspended solid change in time (mg/L).....	57
Figure 4.14 : Total chlorophyll and carotenoid pigment contents in different IVRs.	58
Figure 4.15 : EPS results of different IVRs such as; (1) 100% algae, (2) 75% algae-25% bacteria, (3) 50% algae-50% bacteria, (4) 25% algae-75% bacteria, 100% bacteria.	58
Figure 4.16 : FTIR analysis of EPS samples.....	59
Figure 4.17 : SEM image of EPS.....	61
Figure 4.18 : EDS spectrum of mineralized products of EPS.....	61
Figure 4.19 : Calibration curves of P-nitrophenol standard solution for CA activity test.....	62
Figure 4.20 : CA concentration change in 1 hour by 10 min intervals.	63
Figure 4.21 : CA activity between 0 to 10 minutes as mU/mg.	63
Figure 4.22 : Chlorophyll gene measurement of the samples via qPCR.	64
Figure 4.23 : Gene quantification for chlorophyll area.....	64
Figure 4.24 : Bacteria gene measurement of the samples via qPCR.	65
Figure 4.25 : Gene quantification for bacteria area.....	65
Figure 4.26 : Calcium ion concentration on OD600 and CA activity (Zheng & Qian, 2019).....	66
Figure 4.27 : Calcium and magnesium ion contents.	66
Figure 4.28 : Concentration of carbonate and bicarbonate ions.....	67
Figure 4.29 : XRD analysis - peak points of 75% algae sample.....	68
Figure 4.30 : SEM micrographs of mineralized products of samples as a. Control (only Zarrouk media), b. bacteria monoculture, c. IVR 3:1 coculture, d. algae monoculture.	69
Figure 4.31 : EDS spectrums of mineralized precipitation samples, a. Control (Zarrouk media only), b. bacteria monoculture, c. coculture IVR 3:1, d. algae monoculture.	70
Figure 4.32 : pH and aquatic temperature changes by time.	71
Figure 4.33 : OD600 value change by time.	72
Figure 4.34 : Last day of the 35-day cultivation experiment. Coculture and monoculture, respectively.	73
Figure 4.35 : Total chlorophyll concentration change in raceway by time.....	74
Figure 4.36 : Total carotenoid concentration change in raceway by time.	74
Figure 4.37 : TSS and VSS change of both monoculture and coculture experiments.	75
Figure 4.38 : Enzyme activity change in raceways by time.....	77

Figure 4.39 : EPS concentration in algae monoculture raceway pond (1) 18.10.2024, (2) 25.10.2024, (3) 03.11.2024, (4) 07.11.2024, (5) 11.11.2024.....	78
Figure 4.40 : EPS concentration in coculture raceway pond (1) 18.10.2024, (2) 25.10.2024, (3) 03.11.2024, (4) 07.11.2024, (5) 11.11.2024	78
Figure 4.41 : Carbonate and bicarbonate ion concentrations change in time.	79
Figure 4.42 : SS and VSS Change by Time for Entire Cultivation.	80
Figure 4.43 : Total chlorophyll content of PBR experiments.....	81
Figure 4.44 : Total carotenoid content of PBR experiments.....	81
Figure 4.45 : VSS and mineral content in algae monoculture bubble type photobioreactor for calcification period.	82
Figure 4.46 : VSS and mineral content in coculture bubble type photobioreactor for calcification period.	83
Figure 4.47 : Enzyme activity change in PBR by time.....	85
Figure 4.48 : EPS concentration in algae monoculture PBR (1) before calcium addition, (2) after 2 days of calcium addition, (3) after 4 days of calcium addition.	85
Figure 4.49 : EPS concentration in coculture PBR (1) before calcium addition, (2) after 2 days of calcium addition, (3) after 4 days of calcium addition..	86
Figure 4.50 : Carbonate and bicarbonate ion changes in PBR.....	86
Figure 5.1 : Hierarchy for feasibility of carbon capture technologies.	88
Figure A.1 : Control sample (Zarrouk media only).	102
Figure A.2 : IVR:1/1 sample.....	102
Figure A.3 : <i>Spirulina</i> monoculture sample.....	103
Figure A.4 : <i>Bacillus</i> monoculture sample.....	103
Figure A.5 : IVR: 1/3 sample.....	104



CARBONDIOXIDE CAPTURING FROM INDUSTRIAL FLUE GAS VIA CALCIUM CARBONATE INDUCING MICROORGANISMS

SUMMARY

The increase in greenhouse gases, primarily caused by human activities in the past century, has led to the effects of global climate change becoming increasingly evident. Legal regulations in Europe and neighboring countries are becoming more stringent, and new taxation systems such as the Carbon Border Adjustment Mechanism are pushing industries with high carbon emissions to seek different solutions. In the near future, where conventional flue gas treatment methods alone will be insufficient, carbon capture technologies have been improved in recent years by scientists and even industry's research and development departments.

Solutions involving microorganisms allow for many options with individual benefits, such as atmospheric and closed-loop systems. Carbon capture using microorganisms, especially algae, offers a promising solution. Within the scope of this study, experiments were conducted on two algae species with coccus and filamentous morphological structures obtained from Lake Salda together with *Chlorella vulgaris*, *Spirulina*, *Chlamydomonas reinhardtii* species. Many analyses were conducted on these algae including growth rates, growth periods, pigment contents such as chlorophyll and carotenoid, carbonic anhydrase enzyme activity values, biochemical content, and fatty acid types. The fact that Lake Salda is in the high pH category with a pH value greater than 9 was an effective factor in including the samples obtained from here in the study. In all analyses, the pH at which the relevant algae species showed the most growth between pH 8 and 11 at 0.5 intervals was examined. The two species obtained from Lake Salda, which were subjected to the same growth conditions as other algae species using BG11 medium, were not included in further studies as they grew relatively less. In addition, the measurement of carbonic anhydrase enzyme activity was considered as a parameter at least as important as growth during species selection. The presence of the relevant enzyme that enables the gaseous carbon dioxide to be converted into dissolved gas was evaluated as a factor that needs to be developed for carbon dioxide capture studies. The species selection was made as *Spirulina* with the help of the Analytical Hierarchy Process method, which takes into account all other effective factors as well as growth and enzyme activity.

In the second phase of the experiment, the optimum mixture ratio of algae and bacteria coculture was examined in order to increase enzyme activity. Here, the *Bacillus pasteurii* species that secretes the relevant enzyme was selected. In addition to 100 ml of algae and bacteria monocultures in individual sterile bottles, 3:1, 1:1, 1:3 ratios were also added to the experimental set as two sets. After 12 days of incubation, the highest enzyme activity value was measured as 1.33 mU/mg for the algae-bacteria mixture ratio of 3:1. In growth values, the same culture stood out as 2.4 g/L. The same set of experiments was run for a third set, this time with only the

Zarrouk medium in a different conical flask. Here, just before the 15-day incubation period was started, CaCl_2 was added to the medium so that there would be 60 mM calcium ions in the medium. Advanced experiments such as XRD analysis, SEM imaging and qPCR analysis were performed on the precipitate obtained at the end of 15 days. The coculture 3:1 mixing ratio stood out again, especially due to the high impurity in the calcite it formed.

In the third phase of the experiment, while moving on to pilot scale studies, the coculture mixture ratio was decided and it was progressed in a way. First, the study was carried out in atmospheric and agitated tanks positioned side by side in 200 L volume. Incubation lasting 35 days was carried out in October and November. 22 days of this was the time spent only for the growth of microorganisms in the aquatic environment, and CaCl_2 was added to the medium in the last 13 days and the calcification process was followed. At the end of the total study, the VSS concentration in the coculture increased by 1.7 times, while the VSS concentration in the monoculture increased by only 1.4 times. At the end of the study, the VSS concentration in the monoculture was measured as 1.1 g/L, and the temperature has a great effect on the relatively low result.

With bubble type photobioreactor, 4 days of calcification were performed in monoculture after 4 days of growth, and 4 days of calcification were performed in coculture after 8 days of growth. In the results, 2.12 g/L VSS was observed in coculture, while 4 g/L VSS was observed in monoculture. Despite the remarkable growth in monoculture, almost equal amounts of TSS were measured at the end of both studies as 14.64 g/L in monoculture and 14.42 g/L in coculture, respectively. As a result, it was determined that much more calcite was produced with much lower biomass in coculture.

This study elucidates the multifaceted potential of microalgae, specifically *Spirulina* sp., in diverse biotechnological applications. The comprehensive analyses and experiments conducted have provided critical insights into optimizing conditions for enhanced biomass productivity and efficient CO_2 utilization. The investigation into the properties of calcium carbonate (CaCO_3) and the enzyme activity of carbonic anhydrase (CA) revealed valuable information for optimizing biomass productivity and CO_2 utilization. Experiments conducted in closed photobioreactors demonstrated the advantages of regulating environmental parameters to maximize algal growth and productivity. The evaluation of suspended solids and volatile suspended solids yielded critical data on the overall efficiency and sustainability of the cultivation processes. Furthermore, the structural and compositional attributes of CaCO_3 were found to be essential for its application in various industrial processes. The enzyme activity studies highlighted the pivotal role of CA in facilitating CO_2 capture and conversion, underscoring its potential in mitigating greenhouse gas emissions. Additionally, the extracellular polymeric substances (EPS) analysis illuminated the complex nature of the extracellular matrix, suggesting avenues for further research into biofilm formation and stability.

The study also compared carbon capture via algae with conventional carbon capture and storage (CCS) technologies, noting both advantages and challenges. Despite the benefits, scaling up algae-based capture in energy-intensive sectors remains challenging. Absorption and adsorption are considered more economical and advanced methods for substantial CO_2 capture.

Using the Analytic Hierarchy Process (AHP) method, the study evaluated various CCS technologies based on factors such as CO₂ capture capacity, cost, operational difficulties, scalability, and space requirements. Algae-based CCS technologies face significant economic and spatial challenges, with costs ranging from \$702 to \$1,585 per ton of CO₂ captured, compared to \$15 to \$340 for conventional methods.

In conclusion, while microalgae demonstrate significant promise in addressing environmental and energy challenges, further research and development are necessary for industrial-scale applications. Continued collaboration and research will advance the field of microalgal biotechnology, fostering sustainable development.





KALSIYUM KARBONAT OLUŞUMUNU TETİKLEYEN MİKROORGANİZMALAR İLE KARBONDİOKSİT YAKALAMA

ÖZET

Geçtiğimiz yüzyılda öncelikli olarak insan faaliyetleri sonucunca oluşan sera gazlarındaki artış küresel iklim değişikliğinin etkilerinin giderek belirginleşmesine yol açmaktadır. Avrupa ve komşu ülkelerindeki yasal düzenlemeler daha keskin hale gelmektedir ve Sınırda Karbon Vergisi gibi yeni vergilendirme sistemleriyle birlikte karbon emisyonu yüksek sanayileri farklı çözümler aramaya itmektedir. Yalnızca konvansiyonel baca gazı arıtma yöntemlerinin yetersiz kalacağı yakın gelecekte karbon yakalama teknolojileri son yıllarda araştırmacılar ve hatta endüstri temsilcileri tarafından geliştirilmektedir.

Mikroorganizma içeren çözümler, atmosferik ve kapalı devre sistemler gibi bireysel faydalıları olan birçok seçenek olanağı sunmaktadır. Özellikle algler olmak üzere mikroorganizmalar kullanılarak yapılan karbon yakalama, umut verici bir çözüm sunmaktadır. Bu çalışma kapsamında *Chlorella vulgaris*, *Spirulina*, *Chlamydomonas reinhardtii* türleriyle birlikte Salda Gölü'nden temin edilen kokus ve filamentli morfolojik yapıda olan iki alg türü üzerinde çalışmalar yapılmıştır. Alglerin büyümeye hızları, büyümeye süreleri, klorofil ve karotenoid gibi pigment içerikleri, karbonik anhidraz enzim aktivitesi değerleri, biyokimyasal muhteviyatı, yağ asidi tipleri olmak üzere bu algler üzerinde bir çok analiz yapılmıştır. Salda Gölü'nün pH değerinin 9'dan büyük olarak yüksek pH kategorisinde yer olması, buradan temin edilen numunelerin çalışma kapsamına alınması konusunda etkin faktör olmuştur. Bütün analizlerde ilgili alg türlerinin 0,5 aralıklarla pH 8 ile 11 arasındaki en çok büyümeye gösterdiği pH irdelenmiştir. BG11 besiyeri kullanılan ve diğer alg türleriyle aynı büyümeye şartlarına tabi tutulan Salda Gölü'nden temin edilmiş iki türün de görece çok daha az çoğalmaları nedeniyle ileriki çalışmalara dahil edilmemişlerdir. Bunun yanında karbonik anhidraz enzim aktivitesi ölçümlü tür seçimi sırasında en az çoğalma kadar önemli bir parametre olarak kabul edilmiştir. Gaz formundaki karbon dioksitin çözünmüş gaz formuna geçmesini sağlayan ilgili enzimin varlığı karbon dioksit yakalama çalışmaları için geliştirilmesi gereken unsur olarak değerlendirilmiştir. Büyümeye ve enzim aktivitesinin yanı sıra diğer tüm etkileyici faktörlerin de hesaba katıldığı Analitik Hiyerarşî Prosesi metodu yardımıyla tür seçimi *Spirulina* olarak yapılmıştır.

Deneyin ikinci safhasında enzim aktivitesini artırmabilmek adına alg ile bakteri kokültürü yapmanın optimum karışım oranı irdelenmiştir. Burada ilgili enzimi salgılayan *Bacillus pasteurii* türü seçilmiştir. Steril şişelerde 100'er ml kadar alg ve bakteri monokültürlerinin yanı sıra karışım oranı olarak 3:1, 1:1, 1:3 oranları da deney setine ikişer set olarak eklenmiştir. 12 günlük inkübasyon akabinde en yüksek enzim aktivitesi değeri 1,33 mU/mg olarak alg-bakteri karışım oranı 3:1 için ölçümlenmiştir. Büyümeye değerlerinde ise 2,4 g/L olarak yine aynı kültür öne çıkmıştır. Aynı deney seti, bu kez sadece Zarrouk medyasının farklı bir erlende

olduğu üçüncü bir set için daha çalıştırılmıştır. Burada 15 günlük inkübasyon süresi başlatılmadan hemen önce ortamda 60 mM kalsiyum iyonu olacak şekilde ortama CaCl_2 ilavesi yapılmıştır. 15 gün sonunda elde edilen çökelek üzerinden ise XRD analizi, SEM görüntülemesi ve qPCR analizi gibi çalışmalar yapılmıştır. Özellikle oluşturduğu kalsitteki yüksek safsızlığa istinaden kolkültür 3:1 karışım oranı yine öne çıkmıştır.

Deneyin üçüncü safhasında pilot ölçekli çalışmalara geçerken kokültür karışım oranına da karar verilebilmiş bir şekilde ilerlenmiştir. Öncelikle 200 L hacminde yan yana konumlanmış, atmosferik ve karıştırıcı havuzlarda çalışma yapılmıştır. Ekim ve Kasım aylarının içinde kalacak şekilde 35 gün süren inkübasyon gerçekleştirılmıştır. Bunun 22 günü sadece sucul ortamda mikroorganizmaların çoğalması için geçen süre olmakla birlikte son 13 gündə ortama CaCl_2 ilavesi yapılmış olup, kalsifikasiyon süreci takip edilmiştir. Toplam çalışmanın sonunda kokültürdeki UAKM konstantrasyonu 1,7 kat artarken, monokültürdeki UAKM konsantrasyonu sadece 1,4 kat artmıştır. Çalışmanın sonunda monokültür UAKM kontantrasyonu 1,1 g/L olarak ölçülmüştür, düşük sıcaklığın bu farka neden olduğu söylenebilmektedir.

Kabarcık tip fotobioreaktör ile monokültürde 4 gün büyümeye üzerine 4 gün kalsifikasiyon, kokültürde ise 8 gün büyümeye üzerine 4 gün kalsifikasiyon gerçekleştirılmıştır. Alınan sonuçlarda, kokültürde 2,12 g/L UAKM gözlenirken, monokültürde 4 g/L UAKM gözlenmiştir. Monokültürdeki dikkate değer büyümeye rağmen her iki çalışmanın sonunda sırasıyla monokültürde 14,64 g/L ve kokültürde 14,42 g/L neredeyse eşit miktarda AKM ölçümü yapılmıştır. Sonuç olarak kokültürde çok daha düşük biyokütle ile çok daha fazla kalsit üretimi gerçekleştiği tespit edilmiştir.

Bu çalışma, özellikle *Spirulina* sp. için çeşitli biyoteknolojik uygulamalardaki çok yönlü potansiyelini açıklamaktadır. Yapılan kapsamlı analizler ve deneyler, biyokütle verimliliğini artırmak ve CO_2 kullanımını optimize etmek için kritik bilgiler sağlamıştır. Kalsiyum karbonat (CaCO_3) ve karbonik anhidraz (CA) enzim aktivitesinin özelliklerini incelemiş ve biyokütle verimliliğini ve CO_2 kullanımını optimize etmek için değerli bilgiler elde edilmiştir. Kapalı fotobioreaktörlerde yapılan deneyler, çevresel parametreleri düzenlemenin alg büyümemesini ve verimliliğini maksimize etmenin avantajlarını göstermiştir. Askıda katı maddeler ve uçucu askıda katı maddelerin değerlendirilmesi, yetişirme süreçlerinin genel verimliliği ve sürdürülebilirliği hakkında kritik veriler sağlamıştır. Ayrıca, kalsiyum karbonatın yapısal ve bileşimsel özelliklerinin çeşitli endüstriyel süreçlerdeki uygulamaları için önemli olduğu bulunmuştur. Enzim aktivitesi çalışmaları, CA'nın CO_2 yakalama ve dönüştürme sürecindeki kritik rolünü vurgulayarak sera gazı emisyonlarını azaltma potansiyelini ortaya koymuştur. Ek olarak, hücre dışı polimerik maddeler (EPS) analizi, hücre dışı matrisin karmaşık doğasını aydınlatarak biyofilm oluşumu ve stabilitesi üzerine daha fazla araştırma yapılmasını önermektedir.

Çalışma ayrıca algler aracılığıyla karbon yakalama ile geleneksel karbon yakalama ve depolama (CCS) teknolojilerini karşılaştırmış, avantajları ve zorlukları not etmiştir. Faydalara rağmen, enerji yoğun sektörlerde alg bazlı yakalamanın ölçeklendirilmesi zor olmaktadır. Absorpsiyon ve adsorpsiyon, önemli miktarda CO_2 yakalamak için daha ekonomik ve gelişmiş yöntemler olarak kabul edilmektedir.

Analitik Hiyerarşî Süreci (AHP) yöntemi kullanılarak, çalışma CO₂ yakalama kapasitesi, maliyet, operasyonel zorluklar, ölçeklenebilirlik ve alan gereksinimleri gibi faktörlere dayalı olarak çeşitli CCS teknolojilerini değerlendirmiştir. Alg bazlı CCS teknolojileri, ton başına 702,00 ile 1.585,00 USD arasında değişen maliyetlerle önemli ekonomik ve mekansal zorluklarla karşı karşıya kalmaktadır, bu maliyetler geleneksel yöntemler için ton başına 15,00 ile 340,00 USD arasında değişmektedir.

Sonuç olarak, mikroalgler çevresel ve enerji zorluklarını ele almak için önemli bir potansiyel gösterse de, endüstriyel ölçekli uygulamalar için daha fazla araştırma ve geliştirme gerekmektedir. Sürekli işbirliği ve araştırma, mikroalg biyoteknolojisi alanını ilerleterek sürdürülebilir kalkınmayı teşvik edecektir.





XXX

1. INTRODUCTION

1.1 Significance of the Thesis

The increase of greenhouse gases in the atmosphere is largely due to human activities over the past century. Human beings have been suffering from natural disasters such as floods, hail, or extreme droughts more frequently in the last few years as a result of global climate change.

As one of the important legally binding international contracts, the Paris Agreement was adopted by 196 nations during the Paris Climate Conference (COP21), organized by the United Nations Framework Convention on Climate Change (UNFCCC). In line with the Paris Agreement, the goal is to limit global warming to below two degrees Celsius, preferably 1.5 degrees Celsius in comparison with pre-industrial levels (UNFCCC, n.d.). After the Paris Agreement, the European Union (EU) first took concrete action with the Carbon Border Adjustment Mechanism (CBAM) tool, which claims to put a fair price on the carbon emitted by production processes of carbon-intensive goods that the EU imports. As a consequence, non-EU countries that export goods to the EU will try to reduce carbon emissions and search for cleaner production technologies to avoid intensive CBAM taxes. The CBAM will apply to its definitive regimes such as cement, iron and steel, aluminum, fertilizers, electricity, and hydrogen production facilities by 2026 (Carbon Border Adjustment Mechanism, n.d.).

Europe's Emissions Trading System (ETS), first started in 2005, is a cap-and-trade system limiting greenhouse gas emissions. Companies receive or buy emission allowances and can trade them. The cap decreases over time, pushing businesses to adopt cleaner technologies. The ETS now also includes sectors like aviation and maritime transport, enhancing its role in reducing CO₂ (European Commission, 2023). In addition to market-based approaches, European countries have introduced legal bans and regulations to phase out high-carbon activities. For example, several nations, including Germany and France, have committed to ending coal-fired power

generation by 2030. Furthermore, the Renewable Energy Directive mandates that at least 32% of Europe's energy consumption must come from renewable sources by 2030, driving the shift away from fossil fuels.

While the regulations are getting more and more strict, the conventional treatment techniques for emissions are becoming less efficient than ever. Thus, new approaches need to be promoted and become widespread. At this point carbon capture by microorganisms will be a great solution. There are a lot of papers regarding the carbon capture by algae and this is a really trending topic in academic area. However, there are much less pilot scale facilities operated and there are small proportion of industrial scale facilities exist. This situation points out that the cost efficiency and scalability of the technology is not feasible yet and research are needed to carry out.

The novel idea of this thesis is coculturing algae with bacteria in order to increase growth and so increase carbon capture rates. In addition, by addition of calcium to the media, calcite precipitation is the second crucial outcome of the study.

1.2 Purpose and Scope of the Thesis

Industries came across a decision as making investments on the carbon capture technologies or purchasing the carbon credits according to EU legislation. Purchasing carbon credits can be feasible nowadays by comparing to 2023 market prices because the unit price decreased to 68,00 EUR level from 100 EUR in past 2 years (Trading Economics, 2024). However, due to the increase in population and geopolitical developments, can make the unit prices higher than ever. Hence, feasibility will be change in near future to investing on treating the industrial emissions.

Calcite is a mineral name and the chemical structure of this mineral, which forms carbonate rocks, is CaCO_3 . It has a glassy shine and a colorless transparent structure. It is easily ground, and a white powder is obtained. Its hardness is 3 according to the Moh's scale and its density is between 2.6-2.7 g/cm³. Silica, iron, and magnesium are counted as impurities, and they are at the lowest level in Turkey's mines. Calcite has various usage areas such as paper, paint, plastic and cable, construction, adhesives, food, ceramic, carpet base, floor linoleum, pharmaceutical sectors (MTA, n.d.).

Firstly, selecting the most effective algae species was one of the vital steps of this experimental series. *Chlorella vulgaris*, *Spirulina sp.*, *Chlamydomonas reinhardtii*, coccus type algae from Lake Salda and filamentous type algae from Lake Salda, constitutes the 5 options on list. Not only the species compared, but also the pH levels from 8 to 11 were monitored and compared also. Biomass concentrations, biomass duration, media type, pigment content, enzyme activity and persistency to impurities were the primary factors affecting the select the effective option. Analytical Hierarchy Process method was used for decision-making step and scores were provided via both experimental results and literature. According to that study, *Spirulina sp.* at pH 10.5 was the most effective one.

After determining the algae species and the growing media pH, coculture experiments were conducted. *Bacillus pasteurii* was used for the bacteria culture. Different Inoculation Volume Ratios (IVR) as algae over bacteria were studied in order to figure out the optimum growth. 3:1, 1:1 and 1:3 were the coculture ratios and there were control groups as only Zarrouk medium, monoculture of algae and monoculture of bacteria. One set of experiments was conducted without any calcium addition, only for observing the growing curves and the other set of experiments was conducted with the same amount of CaCl_2 addition to system to observe precipitation quality. In addition to spectrophotometry analysis, XRD analysis, SEM monitoring, qPCR measurement, enzyme activity, carbonate and bicarbonate ion concentrations were determined through the methods which explained through the thesis. IVR 3:1 was found out for the optimum growth and purity of calcite precipitation.

After lab scale experiments results were collected, pilot scale experiments were conducted. Double open raceway ponds with empty volume of 200 L each were operated, one as Spirulina monoculture and the other one as coculture with IVR 3:1. Total cultivation lasted 35 days, however it was autumn session water temperature was not warm enough to support cultivation. On the other hand, calcite precipitation was collected from both ponds and the mass balances are calculated accordingly. The other pilot scale experiment was conducted via bubble type photobioreactor with air compressor connected. Because there is only one PBR set up is available in the laboratory, monoculture and coculture experiments were conducted sequentially. Monoculture's total cultivation duration was 8 days while coculture's duration was

12 days. On the other hand, the calcification process took same duration as 4 days in both systems and there was slight extra gaining in the coculture system.

Mitigation of CO₂ from industrial flue gases and decrease its harmful effects to the atmosphere by support of the microorganisms are the origin of the study. Converting carbon dioxide to calcium carbonate and harvesting the calcite precipitation from the media is the value-added approach to the treatment system. Not only monoculture but using coculture by endeavoring the microorganism to grow much more efficiently is the novel idea of this thesis.

2. LITERATURE REVIEW

2.1 An Overview of Conventional Carbon Capture

CO₂ constitutes 76% of greenhouse gases and is divided into 65% from fossil fuel and industrial processes and 11% from forestry and other land use. Other components can be counted as methane, nitrous oxide, and fluorinated gases as 16%, 6% and 2% respectively (EPA, n.d.).

The impacts of industries on society are so high that mitigating industrial emissions is one of the biggest concerns. Carbon Capture and Storage (CCS) technologies have been developed in recent years. CO₂ can be captured directly from the air, or from a point source. Many point source CCS technologies are available, including pre-combustion capture, post-combustion capture, oxy-combustion, and chemical looping to mitigate CO₂ levels (Shaw & Mukharjee, 2022). Basic process flow diagrams were given in Figure 2.1.

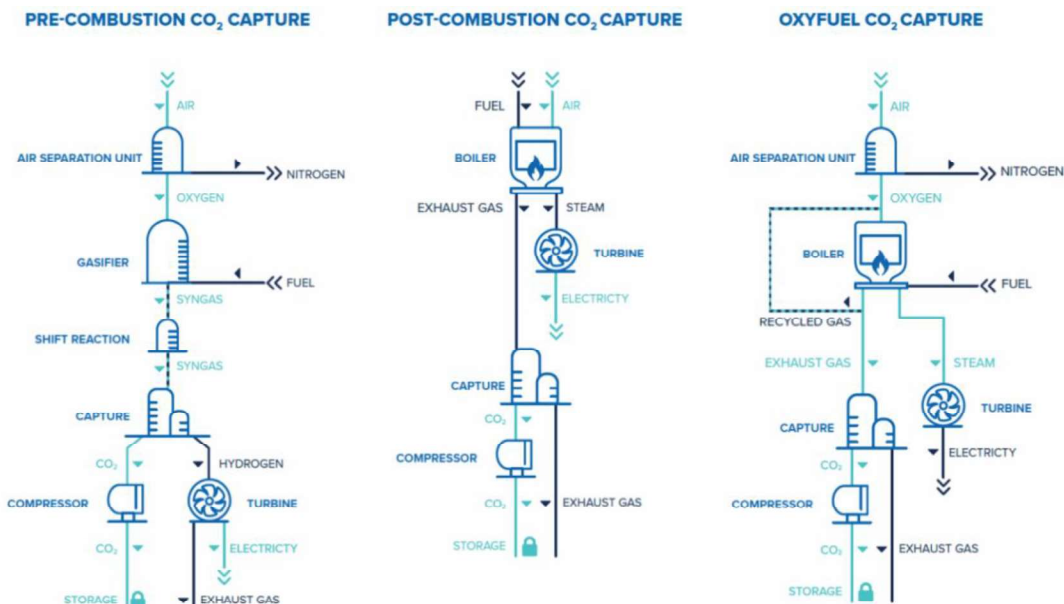


Figure 2.1 : Most common CCUS methods in use (Global CCS Institute, 2023).

- Pre-combustion : In this process, CO₂ was captured just before

combustion. Fuel was converted to hydrogen and CO₂. The hydrogen was separated from mixture and can be burnt purely. On the other hand, CO₂ can be compressed and sent to be stored.

- Post-combustion : CO₂ was captured after the combustion exhaust gases, mainly via liquid solvent named as adsorption. It was the most common approach in use. Numerous ways were existing like dry, semi-dry and wet systems. Electro-static precipitator (ESP), cyclones, fabric filters, selective catalytic reduction (SCR), non-selective catalytic reduction (NSCR), spray dry absorber, scrubbers non-thermal plasma technology were some of major technologies in use by this concept (Singh et al., 2019).
- Oxy-combustion : Not the air, but the pure oxygen was used for combustion of fuel. At the end, exhaust gas consist of mainly water vapor CO₂ can easily extracted from the stream.
- Chemical looping : It was a cost-effective alternative to methods mentioned above due to energy savings. Metal oxide was the oxygen source and reaction was carried out in two chambers, oxidation and reduction. However there is no actual operating facilities applying this technology.

2.2 Carbon Capture via Microalgae

Rather than conventional CCS methods, using microalgae for biological fixation of flue gas has been revealed as a novel alternative with high CO₂ fixation capacities (Alami et al., 2021). Compared to terrestrial plants, it is 10-15 times more efficient at photosynthetically converting carbon dioxide into energy. In many instances, it is not necessary to pre-treat flue gas before sending it to microalgae media. Additionally, microalgae are capable of consuming impurities such as sulphur and nitrogen which are contaminated with heavy metals as nutrients (Anwar et al., 2020). A fossil fuel boiler or furnace has a CO₂ content ranging between 3% and 20%. To be sustainable, the process must be gradually adapted, and the temperature controlled so that microalgae can readily capture it. Light penetration will likely limit the rate at which photoautotrophic microalgae will be able to fix CO₂. There are a number of cultivation processes that have been developed to maximize photosynthetic efficiency, biomass production, and the fixation of CO₂. In contrast to open pond

cultivation, tubular reactors, plastic bag reactors, airlift reactors, and flat pane reactors are examples of closed systems (Choi et al., 2019).

It is very effective to capture CO₂ in gas form using photobioreactors. *Chlorella vulgaris* can grow in fresh water and nutrient-rich waters such as wastewater. Early studies showed that without additional CO₂ supply when algae only use atmospheric CO₂ in open photobioreactors, the system fails due to a lack of metabolic carbon. Also, the increase in dissolved oxygen produced by photosynthesis results in inhibition in the system. By incubating *Chlorella vulgaris* in an open-air reactor for 24 days, CO₂ levels can be lowered (Kim & Otim, 2019). 1 g of algae biomass produced, 1.8 g of CO₂ was utilized based on the assumption that algae biomass consists of 50% carbon (Sudhakar et al., 2011). By merging two articles, it could be claimed that 2.48 g of CO₂ can be utilized theoretically and considered worth conducting advanced academic research on.

Aqueous CO₂ solution transforms into HCO₃ and then CO₃ by pH increase. As the pH rises from 7.5 to 8.5, the entire amount of soluble carbon dioxide reacts with CO₃ and H₂O to form HCO₃. Hence, cultivation mediums shall comply with that minimum requirement to maximize CO₂ sequestration. In their research on *Spirulina maxima* cultivation, Sornchai and Iamtham (2013) used pH values of 9.0, 9.5, 10, and 10.5 as the pH range. In addition, *Chlorella sp.* can grow in pH ranges from 9-11, grow slowly at pH 7, and hardly grow in pH ranges between 4-6. Other types of algae are also capable of cultivating efficiently in higher pH levels as a result of using bicarbonate as their primary carbon source (Jana, 2019).

2.2.1 Open raceway ponds

Raceway ponds are open ponds used for cultivating algae, where algae, water, and nutrients circulate around a race track. These systems are widely used for microalgal growth, and very large commercial systems exist today. Since the 1950s, raceway ponds have been used for mass culture of microalgae.



Figure 2.2 : Open raceway ponds with paddle wheels operated in outdoor mode from UK. Different sizes of the ponds for preparing inoculum cultures (Koller, 2015).

A raceway pond consists of a closed-loop recirculation channel with a water depth of 15-20 cm and a paddlewheel. During daylight, the culture is fed at the front of the paddlewheel, and the broth can be harvested from the same area. The paddlewheel mixes and circulates the algal biomass, preventing sedimentation. These raceway channels are built from concrete or compacted earth and can vary in length and diameter, usually lined with white plastic.

2.2.2 Vertical column photobioreactors (VC-PBRs)

VC-PBRs are usually designed with the radius of 20 cm and up to 4.0 m heights. Increase in radius more than 20 cm can cause low efficiency of cultivation due to less surface-volume (S/V) ratio. Height can be adjust according to performance of gas diffusor. There are different kind of VC-PBRs according to their slight differences of design given below (Qin et al., 2019):

Split column airlift PBR : A flat plate is placed in the middle and separate the diameter of the column as 2 parts such as the riser and the downcomer regions. Air enters the system from the riser and circulate through downcomer.

Internal loop airlift PBR : An internal column is located in a transparent column and air sparger mounted in the middle of inlet column. Degassing occurs at the top of internal column and degassed mixture exist between 2 column skins. Outstanding mixing, easy to clean, great light exposure rates can be counted as the most important benefits.

Bubble column PBR : Air sparger located at the bottom. The movement of air bubbles result in turbulence and the mixing can be achieved.

External loop airlift PBR : Degassing happens at the top of the system and circulation of degassed media is obtained through another circulation column.

2.2.3 Horizontal tubular photobioreactors (HT-PBRs)

HT-PBRs are horizontally placed set of parallel tubes. There are different sequences exist to increase exposing the sun more and more such as spiral, straight, manifold type, serpentine looped, coiled and α -shaped. However plenty of PBR technologies available, HT-PBRs are accepted as most suitable and practical one because of its high S/V ratio, stable and adjustable cultivation conditions (Leong et al., 2023). This type is also convenient to scale up. *Haematococcus* and *Chlorella* species were cultivated in large scale in Israel and Germany, respectively (Torzillo & Zitelli, 2015).



Figure 2.3 : Tubular PBR setup (Torzillo & Zitelli, 2015).

2.2.4 Flat panel photobioreactors (FP-PBRs)

FP-PBRs consist of rectangular transparent boxes such as glass, plexiglass, polycarbonate, etc. with high S/V ratio with short light path due to thin dimensions. The efficiency of the system mainly depends on the light path, dissolved oxygen concentration and panel configurations. They can be implemented horizontally, vertically or inclined according to the best illumination surface area. For outdoor setups, temperature controlling is crucial, and it can be carried out by heat exchangers or water spraying. Due to the system's short light path and no chance to light dilution, there is a risk of photo-inhibition and light oversaturation which lead collapsing the cultivation processes.

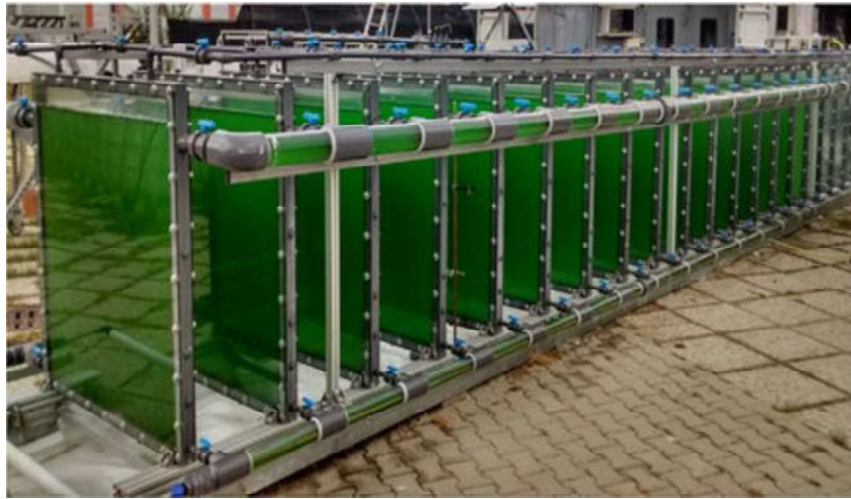


Figure 2.4 : Flat panel photobioreactor setup (Lindblad et al., 2019).

2.2.5 Other innovative photobioreactors

Plastic bag photobioreactors are a cost-effective solution for commercial-scale production. They offer initial sterility due to high film extrusion temperatures. When equipped with aeration systems, these reactors can improve yields. While large polyethylene bag photobioreactors, with capacities up to 2000 liters, were once widely used in aquaculture for algae feed, their usage has decreased but they are still employed to a certain extent (Qin et al., 2019).

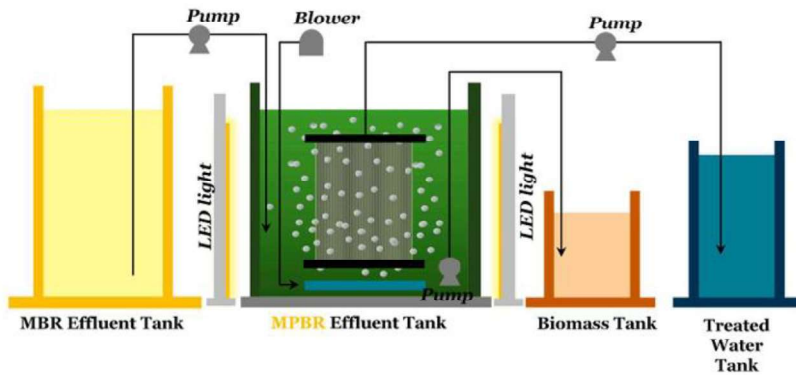


Figure 2.5 : MBPR flow diagram (Theepharaksapan et al., 2023).

Membrane photobioreactors (MBPRs) are used for the further treatment of membrane bioreactor (MBR) effluent water. The main aim is treated to nutrients such as N and P which remain in MBR effluent. Efficient operating condition is determined as 7.7-7.8 days of hydraulic retention time and 60-80 days of solids retention time, by adding bicarbonate as additional carbon source to MBPR. By those retention time 39.3% of $\text{NO}_3\text{-N}$ and 43.8 PO_4 treatment could be achieved. In

addition, not only monoculture of algae, but also coculturing with bacteria provides similar treatment efficiencies. Although lab scale experiments result in successful treatment ratios, scaling up the system comes with the economic problems which needs to be examined deeply in further experiments (Theepharaksapan et al., 2023).

2.2.6 Comparison of the closed photobioreactors

Major closed photobioreactor types are listed above and their most important differentiated features are given in Table 2.1.

Table 2.1 : Comparison between closed type photobioreactors (Qin et al., 2019).

Criteria	VC-PBRs Bubble column	VC-PBRs Airlift	HT-PBRs	FP-PBRs
S/V ratio	Low (2-8 m ² per m ³)	Low (2-8 m ² per m ³)	High (up to 100 m ²)	High (20-80 m ² per m ³)
Mixing mechanisms	Airlift	Airlift	Airlift or pump	Airlift or pump
Mixing efficiency	High	Very high	Low	Low
Degassing efficiency	High	High	Medium	Low
Risk of photo-inhibition	Low	Low	Medium	High
Risk of biofouling	Low	Low	High	High
Space requirement	Low	Low	Medium	Medium
Capital cost	Low	Medium	Medium to high	Medium to high
Scalability	Difficult	Difficult	Easy	Medium

2.3 Importance of carbonic anhydrase (CA) enzyme

CAs are mostly zinc-containing metalloenzymes and hydrate CO_2 to HCO_3^- according to 2 step reaction as given in Equations 2.1 and 2.2, respectively:



CAs can be found everywhere both in prokaryotes and eukaryotes. There are eight different classes of CA enzyme such as α , β , γ , δ , ζ , η , θ and ι . They perform differentiated roles regarding physiological processes, amino acid sequences and 3D tertiary structures (Steger et al., 2022).

One of the major hardships in using enzymes for large-scale industrial applications is maintaining the protein catalysts' thermochemical stability under harsh conditions, such as high temperatures and acid gas contaminants. To figure out this, researchers have isolated carbonic anhydrases (CAs) from thermophiles and immobilized these enzymes on solid support substrates. Other concerns in enzyme management include absorption kinetics over time and the potential for enzyme recovery and reuse. However, it was proved that CA activity is strong against contaminating gases, including H_2S and propane, and industrially relevant concentrations of NO and SO_2 . High concentration of NO and SO_2 results in activity loss, but the enzyme shows high levels of activity retention at lower concentrations which are mostly likely to encounter in industrial effluents (Sharma et al., 2023).

2.4 Coculture Applications

Microalgae often grow with bacteria in natural environments and lab cultures. Heterotrophic bacteria benefit from the oxygen and substances produced by microalgae and provide them with carbon dioxide and vitamins. This synergy has led to an efficient co-culturing mode, which strengthens as the densities of both increase (Han et al, 2016).

Mutualistic symbiosis can arise from exchanging primary metabolites, cofactors and hormones, or creating unique niches within a microbial ecosystem. In algal-bacterial systems, carbon dioxide-oxygen exchange is common. Heterotrophic bacteria

degrade organic material in wastewater, producing carbon dioxide for photosynthetic algae, which in turn provides dissolved oxygen to enhance bacterial degradation of organic material. Co-cultures consume substrates faster than individual organisms. The presence of *E. coli* nearly doubled the neutral lipid and fatty acid content in *A. protothecoides*, enhancing substrate uptake and nitrogen removal. This shift in the fatty acid profile could improve biodiesel's oxidative stability from algal lipids. These findings indicate that co-culturing can boost water treatment performance and biofuel production in algae (Higgins et al., 2016).

Furthermore, vitamin B12 (cobalamin), which is nature's most complex metabolite, requiring at least 19 separate enzymatic steps for its synthesis from uroporphyrinogen III, is crucial benefit of the symbiotic environment. In their natural environment, vitamin B12-dependent algae must be able to obtain the vitamin from an external source. Reported levels of free cobalamin are usually about 2–6 ng.L⁻¹ in fresh water and up to 3 ng.L⁻¹ in sea water. The growth studies suggested that this could be insufficient to boost algal growth. Thus, coculturing with bacteria can increase the vitamin B12 levels to encourage algal growth (Croft et al., 2005).

2.5 Effects of Flue Gas Input

Flue gas can serve as a carbon and nutrient source for microalgal cultivation, offering sustainable environmental benefits. However, using flue gas is more challenging than normal CO₂. Factors like water and oxygen impact growth similarly with both sources, but many aspects of flue gas significantly affect microalgae growth. Therefore, strategic use is crucial to maximize benefits. The following factors presents the positive and negative effects of flue gas components on microalgae (Choi et al., 2019):

- CO₂ : Industrial flue gas contains high levels of CO₂, depending on the process and feedstocks. CO₂ provides inorganic carbon for microalgae during photosynthesis. In fact, if the CO₂ level get higher uncontrollably, it could have toxic effects on culture because of acidification.
- NO_x : NO_x compounds are utilized as a source of nitrogen for microalgae growth, hence greater growth removes NO_x through uptake form flue gas effectively. Dissolution of NO_x compounds stabilize the rise in pH

which occurred through microbial growth. High NO_x concentrations like CO₂ could inhibit the cultivation.

- SO_x : In low concentrations it can serve the culture as sulphure source by its oxidized form as sulfate.
- CO : After oxidizing CO to CO₂, it could be consumed by algae.
- Heavy metals: Many heavy metals provide essential trace elements and can alter algal metabolism, affecting carbonic anhydrase activity. High concentrations found in flue gas and their strategic use can enhance microalgae growth and lipid accumulation. If the concentration exceeds the design parameters, then the inhibition will be unavoidable.
- Hydrocarbons: They also can serve as carbon source to algae species.
- O₂ : Oxygen served as an electron acceptor for photorespiration and microalgal cell membranes likely to be damaged by various toxic oxygen radicals and oxygen also decreases CO₂ uptake by competing for RuBisCO.
- Water: Water acts as an electron donor during the photosynthesis of microalgae. It is a crucial compound for various metabolic activities essential for survival and is extensively utilized by microalgae during the process of photosynthesis.

2.6 Calcite Recovery by Precipitation

Stromatolites like those existing in Lake Michigan and the Great Bahama Bank are CaCO₃ formations caused by collaborative actions by microalgae and bacteria (Jansson&Northen, 2010). Thus, not only algae monocultures, but also algae-bacteria co-cultures can reveal more realistic and efficient CaCO₃ precipitation results. Many of these co-culture systems are used in wastewater treatment systems efficiently. It is claimed that Chlorella minutissima grows faster when co-cultured with Escherichia coli. Furthermore, triglyceride production can be increased under the mixed culture of Chlorella vulgaris and Pseudomonas sp. which points to another efficiency increment. According to study conducted with Chlorella sp. with Sporosarcina pasteurii (S.pasteurii) shows that 3:2 (v:v) inoculation volume ratio (IVR) respectively results in maximum chlorophyll-a concentration. Under this IVR condition, the growth of Chlorella sp. increased up to 37.74% (Xu et al., 2020).

In order to generate CaCO_3 , using carbonic anhydrase enzyme-producing bacteria is more logical than using urease enzyme-producing bacteria. This is due to the efficiency of transforming the gaseous form into a soluble form without causing excessive ammonia. *Bacillus mucilaginosus* was used as a microorganism, and maximum cultivation was observed when the pH was 9–10 and the temperature was 25°C. As a result of the experiment biotic CaCO_3 was obtained successfully (Zheng, 2021). CO_2 sequestration can be enhanced by carbonic anhydrase enzyme function (de oliveira Maciel et al., 2022).

It is common practice in many cases to convert calcium carbonate into calcium oxide (limestone). As part of mineral carbonation processes, microorganisms can contribute carbon dioxide, which can influence these processes, and carbon dioxide can be utilized by these microorganisms for the formation of carbonate minerals. Microorganisms use a natural mineralization mechanism for producing carbonate minerals; however, the feasibility of these processes on a commercial scale remains in the research phase. According to recent studies, biomimicry is a very niche technology, and there is a long way to go to determine the efficiencies of this technology. It can be settled near coal-fired power plants, natural gas systems, municipal solid waste combustion, and other CO_2 -emitting industries (Jansson & Northen, 2010).



3. MATERIAL AND METHODS

3.1 Experiments with Algae Species

To identify the most effective culture in an alkaline settling, several experiments were performed using strains from the Cukurova University Algal Biotechnology Laboratory (*Chlamydomonas reinhardtii*, *Arthrospira platensis* (*Spirulina*), and *Chlorella vulgaris*). These results were then compared to those from strains isolated from Salda Lake (coccus-type and filamentous-type), which is alkaline (0.015-0.041 mol/L) and rich in magnesium (Balci et al., 2020). Algae, growth durations and used specific culture media are given in Table 3.1.

Table 3.1 : Growth durations and studied culture media.

Species	Growth duration (Day)	Culture Media
<i>C. reinhardtii</i>	5	Tris-Acetate Phosphate (TAP)
<i>A. platensis</i> (<i>Spirulina</i>)	36	Spirulina medium*
<i>C. vulgaris</i>	20	Blue-Green Medium (BG11)
Coccus-type cyanobacteria from Salda Lake	34	BG11
Filamentous-type cyanobacteria from Salda Lake	14	BG11

*The ingredients of this medium consists of the following composition (g/L): 18.6 NaHCO₃, 8.06 Na₂CO₃, 1.00 K₂HPO₄ 5.00 NaNO₃, 2.00 K₂SO₄, 2.00 NaCl, 0.40 MgSO₄.7H₂O, 0.02 CaCl₂.2H₂O, 0.02 FeSO₄.7H₂O, 0.16 EDTANa₂ and micronutrient elements (0.001 ZnSO₄.7H₂O, 0.002 MnSO₄.7H₂O, 0.01 H₃BO₃, 0.001 Na₂MoO₄.2H₂O, 0.001 Co(NO₃)₂.6H₂O, 0.00005 CuSO₄.5H₂O, 0.7 FeSO₄.7H₂O, 0.8 EDTANa₂) were added 10 mL to 1 L (Zarrouk, 1966).

DNA was isolated using a FastDNA® SPIN Kit for Soil and FastPrep® Instrument (MP Biomedicals, Santa Ana, CA). A Bio-Rad MyCycler System was used to amplify the selected regions. The used primers are listed in Table 3.2.

A 1% (w/v) TAE agarose gel stained with ethidium bromide was used to visualize dPCR products. Evolutionary relationships in taxa history were inferred using the UPGMA method (Corliss et al., 1973). The optimal tree is shown in Figure 3.1.

Table 3.2 : The primers used for sequencing the strains.

Primer ^b	Sequence (5'-3')	Region
8F*	AGAGTTTGATCCTGGCTCAG	16S rRNA
1492R	GGTTACCTTGTACGACTT	16S rRNA
518R	GTATTACCGCGGCTGCTGG	16S rRNA
515F	GTGCCAGCMGCCGCGGTAA	16S rRNA
1100R	GGGTTGCGCTCGTTG	16S rRNA
18SEUKF (6F)	ACCTGGTTGATCCTGCCAG	18S rRNA
18SEUKR (5R)	TGATCCTCYGCAGGTTCAC	18S rRNA
Euk515R	ACCAGACTTGCCTCC	18S rRNA
Ami6F1	CCAGCTCCAATAGCGTATATT	18S rRNA

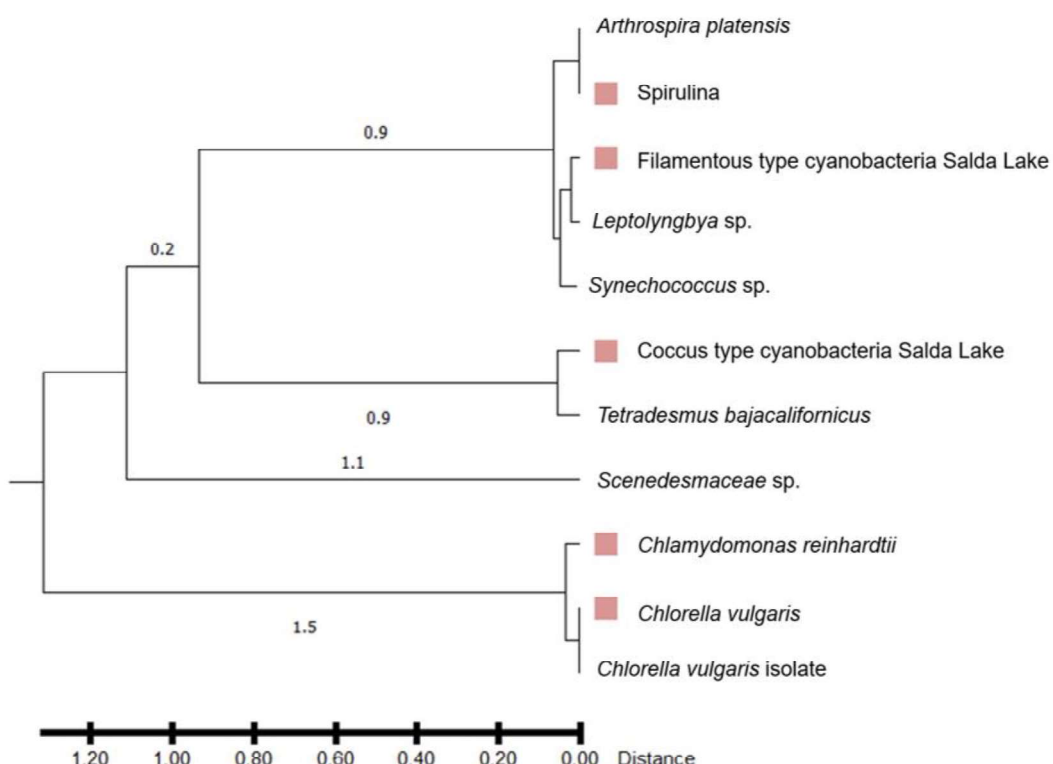


Figure 3.1 : Evolutionary relationship of the strains.

3.1.1 Growth conditions

Twelve flasks per species were prepared, each containing 200 mL of medium and covered with cotton and aluminum foil. They were autoclaved at 105 °C for 20 minutes. The pH levels were adjusted from 8.5 to 11 in 0.5 intervals by adding sterilized 20% KOH solution until the pH indicator strips matched the corresponding color on the box. MQuant pH indicator strips with a range of 7.5–14 were used in the experiment. Species grown in high alkalinity environments experience stress

(Alkhamis et al., 2022), and high light intensity can add additional stress, causing photoinhibition. Although the optimal light intensity for the strains was found to be 30–100 $\mu\text{mol photons/m}^2/\text{s}$ in preliminary experiments, a continuous light intensity of 30 $\mu\text{mol photons/m}^2/\text{s}$ was used to avoid photoinhibition in all setups. An optimal temperature of 28 ± 2 $^{\circ}\text{C}$, determined during initial screenings, was maintained. Optical density (OD) was measured at 540 nm, 690 nm, and 750 nm wavelengths (Akca et al., 2023). OD was monitored daily for *C. reinhardtii*, every four days for *C. vulgaris*, and every other day for the other species.



Figure 3.2 : 8th day of incubation - *Spirulina* sp.

3.1.2 Biomass, total chlorophyll and carotenoid

At the end of each growth cycle, measurements of biomass, total chlorophyll, and carotenoid levels were taken. For dry cell weight (DCW) measurements, microalgae cultures were filtered through pre-weighed filter papers, then dried at 105 $^{\circ}\text{C}$ until a constant weight was achieved (Visentin et al., 2023). Biomass was evaluated based on the correlation between optical density (OD) and DCW. For the analysis of total chlorophyll and carotenoid contents, 10 mL samples were placed in 15 mL Falcon tubes and centrifuged for 7 minutes at 3,000 rpm. After centrifugation, the water layer was removed, a pinch of CaCO_3 was added, and the mixture was vortexed. Next, 1.8 mL of 90% acetone solution was added, and the mixture was incubated at 45 $^{\circ}\text{C}$ for one hour. Absorbance wavelength measurements were taken at 466, 632, 649, 665, and 696 nm. The total chlorophyll and carotenoid contents were calculated using Equations 3.1 and 3.2 (Polat et al., 2020; Ritchie, 2006).

$$\begin{aligned} \text{Total Chlorophyll } (\mu\text{g. mL}^{-1}) = & 24.1209 \cdot A_{632} + 11.2884 \cdot A_{649} + \\ & 3.7620 \cdot A_{665} + 5.8338 \cdot A_{696} \end{aligned} \quad (3.1)$$

$$\text{Total Carotenoid } (\mu\text{g. mL}^{-1}) = 4.74 \cdot A_{466} \quad (3.2)$$



Figure 3.3 : Suspended solid measurement of coccus culture from Lake Salda.

3.1.3 Biochemical structure

Protein extraction is performed using the cold extraction method (Östbring et al., 2019). In order to extract the samples, 1 mL of 0.1 M NaOH solution was added, and the samples were frozen at -20 °C. When the samples reached room temperature, they were centrifuged at 4 °C for 30 minutes at 5,000 g. One mL 0.1 M NaOH solution was added to the bottom part, and the same freeze-thaw process was applied again. Citric acid was added to the collected upper parts to adjust the pH to 5. Rapid heating to 80 °C in 4 minutes and incubated for 30 minutes. Quick cooling in a water bath was applied and then centrifuged at 5,000 g for 30 minutes at 4 °C. The bottom part is used for protein extraction measurements. Spectrophotometric measurement of total protein was performed using the Lowry method against a BSA standard (Lowry et al., 1951).

Lipid measurement was performed using a sulfo-phospho-vanillin (SPV) assay (Khaligh et al., 2023). The main stock was prepared as 1 mg/mL for calibration. Five mg of vegetable oil was dissolved in a hexane solution. Then it was vortexed to get a homogenous solution. Then eight glass tubes were prepared, and the solution was injected as follows: 0µL, 5µL, 25µL, 50µL, 75µL, 125µL, 250µL, and 500µL. 5 mg of biomass from each sample were collected, and their weights were noted. 2 mL of sulfuric acid was added to the samples and the calibration solutions. All samples were vortexed and kept at 100 °C for 10 minutes. 4 mL of SPV solution was added to

each sample and vortexed again. After putting the samples at 37 °C for 15 minutes, they were measured at 530 nm, 540 nm, and 750 nm wavelengths in a spectrophotometer.

In glass tubes, 25 mg of biomass from each sample is added to extract carbohydrates (Polat et al., 2020). 250 μ L 72% (w/w) sulfuric acid was added to the biomass. Then the mixtures were vortexed. Samples were incubated in a water bath at 30 °C for 1 hour. During incubation, samples were vortexed for 30 seconds every 5 minutes. The sulfuric acid concentration decreased to 4% after incubation with 7 mL of dH₂O added to the samples. Samples were vortexed again. The glass tubes were capped and autoclaved at 121 °C for 1 hour. After autoclave, samples were filtered through 0.22 nm filters. Carbohydrate quantification is done via the modified anthrone method (Ludwig & Goldberg, 1956). Ice baths were used to prepare samples and solutions. At the same time, a 100 °C hot water bath was prepared. For the calibration curve, glucose solutions at different concentrations were prepared. 1 mL of sample was put into a glass tube, 2 mL of 75% sulfuric acid was added, and the mixture was vortexed. 4 mL of anthrone solution was added to the sample and vortexed again. Samples were incubated at 100°C for 15 minutes and then cooled to room temperature. At the end, samples were measured at 630 nm against distilled water in a spectrophotometer.

3.1.4 Amino acid extraction and measurements

10 mL of homogenized 6 N HCl solution was added to a 50 mg sample and incubated for 24 hours at 110 °C (Lee et al., 2022). After cooling down to room temperature, 2 mL of the sample was dried at 50 °C. Derivatization solution (Edman reactive) was prepared by mixing 100 mL ACN with 1.2 mL of phenylisothiocyanate (PITC). 0.5 mL of ACN (acetonitrile): MeOH (methanol): TEA (triethylamine) mixture and 0.1 mL of derivatization solution were added to the samples and then left at 40 °C for 30 minutes (Sanchez-Machado et al., 2003). High-performance liquid chromatographic analysis of amino acids in edible seaweeds after derivatization with phenyl isothiocyanate (Sanchez-Machado et al., 2003). 5 mL of 0.02 M ammonium acetate was added to it after it had dried at 40 °C. Then it was filtrated via 0.45 μ m filters and injected into HPLC equipment. For tryptophan extraction, 15 mL of 4.3 N LiOH·H₂O was added to 100 mg of biomass and

hydrolyzed at 110°C for 16 hours. Its pH was adjusted to 4.5 by adding 0.1 M HCl. After the pH adjustment, the volume was set to 100 mL by adding distilled water. The tryptophan standard was prepared by dissolving 50 mg of tryptophan in 50 mL of 0.1 N HCl. After derivatization, HPLC measurements were conducted.

The amino acid contents were measured by HPLC (High-Performance Liquid Chromatography, Shimadzu Prominence 20, Riverwood Drive Columbia, MD, USA) equipped with a PDA detector and an ODS-3V column (5 μ m, 4.6 I.D. \times 250 mm, GL Sciences Inc., Tokyo, Japan). The mobile phase for tryptophan analysis consisted of an aqueous solution of sodium acetate (AcNa) (5 mM) and acetonitrile (Pinhati et al., 2012). The mobile phase for other amino acid analysis consisted of mobile phase A (0.78 g of sodium dihydrogen phosphate dihydrate and 0.88 g of disodium hydrogen phosphate dihydrate in 1 liter of water) and mobile phase B (ACN) in gradient elution.

3.1.5 Fatty acid methyl ester (FAME) measurement

In situ transesterification of microalgal biomass was performed using hydrochloric acid in methanol as a catalyst (Polat et al., 2020). Lipid composition was determined by gas chromatography (Shimadzu GC-2010) equipped with a flame ionization detector and a TR-CN100 capillary column with a 0.2 m film thickness (Teknokroma, Barcelona, Spain). During the analysis, the oven temperature was first increased to 140 °C and held for 6 minutes, then ramped up to 240 °C at a rate of 4 °C per minute, followed by a 10-minute hold at 240 °C. The carrier gas, helium, was set to flow at 30 mL/min, with hydrogen at 40 mL/min and air at 400 mL/min, using a 100:1 split ratio.

3.1.6 Carbonic anhydrase activity measurement

For measuring carbonic anhydrase enzyme activity, the Carbonic Anhydrase Activity Assay Kit (colorimetric) protocol was followed (Sigma-Aldrich, n.d.). Initially, the cells were lysed by adding 5 mL of cold lysis solution (containing 0.13 g Tris, pH 8) to 50 mg of algal biomass and vortexing the mixture. The sample was then frozen at -20 °C, thawed at room temperature, and vortexed again to achieve a uniform mixture. This freeze-thaw process was repeated three times. To prepare the cells for

the enzyme activity assay, the mixture was centrifuged at 3,500 rpm for 15 minutes at 4°C.

For carbonic anhydrase enzyme activity, a 2 mM Nitrophenol standard, 3 mM Nitrophenyl Acetate substrate, and CA activity buffer were prepared. To make a calibration standard, 2 mM Nitrophenol standard was aliquoted onto 96-well plates in volumes of 0.4, 8, 12, 16, 20, 40, 60, 80, and 100 µL. All sample volumes were set to 100 µL by adding the CA activity buffer. Consequently, nitrophenol standard solutions were obtained at 0, 8, 16, 24, 32, 40, 80, 120, 160, and 200 nmol/well Figure 3.4.

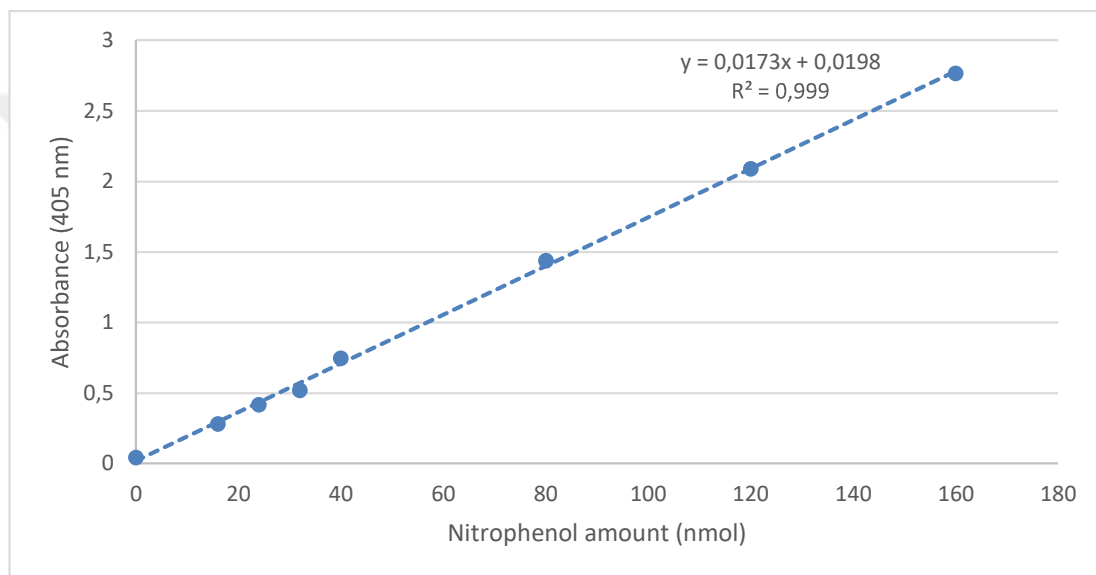


Figure 3.4 : Calibration equation for Nitrophenol standard.

For microalgal biomass samples, 50 µL of cell extract and 45 µL of CA activity buffer were added to each well. Next, 5 µL of Nitrophenyl acetate was added to the samples. Measurements were conducted in a 405 nm wavelength kinetic mode for 1 h at room temperature. Equations 3.3 and 3.4 were used to perform the calculations (Sigma-Aldrich, n.d.).

$$\text{Specific CA Activity (Extract)} = \frac{B \cdot D \cdot 1000}{\Delta t \cdot V} \left(\frac{\text{mU}}{\text{mL}} \right) \quad (3.3)$$

$$\text{Specific CA Activity (Biomass)} = \frac{B \cdot D}{\Delta t \cdot V \cdot P} \left(\frac{\text{mU}}{\text{g biomass}} \right) \quad (3.4)$$

Where;

B = Release Nitrophenol in the sample based on the Standard Curve slope (nmol)

D = Dilution Factor (D = 1 when samples are undiluted)

1000 = 1 mL = 1,000 μ L

Δt = Reaction time (min)

V = Sample volume (μ L)

P = Biomass concentration (g / μ L)

3.1.7 Statistical analysis

To investigate the correlation between pH changes and the biochemical components of microalgae, the Pearson Product correlation test was conducted using Minitab 16.0. Principal component analysis (PCA) was utilized for dimensional reduction and structural modeling of multidimensional data. OriginPro software (OriginLab, version 10.0.0.154) was used for both PCA and hierarchical cluster analysis (HCA). To test for statistically significant differences, one-way analysis of variance (ANOVA) was performed, followed by the post-hoc Tukey Honestly Significant Difference (HSD) test to determine if differences were statistically significant ($p < 0.05$).

3.2 Coculture Experiments with Algae and Bacteria

Coculture experiments were based on *Spirulina* and *Bacillus pasteurii* and they were mixed in different inoculum volume ratios (IVR) such as 0%, 25%, 50%, 75% and 100% respectively. LED lights were mounted on top, internally to shaker's cover. The shaker's heater was adjusted to 30°C degrees and shaking speed was adjusted to 120 rpm. Light intensity was measured between 90–105 μ mol photons. $m^{-2}.s^{-1}$ in different points from the bottom of the shaker. To increase light penetration via reflection the bottom material was covered with aluminum foil.

In the first attempt, 10 small flasks with 50 ml volume each were used, they filled up with Zarrouk medium. Name tags of flasks produced according to algae content, so bacteria content was planned to be remaining part. Each IVR was studied with backups, that's why there were 10 flasks instead of 5. In the first hand starting OD₆₀₀

value was determined for 100% algae flask as 0.3 nm. Then to obtain 0.3 nm, 2.33 ml algae from stock medium added to flask. For 75%, 50% and 25% flasks, 1.75 ml, 1.165 ml and 0.58 ml of algae were added, respectively. There were no algae in 0% flask like there was no bacteria in 100% flask. Then reversely, bacteria additions were conducted. To obtain 0.3 nm value in OD₆₀₀, 1.89 ml of bacteria was added. For 25%, 50% and 75% flasks, 1.42 ml, 0.94 ml and 0.47 ml of bacteria were added, respectively.



Figure 3.5 : Day zero of the coculture setup - first attempt.

Because there was an excessive heat due to setup configuration, the first attempt failed. Thus, there was another experiment with similar IVRs and also with the developed system.

In the second attempt 250 ml flasks were used with 100 ml filled by the medium. The same IVR sequence was preserved. The most important change was that the cover wasn't closed properly on purpose. Fresh air could enter the system, so the interior temperature's unexpected increase was prevented. The growth phase took 12 days long. All of the further analysis was conducted from the samples of the second attempt.

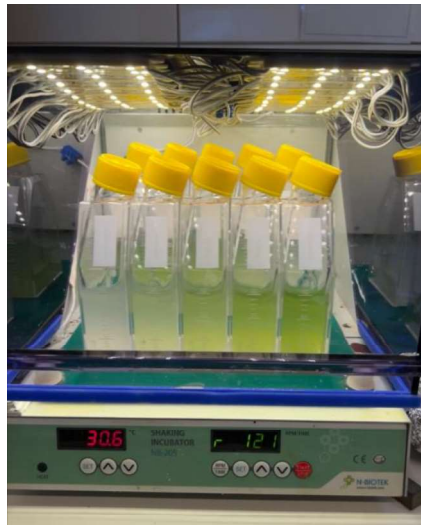


Figure 3.6 : Day zero of the coculture setup - second attempt.

3.2.1 Algal growth, total chlorophyll and carotenoid analysis

OD was monitored every other day for all of the flasks. As the experiment was conducted in sterile conditions, all of the samples were taken in laminar flow cabinet. UV lights and flames were turned on during the uncapping, sampling and recapping.

To determine which wavelength is more representative for coculture components their peak points were executed by the spectrophotometer itself. While the peak point was measured for *A. platensis* as OD₆₈₀, it was OD₆₀₀ for *B. pasteurii*. However, both OD values were read during the experiment, OD₆₀₀ was selected when the common value was required because alga's value changes slightly, while the bacterium's much higher.

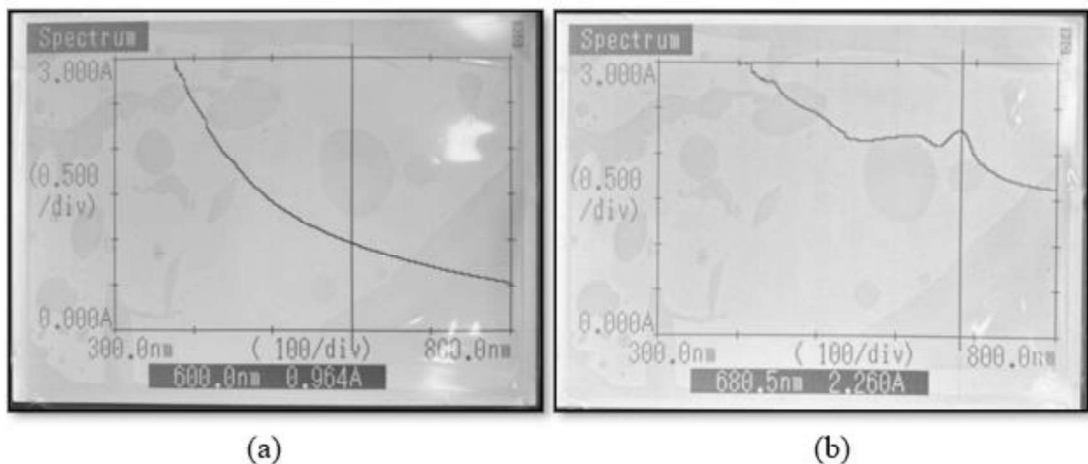


Figure 3.7 : Optical density peak points of (a) *A. platensis* and (b) *B. pasteurii*.

At the end of 12 days growth cycle, measurements of biomass, total chlorophyll, and carotenoid levels were taken. For Dry Cell Weight (DCW) measurements, microalgae cultures were filtered through pre-weighed filter papers, then dried at 105 °C until a constant weight was achieved (Visentin et al., 2023). Biomass was evaluated based on the correlation between Optical Density (OD) and DCW. For the analysis of total chlorophyll and carotenoid contents, 10 mL samples were placed in 15 mL Falcon tubes and centrifuged for 7 minutes at 3,000 rpm. After centrifugation, the water layer was removed, a pinch of CaCO₃ was added, and the mixture was vortexed. Next, 1.8 mL of 90% acetone solution was added, and the mixture was incubated at 45°C for one hour. Absorbance measurements were taken at 466, 632, 649, 665, and 696 nm. The total chlorophyll and carotenoid contents were calculated using Equations 3.1 (Polat et al., 2020) and 3.2 (Ritchie, 2006) as same as monoculture experiments.

3.2.2 EPS analysis

EPS analysis was carried out on samples before and after cultivation. Analyses were carried out by taking into account multiple methods (Choi et al., 2020; Dizge et al., 2011; Mahata et al., 2021). For EPS analysis, 5 mL of sample in Erlenmeyer flask is taken as a suspension and first centrifuged at 4000 rpm at 4°C for 10 minutes. Then, the upper phase is taken into a sterile tube and centrifuged again at 13,200 rpm at 4°C for 20 minutes to ensure that the suspended solids are completely removed. Dissolved protein and polysaccharide analyses were performed in this upper phase obtained by physical extraction. Dissolved protein and polysaccharide give the value of Soluble Microbial Products (SMP) in the medium. In order to detect bounded EPS, the sediment remaining from the first centrifugation was resuspended in 5 mL with sterile distilled water. 6 µl of formaldehyde (37%) was added to this suspension and kept at 4°C for 1 hour, then 0.5 mL of 1N NaOH is added and kept at 4°C for 3 hours. This suspension was centrifuged at 13200 rpm, 4°C for 20 minutes. Bounded protein and polysaccharide analysis was also performed on this supernatant obtained by chemical extraction. These values also gave the value of bounded or extracted EPS. The modified Lowry method for protein analysis and the Antrone method for polysaccharide analysis were carried out.

3.2.3 Enzyme activity analysis

For measuring carbonic anhydrase enzyme activity, the Carbonic Anhydrase Activity Assay Kit (colorimetric) protocol was followed (Sigma-Aldrich, n.d.) again. Initially, the cells were lysed by adding 5 mL of cold lysis solution (containing 0.13 g Tris, pH 8) to 50 mg of algal biomass and vortexing the mixture. The sample was then frozen at -20 °C, thawed at room temperature, and vortexed again to achieve a uniform mixture. This freeze-thaw process was repeated three times. To prepare the cells for the enzyme activity assay, the mixture was centrifuged at 3,500 rpm for 15 minutes at 4°C.

For carbonic anhydrase enzyme activity, a 2 mM Nitrophenol standard, 3 mM Nitrophenyl Acetate substrate, and CA activity buffer were prepared. For preparing a calibration standard, 0 nmol, 2.5 nmol, 5 nmol, 7.5 nmol, 10 nmol, 20 nmol, 40 nmol, 60 nmol, 80 nmol and 100 nmol solutions measured in spectrophotometry equipment with OD₃₄₈ and OD₄₀₅. Then each sample measured in every 10 minutes figure out velocity change by time until 60th minute.

3.2.4 Microbial community analysis via qPCR method

The 410 bp region-specific primer pair p23SrV_f1 (5'-GGACAGAAAGACCCTATGAA -3') p23SrV_r1 (5'-TCAGCCTGTTATCCCTAGAG -3') for the plastid 23S rRNA region of photosynthetic microorganisms, and the 466 bp region-specific primer pair Uni331F (5'- TCCTACGGGAGGCAGCAGT -3') Uni797R (5'-GGACTACCAGGGTATCTAATCCTGTT -3') for the living 16S rRNA region were synthesized (Lee et al., 2015). Each qPCR mixture was prepared in a total volume of 25 µl, consisting of 5 µl of 5-fold diluted DNA, 12.5 µl of master-mix and 400 nM primer pairs. PCR cycling conditions first provide degradation in different chambers with gradient technique to activate DNA polymerization. DNase/RNase distributions water was used as negative control. All measurements are performed with Bio-Rad Real-time PCR detector.

3.2.5 Calcium ion analysis

After cultivation, experiments re-started with fresh inoculums to see CaCO_3 precipitation potential. 1 flask contained only Zarrouk medium without any of organisms and the rest was settled with same IVRs. There was 6 flasks in total.

It has been experimented that the the concentration of Ca^{2+} was as 0 mM, 20 mM, 40 mM, 60 mM, 80 mM, 100 mM, 120 mM, 140 mM, 160 mM, 180 mM, 200 mM and 250 mM, 300 mM. 60 mM concentration has been founded as the one which provides maximum enzyme activity and growth as ≈ 0.7 U and 1.4 OD_{600} , respectively (Zheng & Qian, 2019). Hence, this experiment was conducted directly to obtain 60mM Ca^{2+} . According to that 0.8821 g of $\text{CaCl}_2 \cdot 2\text{H}_2\text{O}$ was added to each flask with 100 ml of media. After retention time passed 10 ml sample have been taken from each flask and filtered through 0.22 mikron filters.

3.2.6 Alkalinity analysis by measuring carbonate and bicarbonate ions

HCO_3^- and CO_3^{2-} concentrations were measured using double indicator neutralization titration. phenolphthalein and methyl orange indicators were used, respectively. 0.5 g phenolphthalein was dissolved in 100 ml of 50% ethanol to make ready the phenolphthalein indicator. On the other hand, 0.1 g methyl orange was dissolved in 100 ml of distilled water.

1 ml of liquid phase of each sample was diluted to 100 ml with distilled water. Then 4 drops of phenolphthalein indicator were added. If the solution didn't show red, it means that the absence of CO_3^{2-} at all. If it was red, titrate with standard HCl solution until the removal of red color after shaking the mixture and the added HCl volumes (V_1) were saved. On the other hand, 4 drops of methyl orange were added to the samples and then titrated with HCl solution again until its color turned from yellow to jacinth. These added volumes (V_2) were saved too. HCO_3^- and CO_3^{2-} concentrations were revealed by Equations 3.5 and 3.6 (Zheng & Qian, 2019):

$$C_{\text{CO}_3^{2-}}(\text{mol/L}) = C_{\text{HCl}} \cdot V_1 / 0.2 \quad (3.5)$$

$$C_{\text{HCO}_3^-}(\text{mol/L}) = C_{\text{HCl}} \cdot (V_2 - V_1) / 0.1 \quad (3.6)$$

The same method was used for open raceway pond and PBR samples.

3.2.7 XRD and SEM Analysis

Precipitated and mineralized products were washed to eliminate microorganism residues and then it dried. Then polymorphs of formations were monitored by XRD. The element species and morphologies of precipitated yield could be analyzed by Scanning Electron Microscope (SEM).

3.3 Design of Pilot Scale Experiment

After the lab-scale experiments carried out, sufficient data were collected for the pilot scale experiments. In order to figure out more realistic solutions, pilot scale experiments will be more effective. Since calcium ion, carbonate and bicarbonate analysis methods were identical with the lab scale coculture samples, they are not mentioned in the context additionally.

3.3.1 Open raceway

There are twin open raceways exist in ITU laboratory's rooftop. Their volume are both 200 L, One of them was chosen for monoculture and the other one for the coculture. Considering the weather conditions, due to it is autumn as well, raceways' volumes were filled by 100 L each.

Spirulina cultures were growing in one of those ponds when the kickoff decision was made and its OD₆₀₀ value was 0.638. To avoid making mistakes by complex mixture rates, it is decided to start with the half of it which is 0.319. So that raceway's volume was decreased 50 L and filled with distilled water until capacity reached to 100 L.

Next pond needs to be prepared for coculture and IVR was selected as 1/3 which means 75 L of it consist of algae and 25 L bacteria. The mixing principle was the same as lab-scale experiment. To achieve starting OD₆₀₀ value 0.319, firstly it was assumed that 100% of algae required and found necessary algae amount. Then it was multiplied by 0.75 and also same processes for bacteria but the coefficient is 0.25 that time. At the end, 42 L of algae media, 1,5 L of bacteria media and 56,5 L of distilled water calculated to reach 100 L.



Figure 3.8 : Open Raceway Setup. 1. Coculture media, 2. Monoculture media.

3.3.1.1 Light intensity, pH, aquatic temperature and growth

Light intensity was measured every 30 minutes for the entire study. The measuring device placed near the raceways and to avoid storm damage it was covered with transparent foil.

In every 2 days the samples about 0.25 mL were taken from raceways. While the samples were collecting, in the meantime aquatic temperature was measured also. pH and optical density measurements were carried out from those samples right after collection.

3.3.1.2 Total chlorophyll and carotenoid

Not from all of the samples, but only the samples from 6th, 13th, 22nd, 26th and 30th days were considered for the analysis. For total chlorophyll and carotenoid measurements, 10 mL samples were put into 15 mL Falcon tubes and centrifuged for 7 minutes at 3,000 rpm. After centrifugation, a layer of water was poured and then a pinch of CaCO₃ was added and vortexed. Then 1.8 mL of 90% acetone solution was added, and the mixture was incubated at 45°C for one hour. Absorbance measurements were conducted at 466, 632, 649, 665, and 696 nm. To calculate the

total chlorophyll and carotenoid contents, Equations 3.1 and 3.2 were used as same as previous ones.

3.3.1.3 Suspended solids and volatile suspended solids

The samples from raceways from day zero, 22nd day and 32nd days were used in this experiment in order to increase representation quality of the results. First, 0.45 μ m filters were sterilized in 105°C incubator for one hour and then put into desiccator for half an hour. After the filters were ready, their weights were measured via scale. Then 10 ml of well mixed samples passed through filters, and they put into 105°C incubator for one hour and then put into desiccator for half an hour again. Then their second weight measurement carried out to find suspended solid (SS) amount. Finally samples were put into 550°C furnace for half an hour and then desiccator for half an hour again. At the end final weight analysis was conducted to find out volatile suspended solids (VSS).

3.3.1.4 CA enzyme activity

For measuring carbonic anhydrase enzyme activity, the Carbonic Anhydrase Activity Assay Kit (colorimetric) protocol was followed (Sigma-Aldrich, n.d.) again. Initially, the cells were lysed by adding 5 mL of cold lysis solution (containing 0.13 g Tris, pH 8) to 50 mg of algal biomass and vortexing the mixture. The sample was then frozen at -20 °C, thawed at room temperature, and vortexed again to achieve a uniform mixture. This freeze-thaw process was repeated three times. To prepare the cells for the enzyme activity assay, the mixture was centrifuged at 3,500 rpm for 15 minutes at 4°C.

For carbonic anhydrase enzyme activity, a 2 mM Nitrophenol standard, 3 mM Nitrophenyl Acetate substrate, and CA activity buffer were prepared. To make a calibration standard, 0 nmol, 2.5 nmol, 5 nmol, 7.5 nmol, 10 nmol, 20 nmol, 40 nmol, 60 nmol, 80 nmol and 100 nmol solutions measured in spectrophotometry equipment with OD₃₄₈ and OD₄₀₅. Then each sample measured in every 10 minutes figure out velocity change by time until 60th minute.

3.3.1.5 Dominance of Algae in Coculture via qPCR

The 410 bp region-specific primer pair p23SrV_f1 (5'-GGACAGAAAGACCCTATGAA -3') p23SrV_r1 (5'-

TCAGCCTGTTATCCCTAGAG -3') for the plastid 23S rRNA region of photosynthetic microorganisms, and the 466 bp region-specific primer pair Uni331F (5'- TCCTACGGGAGGCAGCAGT -3') Uni797R (5'- GGACTACCAGGGTATCTAACCTGTT -3') for the living 16S rRNA region were synthesized (Lee et al., 2015). Each qPCR mixture was prepared in a total volume of 25 μ l, consisting of 5 μ l of 5-fold diluted DNA, 12.5 μ l of master-mix and 400 nM primer pairs. PCR cycling conditions first provide degradation in different chambers with gradient technique to activate DNA polymerization. DNase/RNase distributions water was used as negative control. All measurements are performed with Bio-Rad Real-time PCR detector.

3.3.2 Bubble column photobioreactor

Bubble column PBR was chosen as photobioreactor type to achieve maximum gas contact by the microorganisms. Firstly, *Spirulina* sp. as monoculture was cultivated for 8 days and after that new set of experiment was started with coculture which last for 12 days. Coculture's IVR was set to 3:1. The initial conditions for both experiments are given below:

- *Spirulina* sp. monoculture:
 - Temperature : 23±0,2°C
 - pH : 10,55
 - OD680 : 0,312
- *Spirulina* sp. & *Bacillus pasteurii* coculture:
 - Temperature : 23±0,2°C
 - pH : 10,56
 - OD600 : 0,577
 - OD680 : 0,563

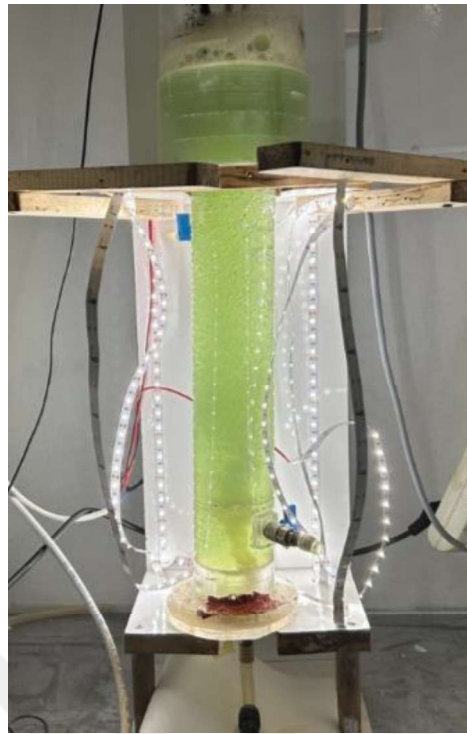


Figure 3.9 : Bubble column PBR, monoculture, day 0.

3.3.2.1 Total chlorophyll and carotenoid

For total chlorophyll and carotenoid measurements, unlike before experiments, 1 mL samples were put into 15 mL Falcon tubes and centrifuged for 7 minutes at 3,000 rpm. After centrifugation, a layer of water was poured and then a pinch of CaCO₃ was added and vortexed. Then 1.8 mL of 90% acetone solution was added, and the mixture was incubated at 45°C for one hour. Absorbance measurements were conducted at 466, 632, 649, 665, and 696 nm. To calculate the total chlorophyll and carotenoid contents, Equations 3.1 and 3.2 were used as same as previous.

3.3.2.2 Suspended solids and volatile suspended solids

The samples from each PBR from the day just before CaCl₂ addition (A), 2nd day after CaCl₂ addition (B) and 4th as last day after CaCl₂ addition (C) were used in this experiment in order to follow change in suspended solids. First, 0.45 µm filters were sterilized in 105°C incubator for one hour and then put into desiccator for half an hour. After the filters were ready, their weights were measured by scale. Then 10 ml of well mixed sample A and 5 ml of each of well mixed sample B and C passed through filters and they put into 105°C incubator for one hour and then put into desiccator for half an hour again. For sample B and C, because of increasing

concentration of the media, lower media volume was passed through the filters to prevent any clogging. Then their second weight measurement carried out to find suspended solid (SS) amount. Finally samples were put into 550°C furnace for half an hour and then desiccator for half an hour again. At the end final weight analysis was conducted to find out volatile suspended solids (VSS). In order to find fixed solids, VSS values were extracted from the total SS values.

3.3.2.3 CA enzyme activity

Exactly same measuring method of enzyme activity which conducted for raceway ponds was applied again.



4. RESULTS AND DISCUSSION

4.1 Assessment of Alkaline pH Effects on Algae Species

4.1.1 Growth, chlorophyll, and carotenoid production

The growth of microalgae is highly sensitive to pH levels, leading to significant variations in their growth rates and biomass production under different pH conditions. This study examined these changes for each species at various pH levels. Due to the heterotrophic nature of TAP media, *C. reinhardtii* grew for 5 days, with the highest growth observed at a pH of 9.5, yielding a biomass of 923 mg/L. In contrast, the biomass at pH 11 was less than half. It was found that *C. reinhardtii*'s growth exceeded 1.6 g/L in 5 days when exposed to different temperatures (25°C, 30°C, and 35°C) and light intensities (50 µE/m²/s, 100 µE/m²/s, and 150 µE/m²/s), with light/dark cycles significantly affecting growth (Zheng et al., 2022).

Spirulina was monitored for 32 days, with the highest biomass of 1,986 mg/L achieved at pH 8.5 (Figure 4.1). Biomass at pH 9 and 9.5 was 1.4 times lower, and at pH 10 and 10.5, it was 1.5 times lower. Chen et al. reported nearly 6 g/L growth in 6 days at 32°C and 700 µmol photons/m²/s light intensity for pH levels of 9.0, 9.5, and 10.0, attributing differences to light intensity in 2016. Also the highest biomass (4.12 g/L) at pH 9 for *Spirulina maxima*, likely due to different strains (Sornchai & Iamtham, 2013).

C. vulgaris achieved a maximum biomass of 469.9 mg/L at pH 10.5. Its ability to grow at alkaline pH values without significant biomass loss suggests high pH tolerance. Previous studies observed around 4 g/L biomass in 26 days in BG11 medium (Silva et al., 2022), linked to initial cell density differences. Higher biomass was seen in BG11 medium at pH 8 (Adam et al., 2022), and in poultry slaughterhouse conditions (pH 9.5-11.5), the highest biomass was at pH 10.5 (Katırcıoğlu Sınmaz et al., 2022), aligning with this study's results.

For Salda Lake coccus-type cyanobacteria, the highest biomass (674 mg/L) was at pH 8.5 after 26 days. Biomass was slightly lower (0.86 to 0.99 times) at other pH

levels, indicating high pH tolerance. Conversely, filamentous-type cyanobacteria from Salda Lake showed the highest biomass (273 mg/L) at pH 11, with a significant decrease at lower pH, reflecting high pH tolerance comparable to *C. vulgaris*, despite lower biomass production.

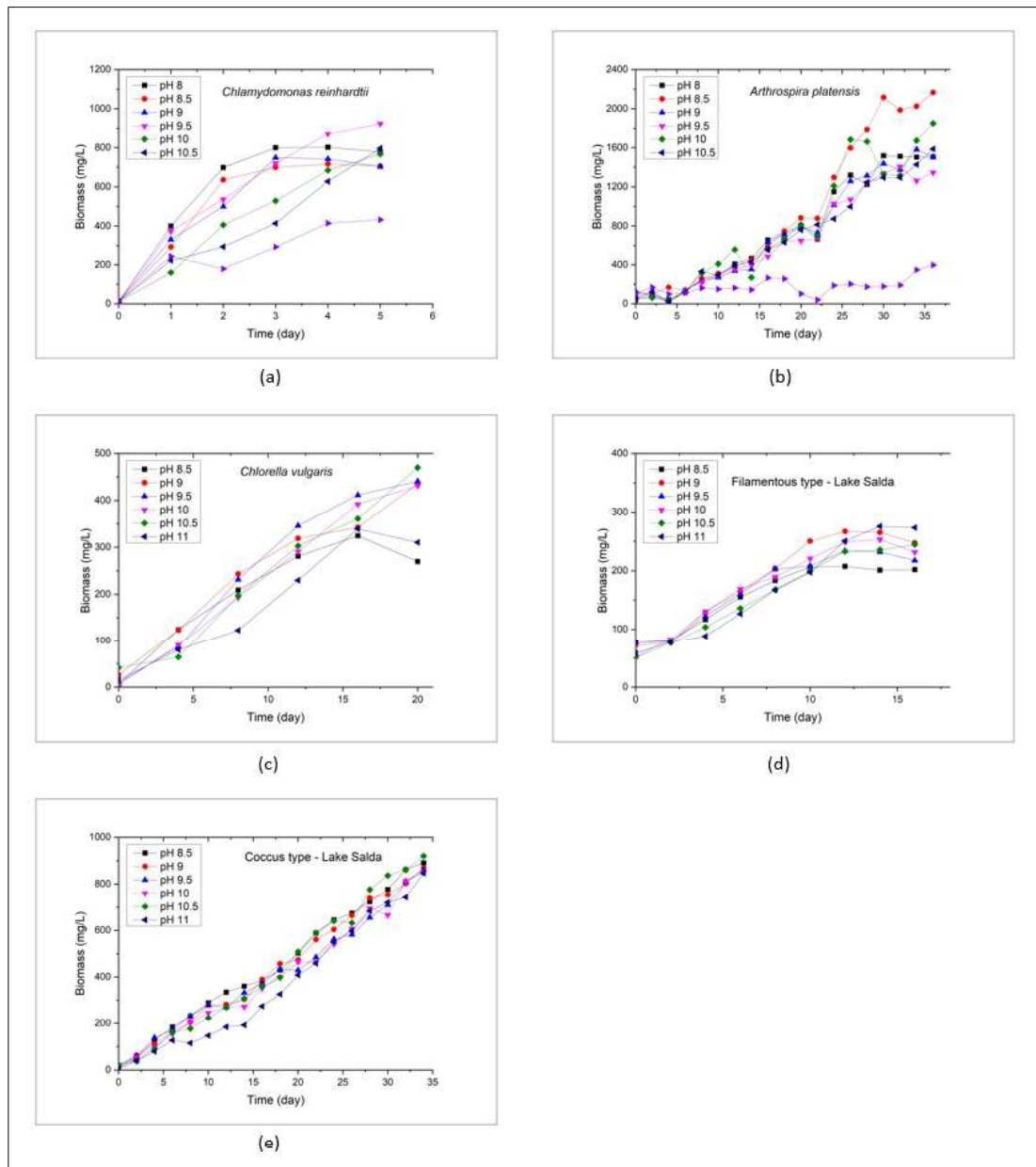


Figure 4.1 : Growth durations of different species such as: (a) *Chlamydomonas reinhardtii*, (b) *Arthrosphaera platensis*, (c) *Chlorella vulgaris*, (d) Filamentous-type cyanobacteria from Salda Lake cultures, (e) Coccus-type cyanobacteria from Lake Salda.

In order to find out the best-growing biomass by comparing 5 samples, *A. platensis*, *C. vulgaris*, and coccus-type from Salda Lake cultures were added to a shortlist, and for the proper comparison, 20 days of growth were noted for each sample. C.

reinhardtii was excluded due to heterotrophic media, whereas the rest are autotrophic. Furthermore, the filamentous-type cyanobacteria from Salda Lake were excluded due to their considerably low biomass yields. pH levels of three shortlisted individual cultures and biomass levels on the twentieth day of growth are given in Table 4.1. Comparing the growth levels of three samples on the twentieth day indicates the potential use of *A. platensis* for advanced research, despite its relatively high standard deviation.

Table 4.1 : The pH levels at which the highest growth was observed, combined with correspondent biomass and incubation time.

	Optimum pH	Biomass (mg/L)	Incubation Time (Day)
<i>A. platensis</i>	pH 8.5	882.9±277.5	20
<i>C. vulgaris</i>	pH 10.5	469.9±137.8	20
Coccus-type cyanobacteria from Salda Lake	pH 10.5	508±21.6	20

The chlorophyll and carotenoid contents of microalgae are essential for determining their carbon capture capability. Chlorophyll is a pigment central to photosynthesis and provides the ability of microalgae to absorb sunlight, convert CO₂ into biomass, and contribute to the fixation of CO₂ by converting light energy into chemical energy (Gerotto et al., 2020). Carotenoids are essential for light harvesting and energy transfer during photosynthesis; examining their amounts with chlorophyll is critical to converting CO₂ into organic compounds through photosynthesis and to understanding the photosynthetic capacities (Varela et al., 2015). In Table 4.2, the total concentrations of chlorophyll and carotenoids produced by microalgae species at various pH levels are presented. The highest chlorophyll content was observed with *C. reinhardtii* at a pH of 9.5, whereas the lowest chlorophyll content was observed with filamentous-type cyanobacteria at a pH of 10.5. Similar results were observed for carotenoid production. High levels of chlorophyll and carotenoids indicate that microalgae can capture more carbon by absorbing more sunlight. ANOVA analysis has been performed to maintain the relationship between samples, and Pearson correlation has been used to analyze the correlation between pH and chlorophyll and carotenoid contents. As well as total carotenoids and total chlorophyll, the results were examined as a ratio. For filamentous-type cyanobacteria from Salda Lake, there was a positive correlation between the total chlorophyll and

carotenoid content ($r = .888$, $p = .018$). For Spirulina, there was a positive correlation between the total chlorophyll and carotenoid content ($r = .894$, $p = .016$). For *C. reinhardtii*, there was a positive correlation between the total chlorophyll and carotenoid content ($r = .957$, $p = .003$). The carotenoid-to-chlorophyll ratio (Car/Chl), an indicator of carotenogenesis, was also evaluated for each species (Chen et al., 2017). The increase in this ratio for Coccus-type cyanobacteria from Salda Lake can be due to the increase in oxidative stress and the change in photosystem II (PSII) activity and photosynthesis (Polat et al., 2020). As carotenoids can form a protective layer to prevent reactive radicals (Shi et al., 2020), the change in the Car/Chl ratio can be due to the adapted culture of Coccus-type cyanobacteria. The original pH of Lake Salda is between 9 and 9.5, and this species showed the lowest Car/Chl ratio at pH in this range.

Table 4.2 : Total chlorophyll and total carotenoids amount with total carotenoids to total chlorophyll ratio of strains in different pH conditions ($\mu\text{g}/\text{mg}$).

pH	<i>C. reinhardtii</i>	<i>A. platensis</i>	<i>C. vulgaris</i>	Coccus-type cyanobacteria from Salda Lake	Filamentous-type cyanobacteria from Salda Lake
Total chlorophyll, $\mu\text{g}/\text{mg}$					
8.5	2.66 \pm 1.55	3.27 \pm 2.8 ^{a,b}	5.32 \pm 1.37	11.60 \pm 4.36	3.80 \pm 1.81
9	5.26 \pm 3.11	7.15 \pm 2.34 ^{a,b}	6.87 \pm 4.88	8.41 \pm 3.12	4.98 \pm 2.17
9.5	23.58 \pm 0.91	9.14 \pm 2.85 ^b	3.69 \pm 0.65	8.63 \pm 3.20	6.30 \pm 2.84
10	6.47 \pm 3.11	3.78 \pm 2.52 ^b	7.38 \pm 4.03	9.59 \pm 3.66	2.61 \pm 1.19
10.5	5.71 \pm 3.39	4.73 \pm 3.34 ^{a,b}	3.62 \pm 0.92	8.06 \pm 3.08	2.10 \pm 0.93
11	8.49 \pm 4.88	3.64 \pm 0.97 ^{a,b}	7.68 \pm 3.39	9.61 \pm 4.03	2.62 \pm 1.10
Total carotenoids, $\mu\text{g}/\text{mg}$					
8.5	1.40 \pm 1.16	1.13 \pm 0.83	2.52 \pm 0.07 ^{a,b}	4.27 \pm 1.56	2.72 \pm 1.26
9	2.45 \pm 2.34	2.33 \pm 0.69	4.64 \pm 0.77 ^a	3.66 \pm 1.40	3.16 \pm 1.37
9.5	10.66 \pm 2.45	2.60 \pm 0.52	3.33 \pm 0.54 ^{a,b}	4.07 \pm 1.51	3.02 \pm 1.37
10	3.55 \pm 1.81	1.85 \pm 1.35	5.66 \pm 0.84 ^a	3.87 \pm 1.54	2.60 \pm 1.15
10.5	3.39 \pm 3.05	2.06 \pm 0.80	0.66 \pm 0.33 ^b	4.10 \pm 1.57	2.35 \pm 1.03
11	1.85 \pm 0.45	1.35 \pm 0.36	0.79 \pm 0.58 ^b	5.00 \pm 2.10	2.29 \pm 0.96

Table 4.2 (continued) : Total chlorophyll and total carotenoids amount with total carotenoids to total chlorophyll ratio of strains in different pH conditions ($\mu\text{g}/\text{mg}$).

Total carotenoids / Total chlorophyll, w/w					
8.5	0.41 \pm 0.20	0.48 \pm 0.16	0.50 \pm 0.12	0.72 \pm 0.01 ^d	0.37 \pm 0.00 ^e
9	0.31 \pm 0.26	0.33 \pm 0.01	1.2 \pm 0.74	0.63 \pm 0.00 ^e	0.43 \pm 0.01 ^c
9.5	0.45 \pm 0.09	0.30 \pm 0.04	0.9 \pm 0.00	0.48 \pm 0.00 ^f	0.47 \pm 0.00 ^b
10	0.54 \pm 0.02	0.45 \pm 0.06	1.00 \pm 0.43	1.00 \pm 0.01 ^b	0.40 \pm 0.01 ^d
10.5	0.43 \pm 0.28	0.63 \pm 0.28	0.17 \pm 0.05	1.12 \pm 0.01 ^a	0.51 \pm 0.00 ^a
11	0.28 \pm 0.11	0.37 \pm 0.00	0.09 \pm 0.04	0.87 \pm 0.00 ^c	0.52 \pm 0.00 ^a

*means that do not share letters are significantly different

4.1.2 Biochemical Contents

Microalgae capture carbon in the form of proteins, starches, and lipids within their cells (Mondal et al., 2017). Measuring these compounds in microalgae is crucial for assessing their environmental benefits. Determining the amount of carbon converted into biomass is important for evaluating the effectiveness of carbon emission reduction strategies (Lin et al., 2018). As a source of proteins, fats, carbohydrates, and vitamins, microalgae biomass is considered a promising raw material for high-value product recovery. Lipid production performance depends on lipid composition and productivity, which is the amount of lipid produced per liter of working volume per day (Udayan et al., 2022). Under stress conditions, oils tend to accumulate in microalgal cells, reducing their growth rate, which is significant when focusing on lipid production.

Figure 4.2 shows the changes in the lipid, protein, and carbohydrate contents of each species. The variation in these contents under different pH conditions reflects the cells' adaptation mechanisms to environmental stress and the reorganization of their metabolic pathways (Sun et al., 2018). High pH conditions cause cells to alter their energy and resource use to survive and grow. pH levels can affect all biochemical processes in algae cells, including protein synthesis and carbohydrate and lipid metabolism (Xia et al., 2015). For *C. reinhardtii*, there was a positive correlation between pH and lipid content ($r = .781$, $p = .038$). For *Spirulina*, there was a negative correlation between pH and protein content ($r = -.878$, $p = .009$) and between pH and lipid content ($r = -.841$, $p = .018$). In Salda Lake coccus-type cyanobacteria, there was

a tendency to accumulate carbohydrates with increasing pH, as pH changes can affect the photosynthesis rate of microalgae, leading to increased carbohydrate production due to higher photosynthesis rates (Cheng et al., 2022).

C. vulgaris had the highest protein content at pH 9, but the highest lipid and carbohydrate contents at pH 11, indicating defense mechanisms against pH stress, observed by decreased protein and increased lipid and carbohydrate stores (Gauthier et al., 2020). Filamentous-type cyanobacteria from Salda Lake showed no significant changes in these molecules. Previous studies showed *Chlorella* sp. achieved the highest lipid yield (167.5 mg/L) at pH 7.0 (Zhang et al., 2014). It was found that *C. vulgaris* accumulated 49% carbohydrates at pH 8, with a carbohydrate content ranging from 16 to 44% of dry cell weight (Cheng et al., 2022). Another study found that *Spirulina* accumulates lipids and proteins between pH 8 and 10 (Mufidatun et al., 2023). *C. reinhardtii* showed 30% lipid accumulation at pH 9.5 in previous studies, while our study observed over 25% at that pH (Zheng et al., 2022).

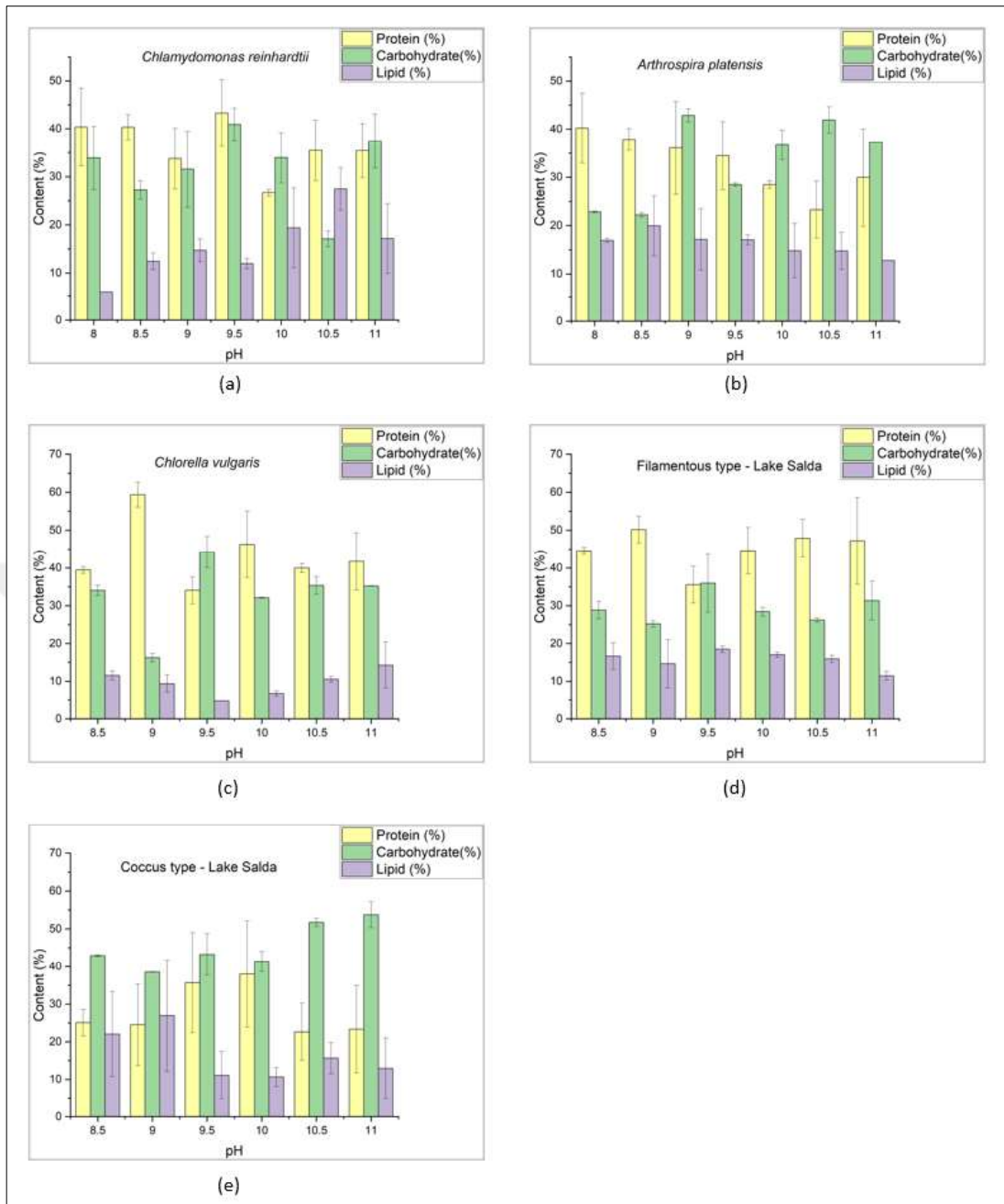


Figure 4.2 : The protein-lipid and carbohydrate contents of the cultures: (a) *Chlamydomonas reinhardtii*, (b) *Arthrosphaera platensis*, (c) *Chlorella vulgaris*, (d) Filamentous-type cyanobacteria from Salda Lake, (e) Coccus-type cyanobacteria from Lake Salda.

4.1.3 Amino acids contents

Amino acid content is important to be measured to investigate the potential of cultivated microalgae biomass as a protein source for humans, farm animals, or farmed fish (Michelon et al., 2021). So, the amino acid contents of different species and pHs have been defined with HCA analysis. Amino acid data were obtained, and

HCA analysis with dendrograms was shown in Figure 4.3. Dendrograms are tree structures that demonstrate similarities and differences between clusters based on hierarchical clustering. The length of branches reflects the differences between clusters, while the length of branches represents the similarities between clusters. Clusters with short branches have a high degree of similarity, while clusters with long branches have a low degree of similarity. Additionally, positive and negative values obtained from Euclidean geometry indicate that the data set is similar or different. Euclidean geometry calculates the distance between two points represented by straight lines. By using the mean and standard deviation for each data point, normalized data (z-scores) allow the distribution of data points to be standardized. When the Z-score is positive (e.g., 1.11), the data point is deemed to be above the mean. The data point falls below the mean when Z-Scores are negative (e.g., -2.22). By the time coccus-type cyanobacteria from Salda Lake, filamentous-type cyanobacteria from Salda Lake and *C. vulgaris* at different growth pHs (8–11), *C. reinhardtii* at pHs of 8, 9, and 10.5, and Spirulina at pH of 10.5, do not share the lines it has with other pH values within its group, they are not closely related. Considering the protein composition, the biomass of species grown at alkaline pH can be recovered, and this can provide a cost-effective biorefinery.

Glutamic acid, tyrosine, and valine are the most abundant amino acids for all species, whereas valine is also counted as essential. There is good agreement between the results of this study and those of previous studies (Andreeva et al., 2021). Glutamic acid is also the most abundant amino acid in Cyanobacteria, Plantae, Cryptophyta, and Bacillariophyta (Leon-Vaz et al., 2023). In the form of glutamate, it acts as an important neurotransmitter in the central nervous system and is involved in ammonia assimilation (Ingrisano et al., 2023). The results show that amino acid distribution varies in different pH environments. pH is a key factor affecting the activity of enzymes in the cell. Each enzyme works most efficiently in its optimum pH range. The activity of enzymes involved in the synthesis and degradation of amino acids may differ at different pH levels, affecting the composition of amino acids. On the other hand, amino acid concentrations of coccus-type species from Lake Salda were found to be significantly different.

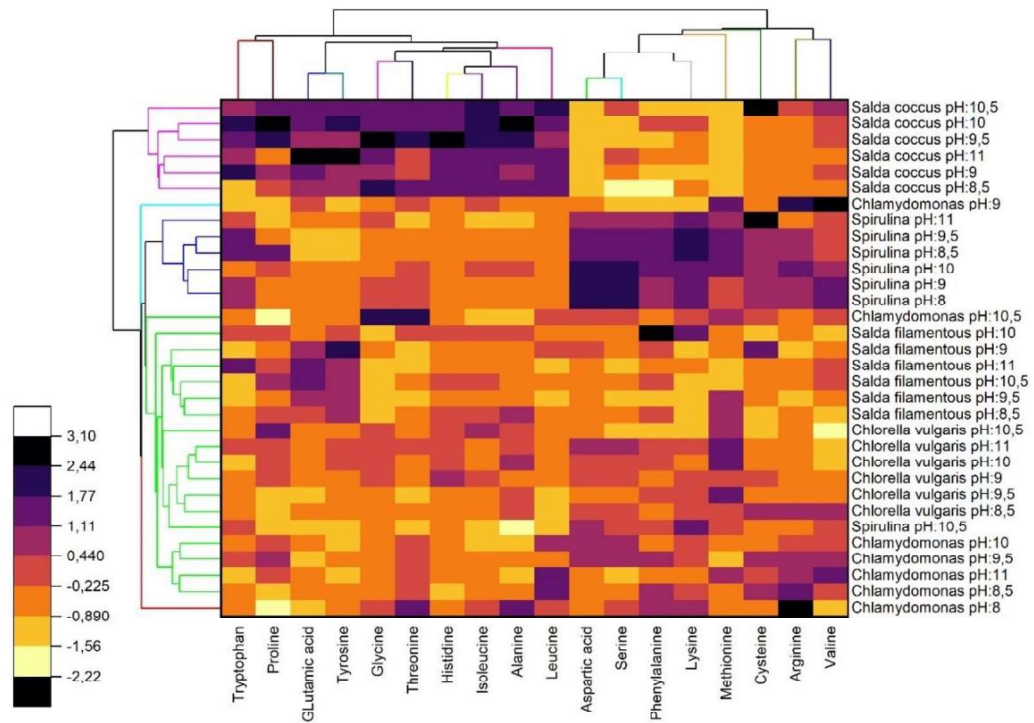


Figure 4.3 : Heat map of the amino acid measurements.

Tryptophane, serine, glycine, and cystine existed less than others. For coccus-type cyanobacteria from Salda Lake, there was a positive correlation between the total phenylalanine content and amino acid amount ($r = .834$, $p = .039$). For filamentous-type cyanobacteria from Salda Lake, there was a positive correlation between the total chlorophyll and glutamic acid content ($r = .891$, $p = .017$). In high concentrations of glutamic acid, chlorophyll biosynthesis is supported, which results in greater photosynthetic efficiency. The reason for this correlation is that glutamate is the essential precursor used to synthesize protoporphyrin IX, which is a structural component of chlorophyll (Weinstein & Castelfranco, 1977). For *Spirulina*, there was a positive correlation between the total amino acid amount and lysine content ($r = .951$, $p = .001$); leucine content ($r = .984$, $p = .000$); and methionine content ($r = .916$, $p = .004$). Curiously, there was a negative correlation for *Spirulina* between tryptophan content and carbohydrate content ($r = -.757$, $p = .049$). This situation can be explained by using carbohydrates as an energy source in cells. It is possible that carbohydrates contributed to synthesizing amino acids such as tryptophan by limiting tryptophan degradation (Gao et al., 2019). It may also indicate that the synthesis of other precursor molecules (serotonin) related to metabolic activity is promoted

(Correa & Vale, 2022). For *C. reinhardtii*, there was a positive correlation between the total amino acid and glutamic acid content ($r = .893$, $p = .007$).

4.1.4 Fatty Acid Methyl Ester Contents

An important source of essential and bioactive lipids is microalgal biomass. As microalgae are quite diverse in terms of their size and diversity, they possess lots of potential, as some of them are the main sources of omega-3 fatty acids (FA) and are the main producers of nutrients that can be used to replace fish oils (Conde et al., 2021). It is important to note that microalgae provide essential FAs that can be metabolized by mammals into eicosapentaenoic acid (C20:5 ω -3; EPA) and docosahexaenoic acid (C22:6 ω -3; DHA) (Conde et al., 2021). Many studies discuss the saturated fatty acid (SFA), monounsaturated fatty acid (MUFA), and polyunsaturated fatty acid (PUFA) contents of microalgae under different growth conditions. This study investigates how FA contents change under alkaline pH conditions.

In this study, except for coccus-type cyanobacteria from Salda Lake grown at a pH of 8.5, all microalgae species contain saturated fatty acids exceeding 60% of total FA (Figure 4.4). Statistical significance has been considered when analyzing the change in FA type. Compared to previous studies, the unsaturated fatty acid/total fatty acid (UFA/TFA) ratio of autotrophic *C. vulgaris* cultured in BG-11 was lower, except for the pH of 9.5 culture. In a study with a CA complex added to *C. vulgaris*, due to the influence of the CA complex, SFA content decreased from 35.8% to 15.6%, while UFA content increased from 64.2% to 84.4% in a BBM medium. The higher SFAs in our study can be attributed to differences in growth medium and cultivation conditions.

Additionally, previous studies with *Spirulina* have shown 45-56 % SFA (Ennaji et al., 2021). But, in this study, the SFA content of *Spirulina* was approximately 70% for all pH treatments. As well, *C. reinhardtii* showed 28% SFA accumulation under the TAP medium (Zhu et al., 2021). For *C. reinhardtii*, there was a negative correlation between the PUFA and SFA content ($r = -.783$, $p = .037$). As a result, this provides essential information regarding the culture's energy storage strategies under alkaline stress conditions.

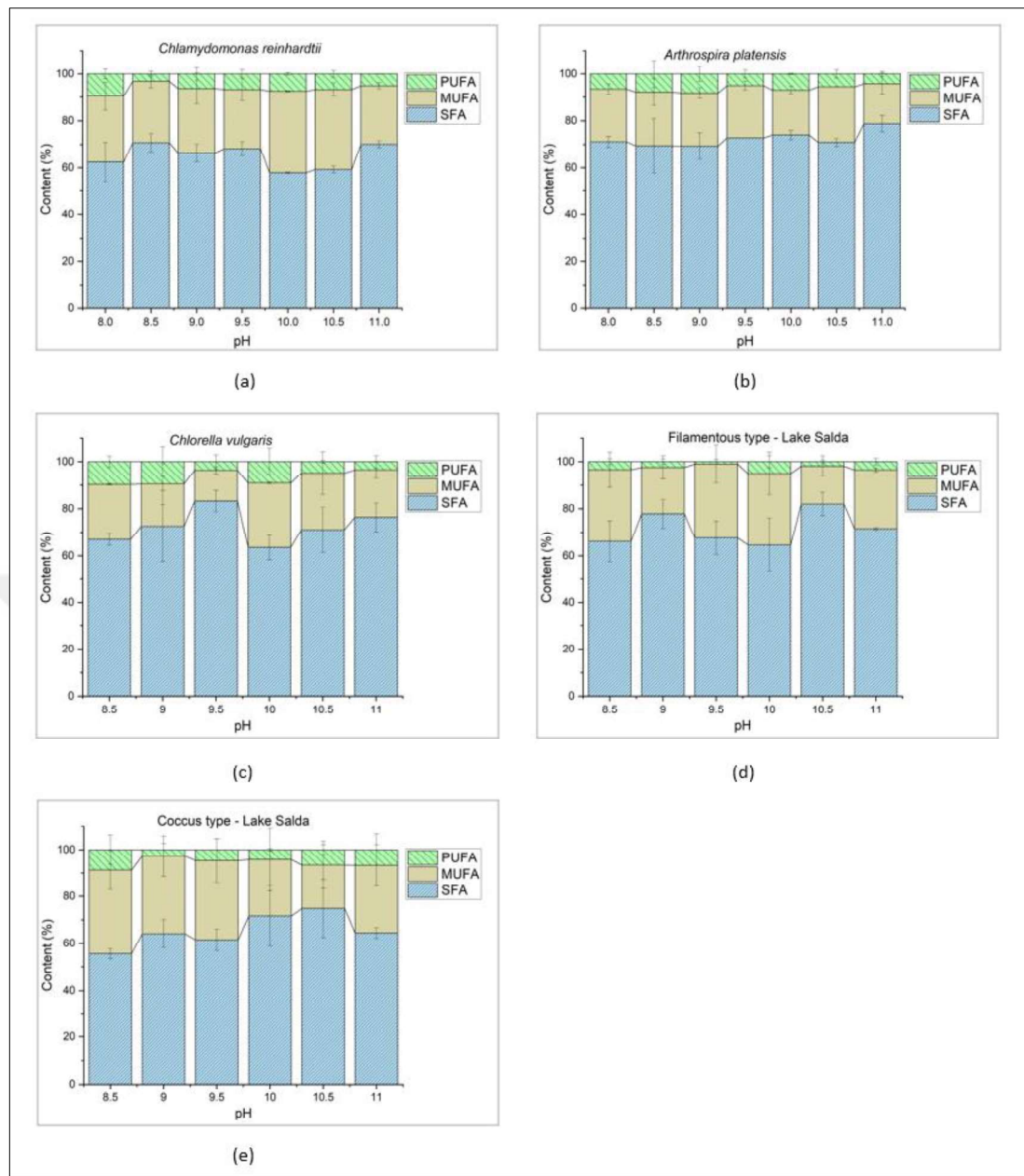


Figure 4.4 : SFA, MUFA and PUFA contents of the cultures changing with pHs: (a) *Chlamydomonas reinhardtii*, (b) *Arthrospira platensis*, (c) *Chlorella vulgaris*, (d) Filamentous-type cyanobacteria from Salda Lake, (e) Coccus-type cyanobacteria from Lake Salda.

The detailed C16-C18 contents of the FAMEs are shown in Figure 4.5. The results obtained from this study will provide information about which microalgae species and pH conditions are suitable for extracting lipids for biodiesel or food. Microalgae species FA values must be interpreted following biodiesel standards if they are to be used for bioenergy and carbon capture. In this study, most of the species had PUFA

values lower than 10%, suggesting that the use of these species in lipid production may also be a crucial biomass valorization stage (Hawrot-Paw et al., 2021).

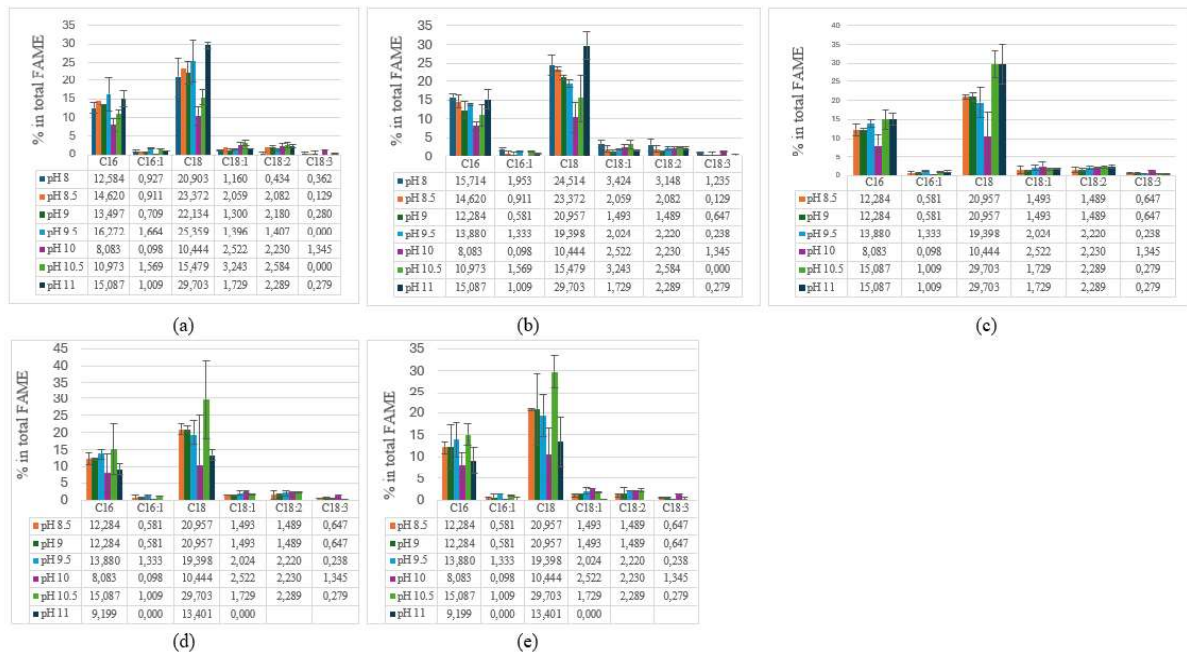


Figure 4.5 : C16-C18 contents of the FAMEs (a) *C. reinhardtii*, (b) *S. Platensis* (c) *C. vulgaris*, (d) Coccus-type cyanobacteria, (e) Filamentous-type cyanobacteria.

4.1.5 Carbonic anhydrase enzyme activity

Carbon fixation performance in microalgae photosynthesis can be evaluated by considering carbonic anhydrase (CA) activity (Yao et al., 2024). Carbonic anhydrase accelerates the conversion of CO₂ into HCO₃⁻ ions. It thus allows microalgae to capture more carbon and convert it into biomass, and for this purpose, CA activity in varied species and pH conditions was investigated in this study. According to the analyses, all species and strains of algae have carbonic anhydrase activity ranging from 0.10 to 3.60 mU/mg dry matter, depending on strain and cultivation conditions. Minimum enzyme activity was previously observed in *C. reinhardtii* under laboratory conditions grown in glass vessels. According to our measurements, *C. reinhardtii* showed carbonic anhydrase activity between 2.31 to 4.68 mU/mg biomass, and the highest activity was observed under a pH of 10 (Table 4). This organism grows photosynthetically using CO₂ or, when in the dark, using acetate as the carbon source. In the light, the CO₂ concentrating mechanism (CCM) of *C. reinhardtii* accumulates CO₂, enhancing photosynthesis.

Carbonic anhydrases (CAs) and bicarbonate transporters in the chloroplast pyrenoid of *C. reinhardtii* increase the concentration of CO₂ at Ribulose 1,5-bisphosphate carboxylase oxygenase (RuBisCO) (Rai et al., 2021).

The results of carbonic anhydrase enzyme activity in Spirulina are consistent with previous studies. For instance, Spirulina has been reported to have high bicarbonate utilization efficiency and strong CA activity (Zhang et al., 2023). According to a similar study, the maximum CA activity of Spirulina cultures was 6.2-8.7 mU/mg using the freeze-thaw method, while 2.5 mU/mg was obtained with homogenization (Ores et al., 2016). Among our results, the highest activity was 4.51 at pH 9. The difference can be attributed to extraction methods and cultivation conditions. CA activity was 2.38-3.40 mU/mg in *C. vulgaris*. The results of this study differ from those of previous studies in some aspects. *C. vulgaris* showed a maximum specific activity of 17 mU/mg after 37 days of cultivation in the BG11 medium. The difference might be attributed to the CA extraction method, which ultrasonic treatment used. Comparing CA activities with other results yields important outcomes. For *C. vulgaris*, there was a positive correlation between total amino acid amount and CA activity ($r = .897$, $p = .015$). Interestingly, for Spirulina, there was a positive correlation between isoleucine content and CA activity ($r = .931$, $p = .002$). Coccus-type cyanobacteria from Salda Lake showed varying levels of carbonic anhydrase activity, with the lowest activity at pH 11 and the highest at pH 9. A previous study of the properties and function of carbonic anhydrase enzymes involved in microalgae's carbon metabolism was conducted to determine how the activity of various forms of such enzyme varies in response to CO₂ and nitrogen concentrations, and it was shown that CA activity is in the range of 0.10-3.60 per mg.

In a previous study, *Bacillus mucilaginosus* was used as a microorganism, maximum cultivation was observed when the pH was 9–10, and biotic CaCO₃ was successfully obtained by this microorganism (Zheng, 2021). The formation of CaCO₃ in co-culture systems involving microalgae may have a positive impact on carbon sequestration. Using carbonic anhydrase enzyme-producing bacteria might be logical for further research.

Stromatolites like those existing in Lake Salda, Lake Michigan, and the Great Bahama Bank are CaCO_3 formations caused by collaborative actions by microalgae and bacteria (Frantz et al., 2015). It is, so, possible to achieve better results for CaCO_3 precipitation by not only growing microalgae monocultures but also growing co-cultures of microalgae and bacteria.

Table 4.3 : Carbonic Anhydrase enzyme activity per biomass in different pH conditions (mU/mg biomass).

pH	<i>C. reinhardtii</i>	<i>A. platensis</i>	<i>C. vulgaris</i>	Coccus-type cyanobacteria from Salda Lake	Filamentous-type cyanobacteria from Salda Lake
8.5	3.25±0.12	3.66±0.07	2.39±0.33	3.24±0.58	2.35±0.45
9	4.32±1.36	4.51±0.76	2.85±0.34	4.44±0.04	2.11±0.08
9.5	3.92±0.22	1.79±0.29	2.38±0.44	2.95±1.70	2.02±0.60
10	4.68±0.42	2.02±0.28	2.46±0.75	2.19±0.68	1.87±0.28
10.5	3.61±1.63	2.89±0.49	3.40±1.22	2.83±0.18	2.43±0.32
11	2.31±0.16	3.10±0.42	2.88±0.95	1.89±0.26	2.24±0.55

4.2 Principal Component Analysis to Evaluate the Results

One of the most popular ways to analyze multivariate data is by performing principal component analysis (PCA). PCA extracts fundamental information from the input data into new orthogonal variables, known as principal components, and then analyzes them as a multivariate result (Destanoğlu, 2022). As PC1 represents the greatest degree of variability in the data, PC2 represents the second highest degree of variability. This allows for the discovery of previously unknown relationships between samples. Over the last few years, numerous PCA studies have evaluated biomass and metabolites, as well as the biostimulatory effects of microalgae (Rugnini et al., 2022). The data points of this study are projected as sample projections in Figure 4.6.

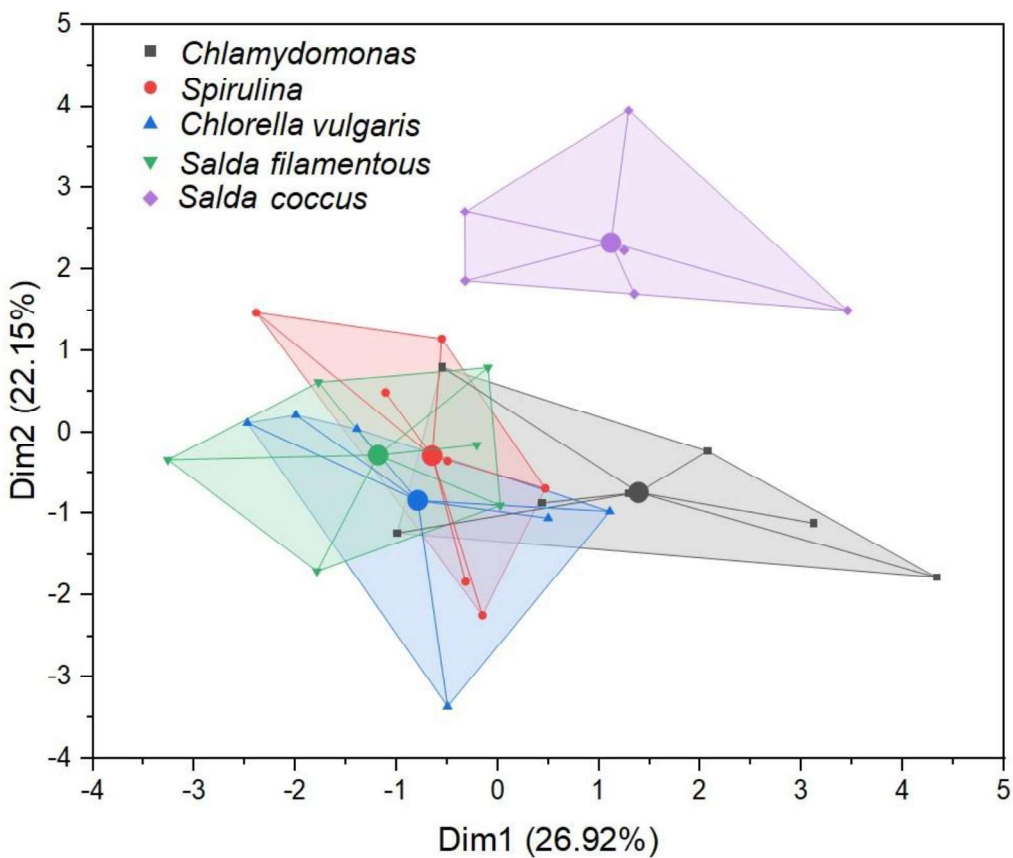


Figure 4.6 : Principal component analysis (PCA). Sample projection of *Chlamydomonas reinhardtii*, *Arthrospira platensis* (*Spirulina*), *Chlorella vulgaris*, Filamentous-type cyanobacteria from Salda Lake (*Salda filamentous*), Coccus-type cyanobacteria from Salda Lake (*Salda coccus*).

In this analysis, the data set was represented in a bivariate plot as a result of principal component analysis. Based on the overall data, it has been determined that the two principal axes, PC1 and PC2, account for 49.07% of the variance (26.92% and 22.15%, respectively) (Figure 4.7). The data set should be considered in light of other components that explain a greater portion of the variance. With 67.12% of the cumulative covariance percentage, a 3D PCA was constructed. Consequently, 3D PCA has been used to analyze the PCA of each strain individually.

In the case of *C. reinhardtii*, PCA plots of PC1 versus PC2 explained 28.28% and 40.26% of the total variance, respectively. Since PC1 and PC2 are responsible for only 68.54% of total variance, other factors shall be examined to explain a higher proportion of variance. Therefore, a 3D PCA was constructed based on 81.23% of the cumulative covariance percentage. As noted, pH, CA activity, MUFA, total AAs, and lipids are negatively correlated with the first component.

The cumulative percentage of covariance of *C. vulgaris* was found to be 82.38% by using 3D PCA plotting. The first component of *C. vulgaris* has a positive correlation with protein, MUFA, PUFA, total chlorophyll, and total carotenoids. In the case of Spirulina, the cumulative percentage of covariance was found to be 83.53% on a 3D PCA plot. A negative correlation exists between the first component of Spirulina and pH, SFAs, total AA, and carbohydrates.

According to PCA plotting of PC1 versus PC2 for filamentous-type cyanobacteria from Salda Lake, PC1 explained 42.91% and PC2 explained 30.90% of the total variance, respectively. Considering that PC1 and PC2 account for only 73.81% of the total variance, it is essential to identify other factors that may account for additional variance. Thus, a three-dimensional PCA was constructed based on 91.14% of the cumulative covariance percentage. A positive association exists between the first component and MUFA, CA activity, total chlorophyll, total carotenoids, carbohydrates, and lipids. In addition, 87.85% of the cumulative percentage of covariance was found for coccus-type cyanobacteria from Salda Lake using 3D PCA. All of these variables are positively correlated with the first component, including pH, PUFA, total AA, CA activity, total carotenoids, and carbohydrates.

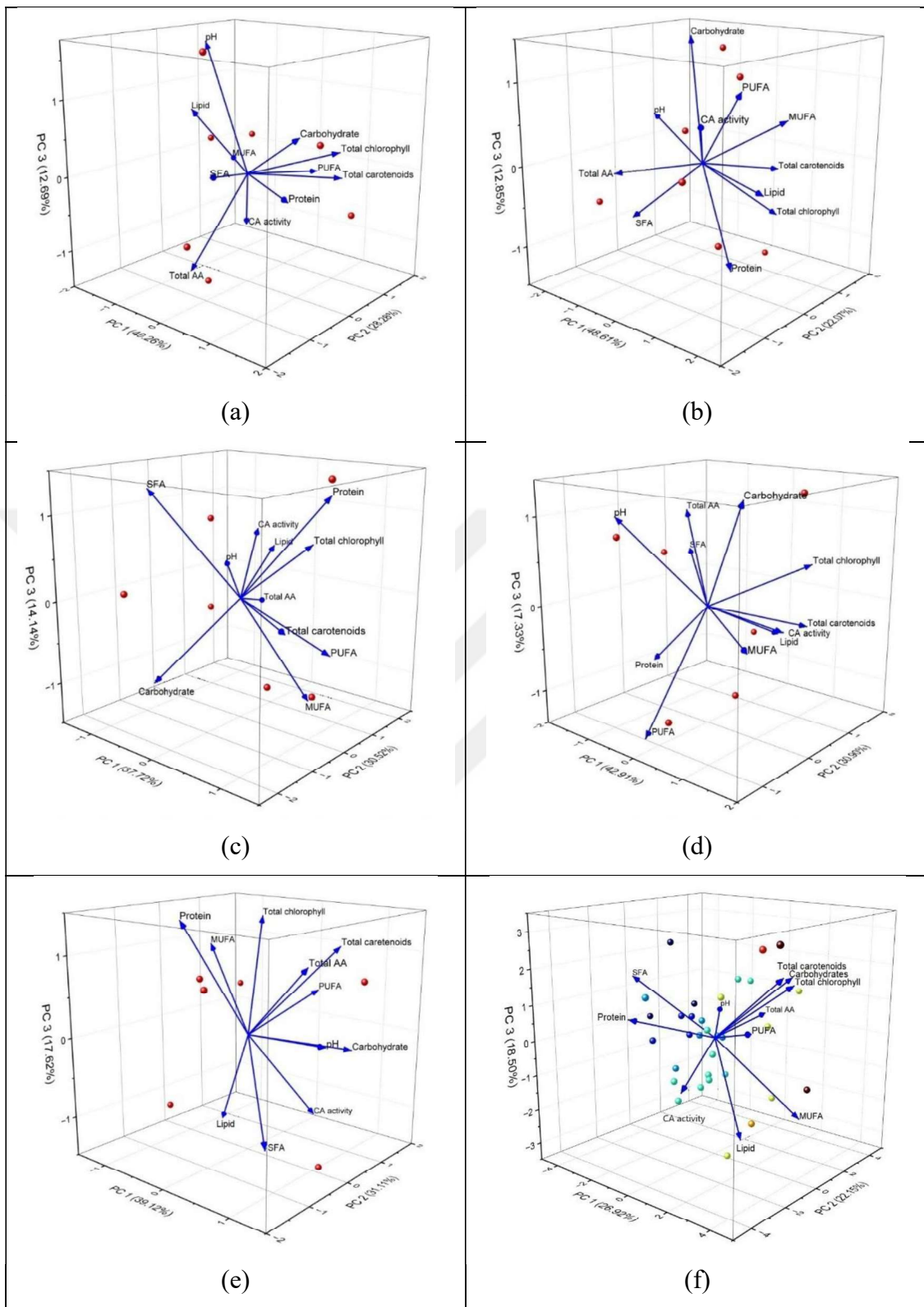


Figure 4.7 : 3D PCA plot of (a) *Chlamydomonas reinhardtii*, (b) *Arthrospira platensis* (*Spirulina*), (c) *Chlorella vulgaris*, (d) Filamentous-type cyanobacteria from Salda Lake (Salda filamentous), (e) Coccus-type cyanobacteria from Salda Lake (*Salda coccus*) and (f) overall data.

4.3 Analytic Hierarchy Process Method to Determine Algae Species

Analytic Hierarchy Process (AHP) is a method used in decision-making, especially in complex and multi-criteria decision problems, allowing the determination of the importance levels of preferences or criteria between different options. This method performs comparative analysis to make systematic and consistent decisions, calculating the relative weight of each option or criterion as a result of this analysis. The multiple data obtained from our lab experiments point out that the most effective microalgae type cannot be easily declared. On the other hand, with the Analytic Hierarchy Process (AHP) method, all the parameters and their values can be defined. The main parameters were determined by growth rate, pigment content, enzyme activity, and persistency against impurities. Concentration, cultivation time, and media type were selected as subparameters of growth rate. Lastly, chlorophyll and carotenoids were selected as subparameters of pigment content.

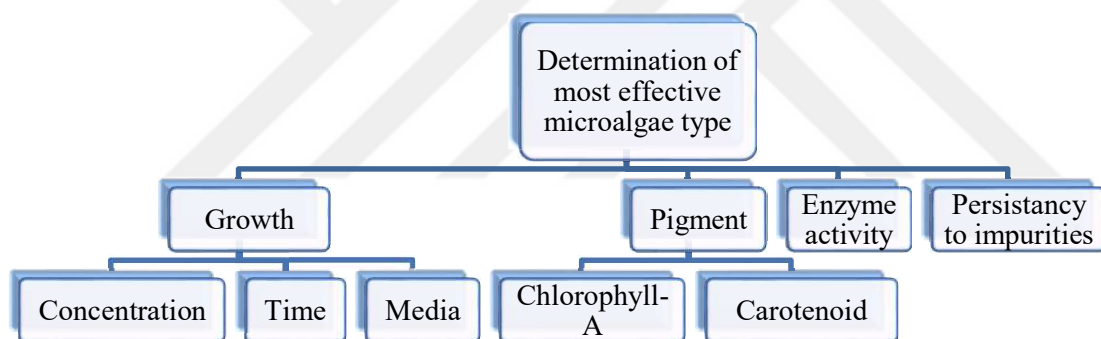


Figure 4.8 : Hierarchy of the Criteria.

After determining the parameters, matrixes were produced, and each parameter could be compared individually by assigning coefficients. Then each alternative species' scores were determined and multiplied by their importance coefficient. For score inputs, actual experiment results were used. The actual values have been scaled accordingly since the scale ranges from 1 to 10. Media and persistence to impurities data were only the ones determined by knowledge. According to the AHP method, *A. platensis* obtained the highest score, and *C. vulgaris* came in second. Cultures from Lake Salda had the lowest scores, so they will not be included in further experiments.

Table 4.4 : Selection of microalgae species for carbon capture using the AHP method.

FACTOR	<i>C. reinhardtii</i>	<i>A. platensis</i>	<i>C. vulgaris</i>	Filamentous-type cyanobacteria from Salda Lake	Coccus-type cyanobacteria from Salda Lake	Importance Score Multiplier
Concentration	4.2	9.85	2.14	1.25	4.18	0.21
Time	10	1.39	2.5	3.57	1.47	0.1
Media	2	7	7	7	7	0.22
Total chlorophyll	9.43	1.31	1.45	1.05	3.22	0.07
Total carotenoids	9.69	1.03	0.6	2.08	3.73	0.03
Enzyme activity	8.23	7.69	7.14	3.97	5.1	0.13
Persistency to impurities	5	6	10	4	4	0.24
TOTAL SCORE	5.53	6.31	5.71	3.79	4.54	

4.4 Coculture Experiments with Algae and Bacteria

The first attempt was carried out via 50 ml flasks. Despite the shaking speed and the light intensity were applied as planned in the beginning of the experiment, the temperature was increased to higher than 40°C degrees unpredictably. The experiment ended due to early decay phase of the algae species. The change in color can be seen in Figure 4.9. pH was decreased similarly in all flasks to around 9.5.

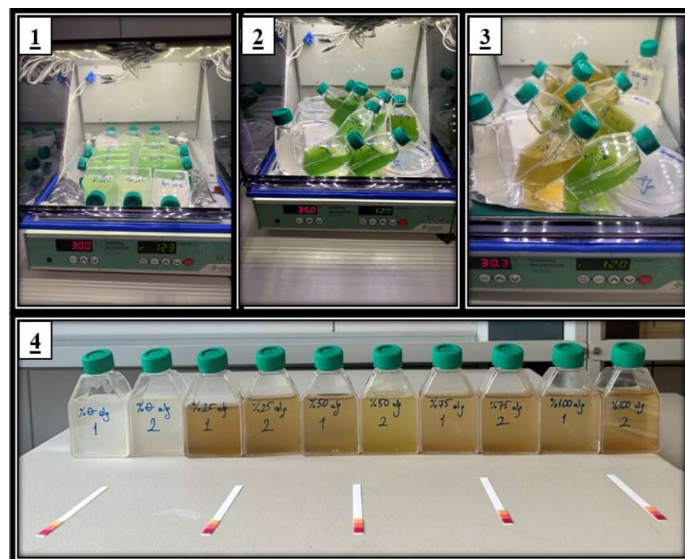


Figure 4.9 : Coculture experiment set (first attempt with failure end). (1) Picture from day 0, (2) Picture from day 1, (3) Picture from Day 2, (4) Picture from Day 3.

4.4.1 Growth, total chlorophyll and carotenoid

However the first attempt was failed due to high temperatures, growing conditions were controlled much more adequately in the second attempt. The cover of the shaker didn't closed completely and the air let in for the cooling. Also heater was remained turn off position, the only heat source were the LED lights. The growing phase lasted in 12th day and Figure 4.10 represents the picure from that day.

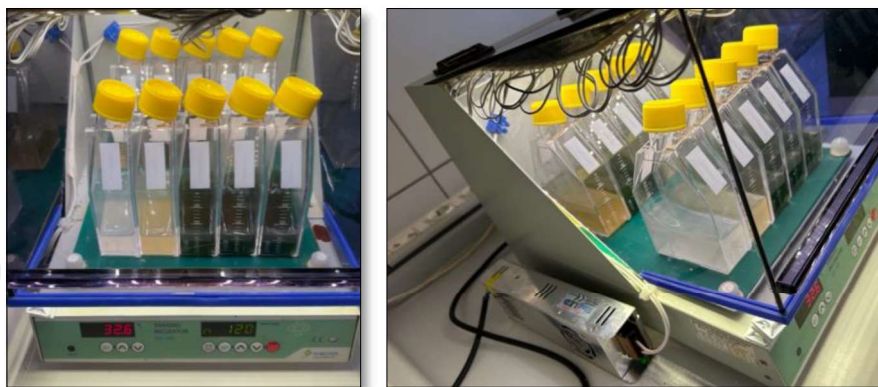


Figure 4.10 : Coculture experiment setup (second attempt) - photos from the 12th day.

In order to obtain 6 point and 5 point calibration curves for algae and bacteria biomass concentration calculations respectively, TSS analysis was carried out. Calibration curve for algae with OD₆₈₀ is given Figure 4.11 and for bacteria with OD₆₀₀ is given in Figure 4.12. By the higher R² value of bacteria's curve, it was applied to optical density measurements by time.

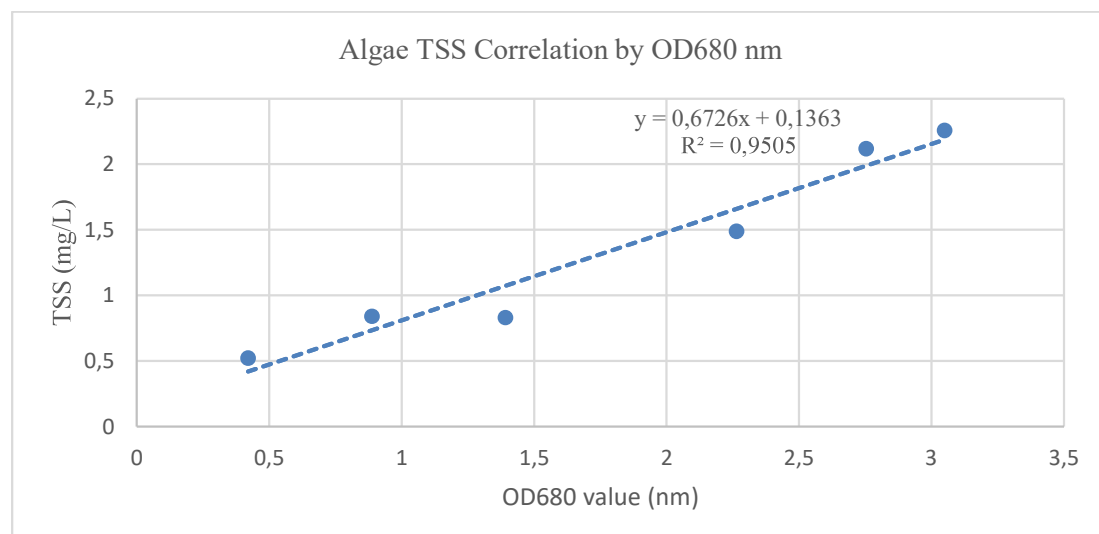


Figure 4.11 : Algae TSS correlation graphic by OD₆₈₀ nm.

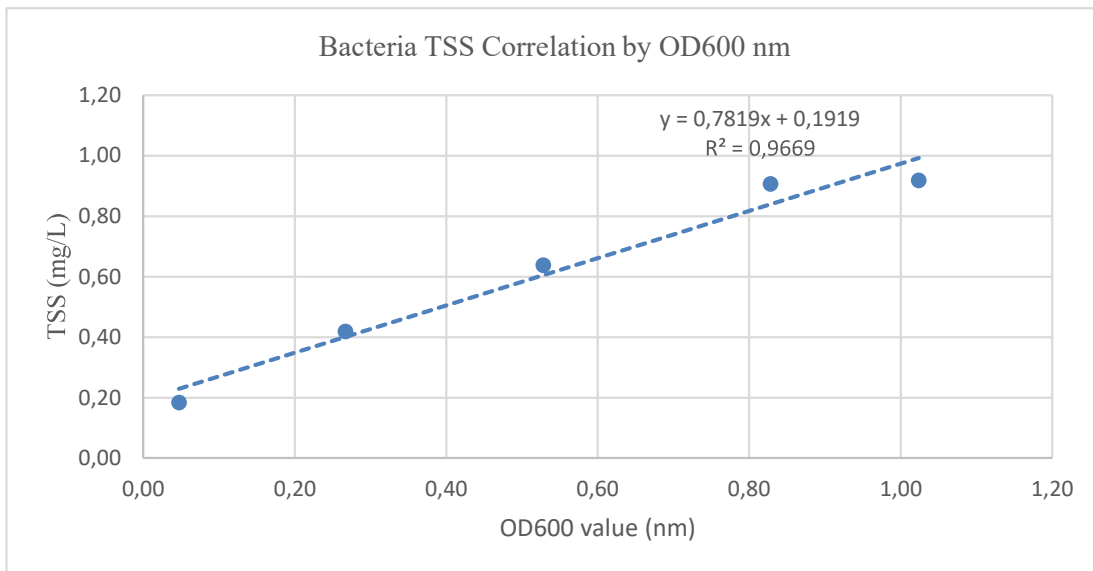


Figure 4.12 : Bacteria TSS correlation graphic by OD₆₀₀ nm.

There was no considerable growth observed in 100% bacteria and 75% bacteria-25% algae medias. On the other hand, biomass concentrations were measured almost the same for the 50%, 75% and 100% algae medias such as 2.328 mg/L, 2.325 mg/L, 2.345 mg/L respectively. It can be examined in Figure 4.13. It was 2.200 mg/L in 36 days during the monoculture experiments and the highest growth rates were achieved by this experiment thanks to improved growing conditions. Coculture growth rates are great for 50% and 75% algae flasks, however monoculture's growth rate is great too. So further experiments were conducted to make a comprehensive decision.

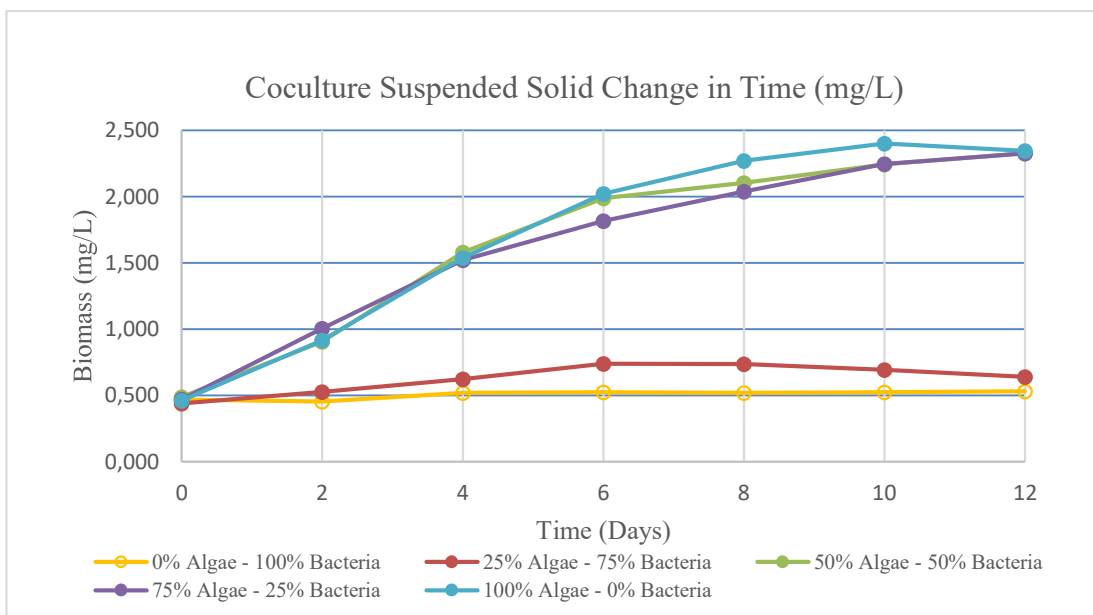


Figure 4.13 : Coculture suspended solid change in time (mg/L).

After measuring the total chlorophyll and carotenoid contents of individual sample, 50%, 75% and 100% algae media samples represented these pigments. As the 25% algae sample's color was yellow and 0% algae sample's color was white, it can be clearly claimed that there are no pigments such as chlorophyll and carotenoids. In Figure 4.14, due to measuring method it looks like the pigments exist; however, they need to be neglected.

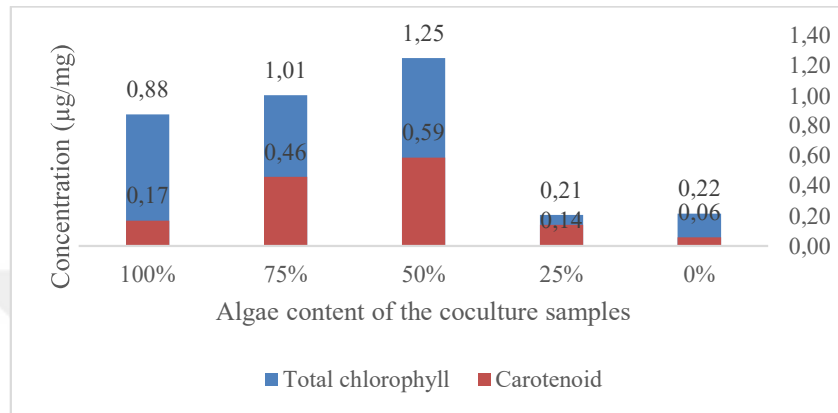


Figure 4.14 : Total chlorophyll and carotenoid pigment contents in different IVRs.

4.4.2 EPS analysis result

EPS was analyzed as both fixed, soluble and total. Like the pigment analysis experiment's results, 100%, 75% and 50% algae samples contain EPS considerably high against to 25% and 0% of algae samples. In all of the samples soluble EPS appears 10 times higher than the fixed EPS.

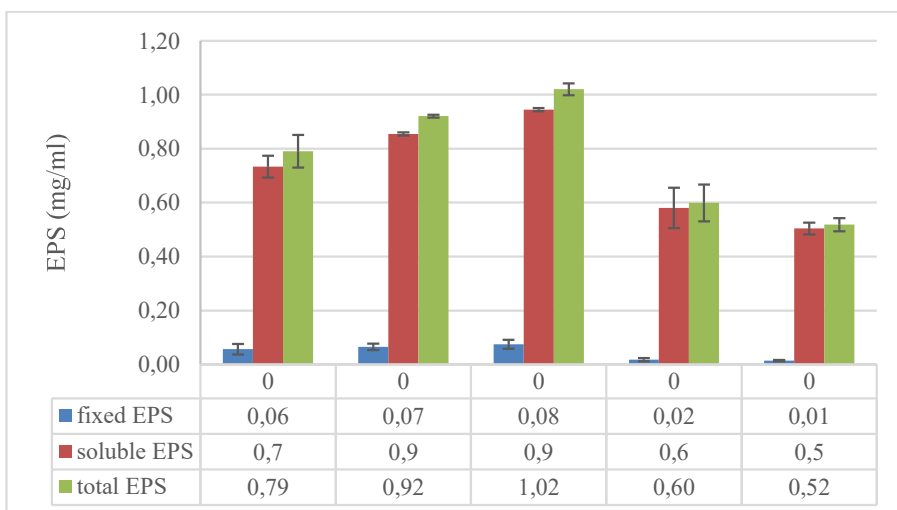


Figure 4.15 : EPS results of different IVRs such as; (1) 100% algae, (2) 75% algae-25% bacteria, (3) 50% algae-50% bacteria, (4) 25% algae-75% bacteria, 100% bacteria.

EPS are promising in biotechnology due to their structures and properties and are used in industries (Sutherland, 2001; Poli et al., 2010; Lordan et al., 2011; Raza et al., 2012). Although the polysaccharide yield in microalgae is lower than in bacteria and fungi, the composition of algal EPS gains importance with its different properties from other polysaccharides (Angelaalincy et al., 2017). FTIR technique can be used to monitor changes in biomass composition of organic compounds such as carbohydrates, lipids and proteins (Bartošová et al., 2015). FTIR spectrum shows the distribution of macromolecules; lipid band (approximately 1740 cm^{-1}), amide I and amide II bands representing proteins (approximately 1660 and approximately 1540 cm^{-1}) and carbohydrate region (1200–900 cm^{-1}) (Bartošová et al., 2015). When the FTIR spectra of EPS from monocultures and cocultures are examined in terms of molecular components, bonding types and functional groups, it is seen that there are significant differences between bacterial monoculture and algae monoculture.

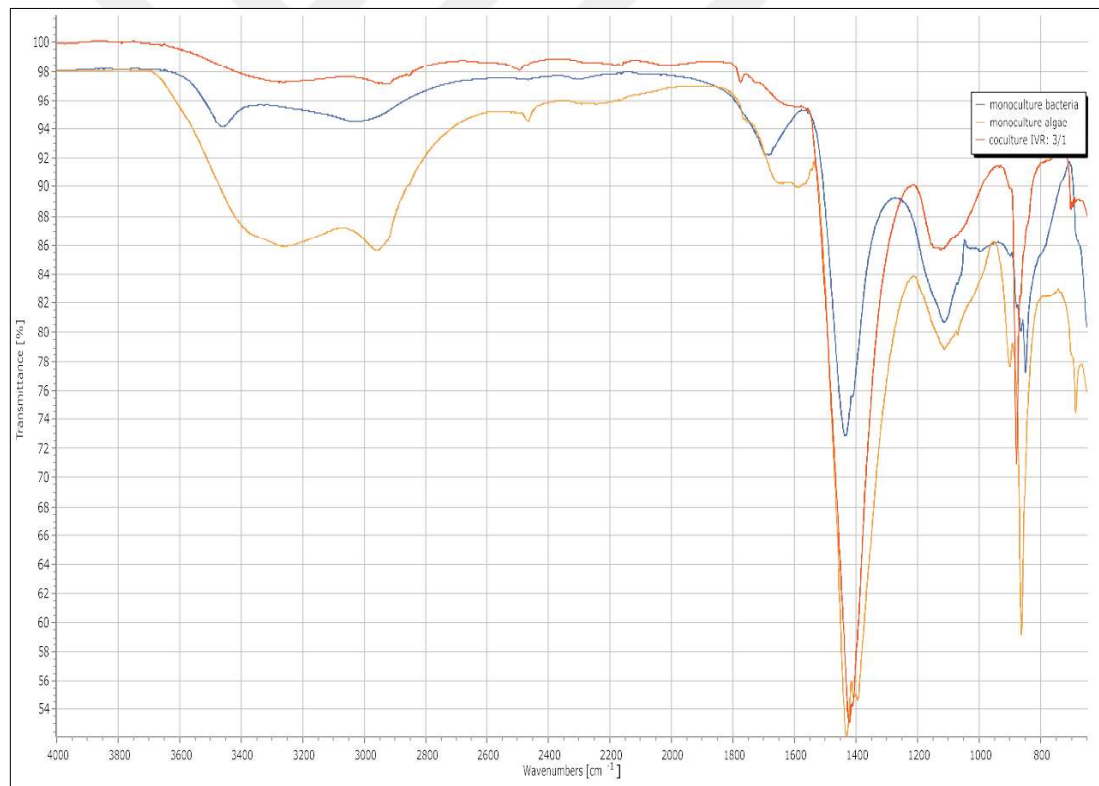


Figure 4.16 : FTIR analysis of EPS samples.

EDS is used during SEM analysis and helps determine the chemical composition of EPS. The basic elements (such as C, O, N, P, S) contained in EPS can be detected. This provides an understanding of the organic and inorganic components of EPS.

The detection of heavy metals or trace elements contained in EPS is important in processes such as bioremediation or biosorption.

Table 4.5 : Band assignments for FTIR of EPS.

Peak (cm ⁻¹)	Functional group	Macromolecule	Peak
688	C–H out of plane	EPS, ribose aromatic	Algae monoculture, coculture
851	Bending –C=O	Inorganic carbonate	Bacteria monoculture
861			Algae monoculture
873			Coculture
1116	νC–O–C/νP=O, νC–O–C	Carbohydrate	Algae monoculture > Bacteria monoculture > Coculture
1420	δas(CH ₂),δas(CH ₃) CH aliphatic CH ₂ , CH ₃	Protein, Lipid	Algae monoculture = Coculture > Bacteria monoculture
1582	δ(N–H), ν(C–N) amide I	Protein	Algae monoculture > Bacteria monoculture > Coculture
2953	νC=O	Lipid	Algae monoculture
3000-3600	O–H	Water stretching	Algae monoculture, Bacteria monoculture, Coculture

•ν = symmetric stretching, νas = asymmetrical stretching, δ = symmetric deformation, δas = asymmetrical deformation, WN= wavenumber

As a result of EDS analysis, elements such as sodium (Na), carbon (C), oxygen (O), sulfur (S) and potassium (K) were observed. However, In the study of (Cheah et al., 2022), metal cations such as Cu, Pb, Zn, Cd and Cr were also detected by EDS and this situation can be explained by the biosorption of metals. Potassium (K) plays an important role in cells of bacteria, especially in activating enzymes and enzyme transport systems and is known to play a role in metal bioaccumulation and can be an indicator of enzyme activities in microbial culture. Sodium (Na) detected in our EPS sample is also found in high amounts in the study (Thakur & Yadav, 2024). This situation was explained by EPS retaining sodium etc. ions as an indicator of the increase in environmental salinity.

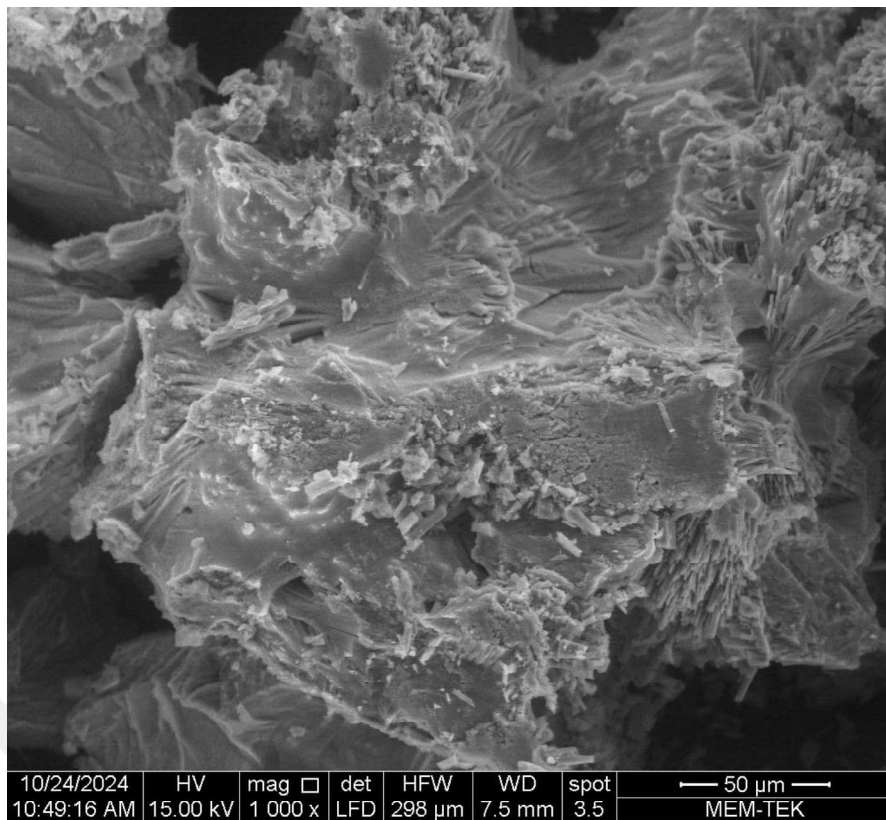


Figure 4.17 : SEM image of EPS.

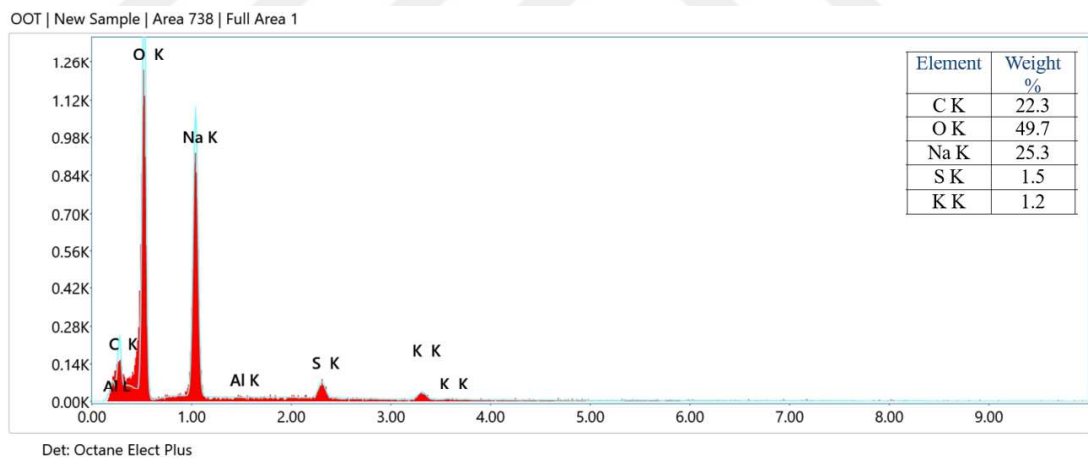


Figure 4.18 : EDS spectrum of mineralized products of EPS.

4.4.3 CA enzyme activity results

Before analyzing the kinetics of CA enzyme activity, standard solution was prepared and read in 2 different wavelengths such as $348\text{ }\lambda$ and $405\text{ }\lambda$. Standard solution's characteristic wavelength was illuminated as $348\text{ }\lambda$ in terms of providing a linear graphic which is given in Figure 4.19.

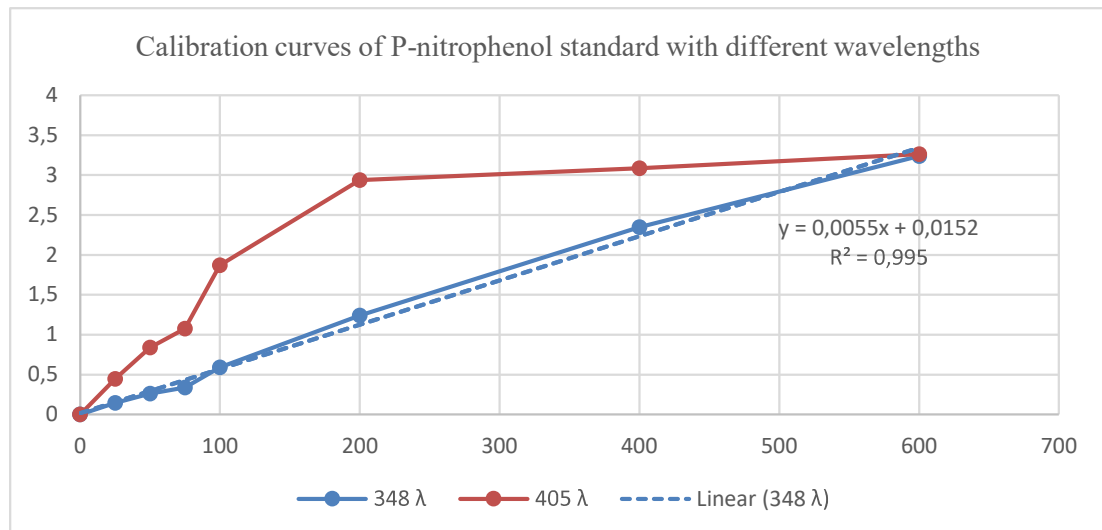


Figure 4.19 : Calibration curves of P-nitrophenol standard solution for CA activity test.

By selecting the wavelength to be used, the concentration values could be calculated accordingly. It was found that the enzyme activity in *Bacillus pasteurii* shows great results both potentially and kinetically as monoculture. On the other hand, 25% algae-75% bacteria sample was the poorest one. Thus, it can be stated that enzyme activity does not change proportionally by the bacteria content decreasing. 100%, 75% and 50% algae content samples took place in the middle range.

However the concentration values different at the end of 1 hour, enzyme activity is measured by the gap with the highest acceleration rate. By checking the Figure 4.20, the highest acceleration rate is started from 0 to 10 min. At this point again the monoculture of bacteria shows the highest value, however due to lack of photosynthesis ability, the second highest value needs to be selected which is 75% algae-25% bacteria sample. By this study the coculturing bacteria as *Bacillus pasteurii* was an excellent choice for the experiment.

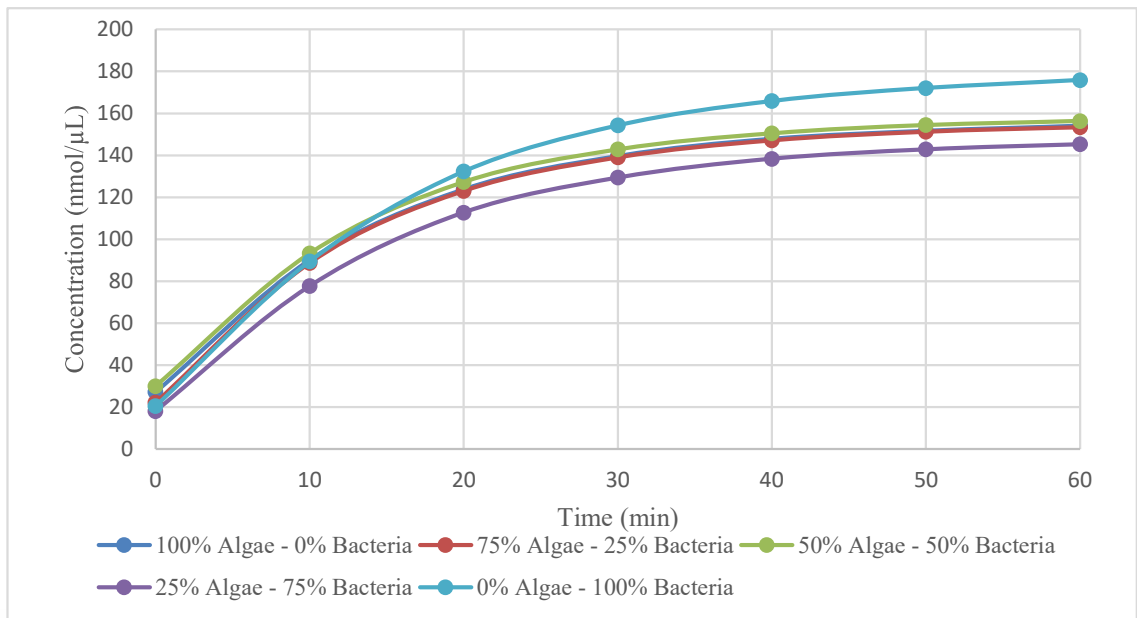


Figure 4.20 : CA concentration change in 1 hour by 10 min intervals.

CA activity measurements are based on the highest acceleration interval. Thus, we were focused on the first 10 minutes. Bacteria monoculture had around 20% higher yield of enzyme activity than algae monoculture in the first 10 minutes. On the other hand, we require photosynthesis pathways more than enzyme activity. Hence, algae must be involved. In terms of cocultures of algae and bacteria, 75% algae content media (IVR:3/1) showed the best performance of enzyme activity by reaching almost 1.5 mU/mg. IVR:1 and IVR 1/3 results were considerably lower than the IVR:3/1, so this option was picked for further experiments.

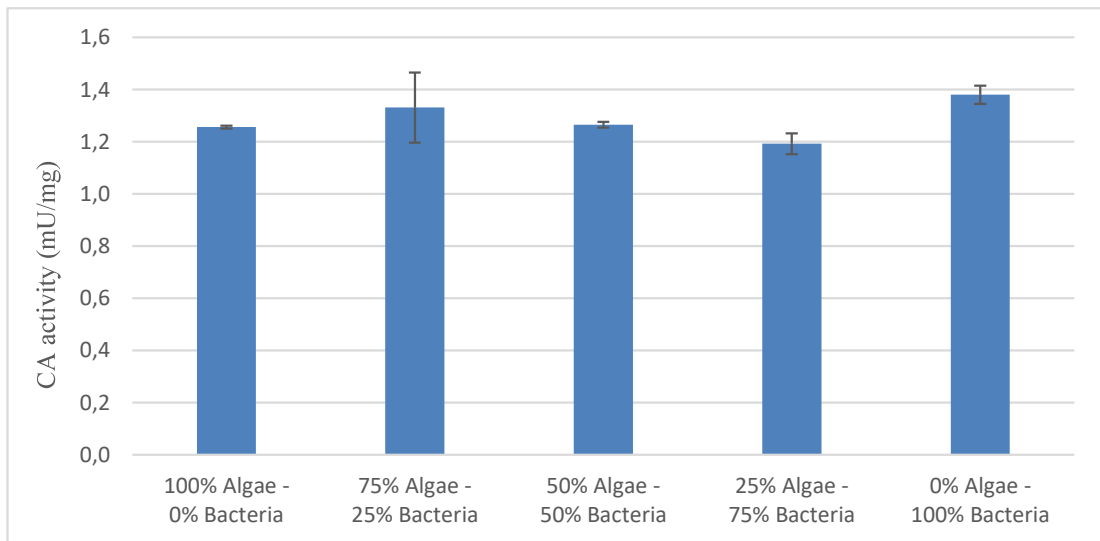


Figure 4.21 : CA activity between 0 to 10 minutes as mU/mg.

Moreover, obtained enzyme activity results of this experiment set was lower than the previous experiment results. It could be happened because of the different incubator usage, lower incubation duration and different ambient temperatures.

4.4.4 qPCR analysis results

In addition to 5 samples algae control and bacteria control samples were included in this measurement. The samples which constitute chlorophyll genes presented a line graphic, and their gene expression numbers are given in Figure 4.22 and Figure 4.23, respectively.

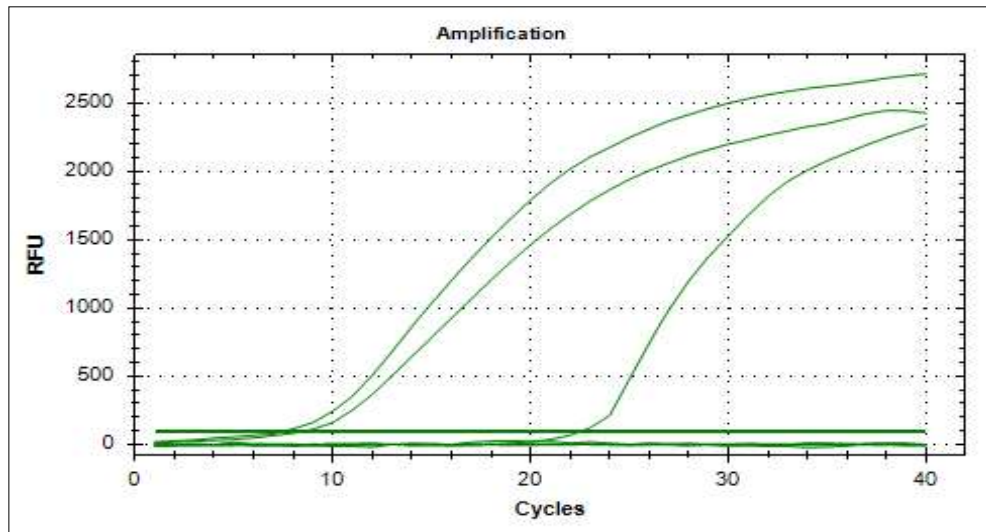


Figure 4.22 : Chlorophyll gene measurement of the samples via qPCR.

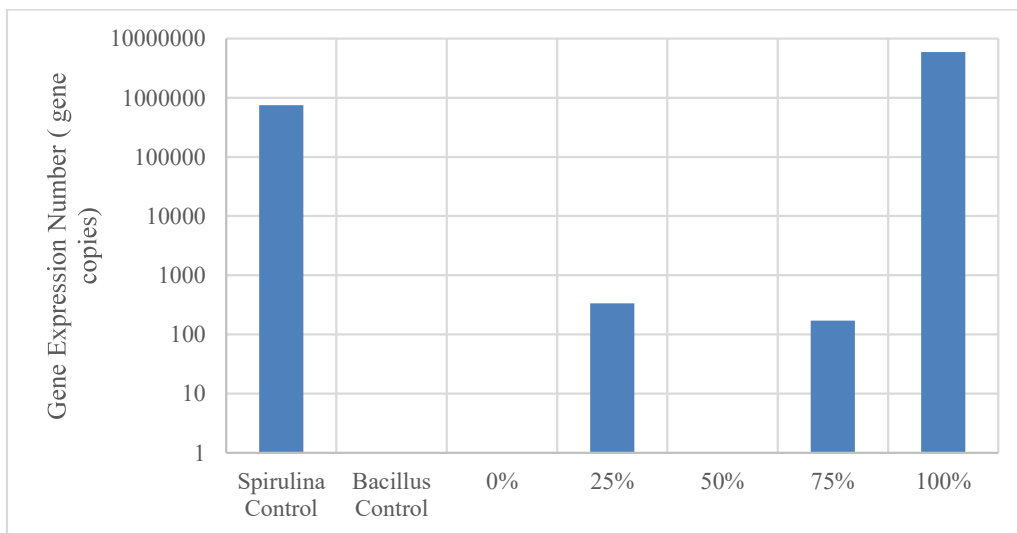


Figure 4.23 : Gene quantification for chlorophyll area.

Similar to chlorophyll area gene analysis, the samples which constitute bacteria genes presented a line graphic and their gene expression numbers are given in Figure 4.24 and Figure 4.25, respectively.

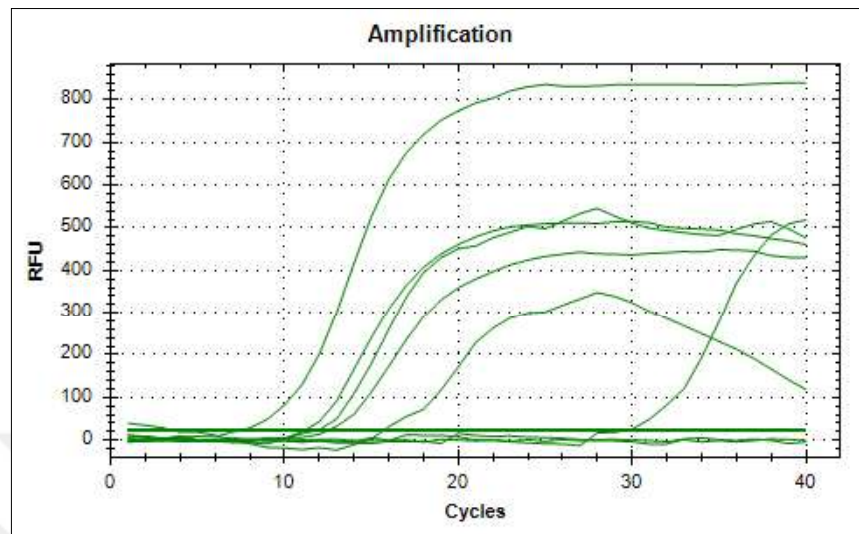


Figure 4.24 : Bacteria gene measurement of the samples via qPCR.

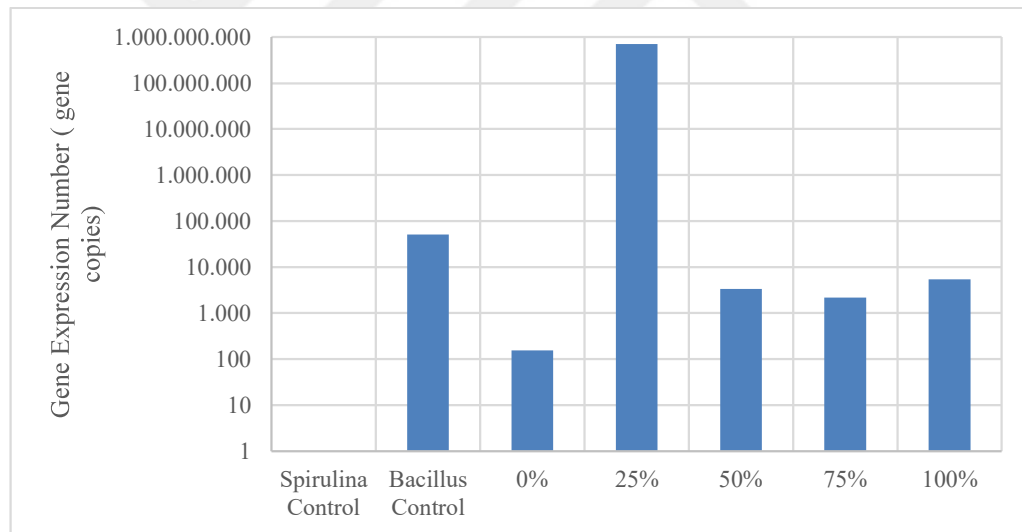


Figure 4.25 : Gene quantification for bacteria area.

4.4.5 Calcium ion content

Zheng and Qian (2019) conducted an experiment to achieve the most effective Ca^{2+} concentration with bacteria. They analyzed the Ca^{2+} concentrations from 0 to 300 mM and found that 60 mM was the one which had maximum growth and enzyme activity. Both growth and enzyme activity values were mostly correlated together and decreased dramatically after 100 mM.

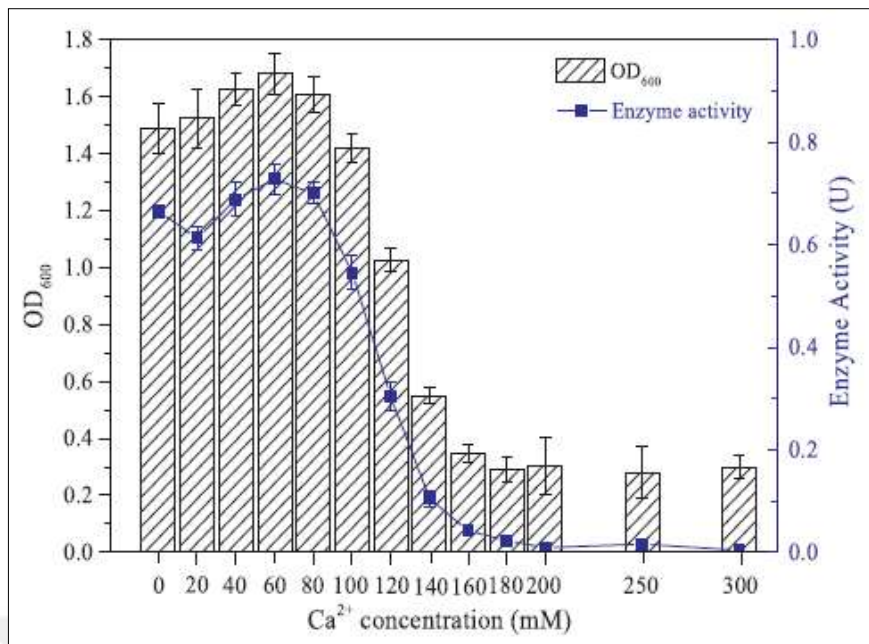


Figure 4.26 : Calcium ion concentration on OD₆₀₀ and CA activity (Zheng & Qian, 2019)

In this experiment, to prevent any inhibition and boost the growth of microorganisms, 60 mM concentration was selected. The minimum concentration of Ca²⁺ was found in IVR: 3/1 sample which points out the rest amount was precipitated as CaCO₃, and the system was very effective. CaCl₂ conversion rate was 99.3%. However, *Spirulina* monoculture and IVR :1/1 option were less effective to obtain that much calcite yield. In control sample, due to not consuming any minerals by microorganisms, they are assumed to interact with the added CaCl₂.

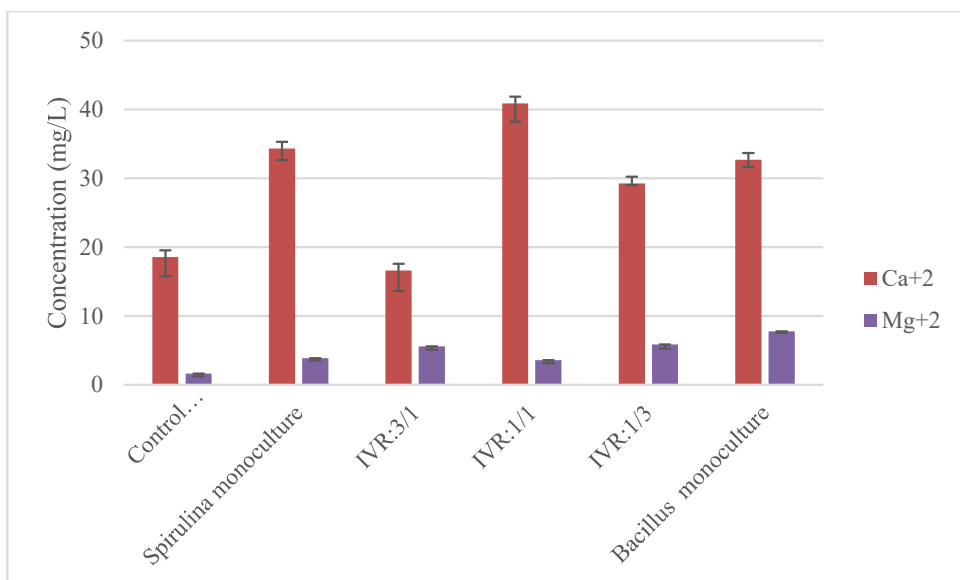


Figure 4.27 : Calcium and magnesium ion contents.

Furthermore, sodium and potassium ions were measured as the lowest value for IVR: 3/1 in comparison to other samples which indicates high salt formation tendency.

4.4.6 Carbonate and bicarbonate ions content

In addition to the calcium ion, the other component of calcite is carbonate. Unlike calcium, carbonate concentrations do not refer to exact results. The results are all distributed. Maximum bicarbonate concentration was observed in IVR: 1/1 sample and the minimum one in Spirulina monoculture. On the other hand, maximum carbonate concentration was observed in monoculture Spirulina and the minimum one in IVR: 3/1 sample. There is a negative correlation between the carbonate and bicarbonate ions due to pH differences. That's the reason why while carbonate concentration was high, bicarbonate concentration was low, relatively to others.

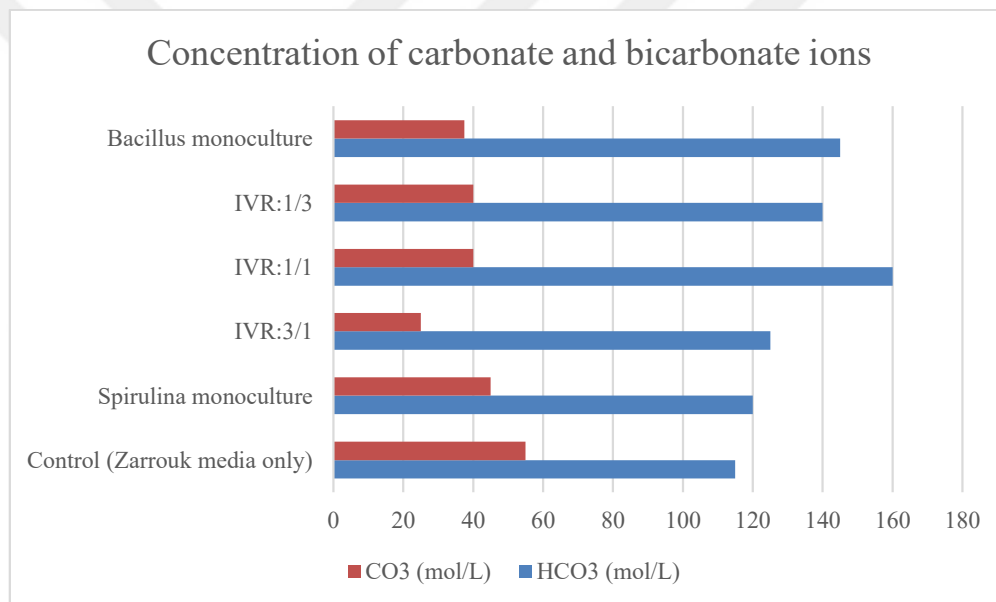


Figure 4.28 : Concentration of carbonate and bicarbonate ions.

4.4.7 XRD and SEM analysis

All the IVRs and the Zarrouk media without any microorganisms were analyzed via XRD. Zarrouk media was analyzed especially in order to find out if the media itself causes calcite formations. According to results achieved from analysis, only the 75% algae composition results in the pure calcite formations. All other coculture IVRs, monocultures and the Zarrouk media resulted in a magnesian calcite which means impurities exist in the precipitated materials. The peak points of XRD analysis are given in Figure 4.29 for 75% algae sample and the others are given in Appendices.

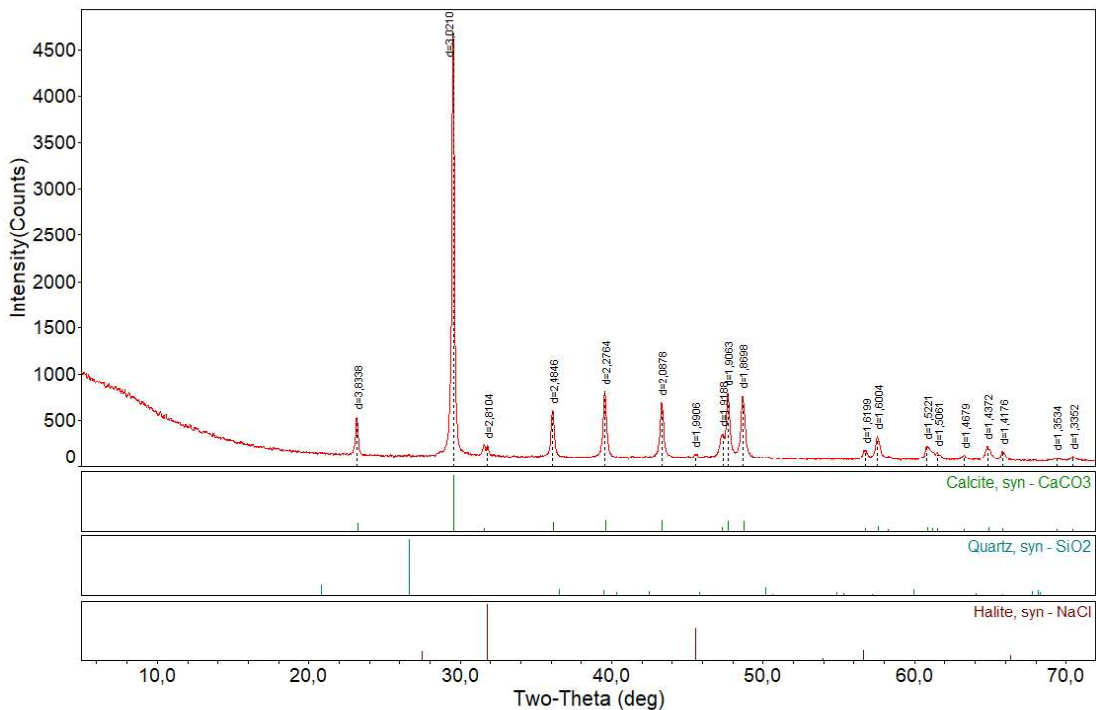


Figure 4.29 : XRD analysis - peak points of 75% algae sample.

Alga monoculture, bacterium monoculture, coculture IVR 3:1 and Zarrouk media as a control group was examined via scanning electron microscope (SEM). The morphologies of the precipitated and mineralized products are given in Figure 4.30. Because the samples were washed with acid beforehand the analysis, there is no microorganism morphology in the images. In the bacteria monoculture and coculture samples fine spherical particles cling on each other and their sizes look alike. Bacteria monoculture's image is 2 times more focused on the sample to show whole group of spherical particles in one image and that is the reason why the community seems quite large. On the other hand, it couldn't be observed any spherical particles algae monoculture nor control sample. There is only irregular shaped small particles

were exist and they are dispersed all around the area. As a result, it can be clearly said that bacteria contribution is vital for producing fine spherical particles.

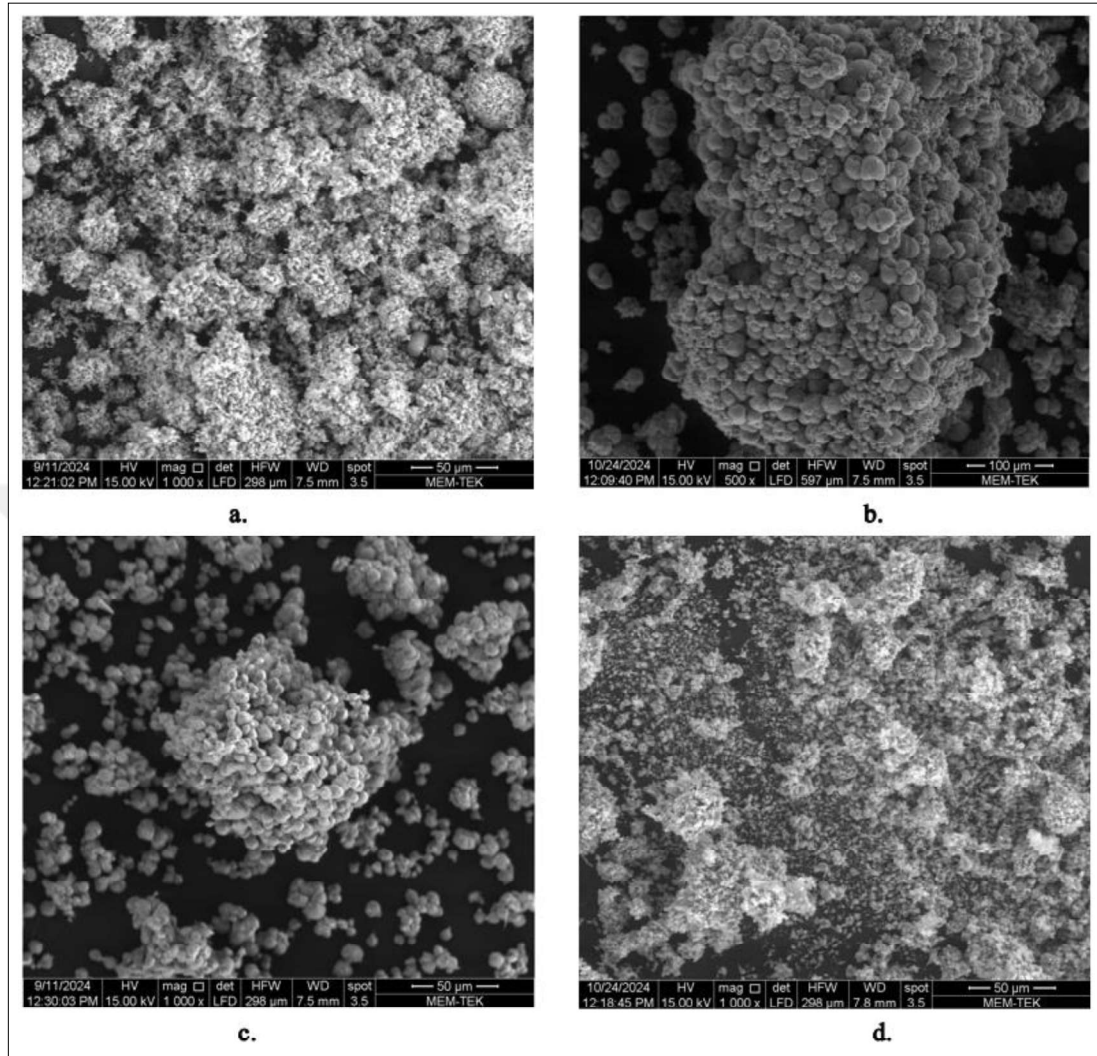


Figure 4.30 : SEM micrographs of mineralized products of samples as a. Control (only Zarrouk media), b. bacteria monoculture, c. IVR 3:1 coculture, d. algae monoculture.

The EDS spectrum of precipitated products points out the major elements were Ca, C and O exist there, given in Figure 4.31. The most important difference of coculture from others was that there were not any impurities, confirming the precipitation in coculture was calcium carbonate. Others' precipitation content includes some other compounds.

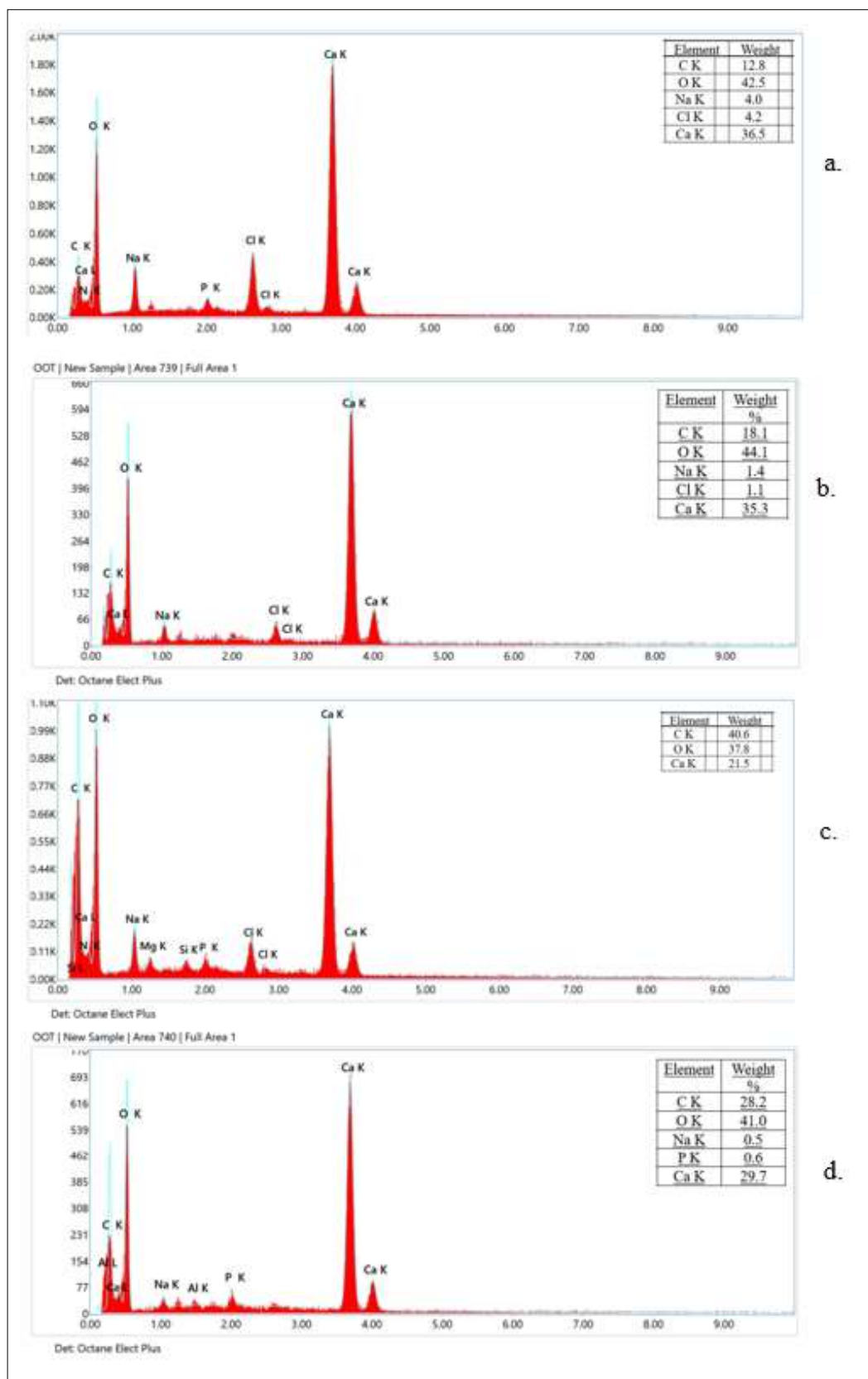


Figure 4.31 : EDS spectrums of mineralized precipitation samples, a. Control (Zarrouk media only), b. bacteria monoculture, c. coculture IVR 3:1, d. algae monoculture.

4.5 Open Raceway Ponds

4.5.1 Light intensity, pH, aquatic temperature and growth

According to recorded real time data, the average sunlight duration during the experiment is 11 hours per day. The remaining time was darkness, and no additional lighting apparatus was used. During the day time maximum light intensity value was $513 \mu\text{mol photons.m}^{-2}.\text{s}^{-1}$ in 25th of October, 2024. In addition the average light intensity was $159 \mu\text{mol photons.m}^{-2}.\text{s}^{-1}$.

Although pH was set to 10.5, it did not remain same for the experiment time. It started to decrease right after the kickoff until 9.5 in both raceways. It was monitored for a while to observe if there would be any further change. The value remained the same after 9.5 for almost 10 days. As the main purpose was proceeding the experiment at 10.5, alkalinity was added to the raceways on the 12th day. As a result, pH could be increased. At the end, pH was 9.8 in monoculture and 9.7 in coculture.

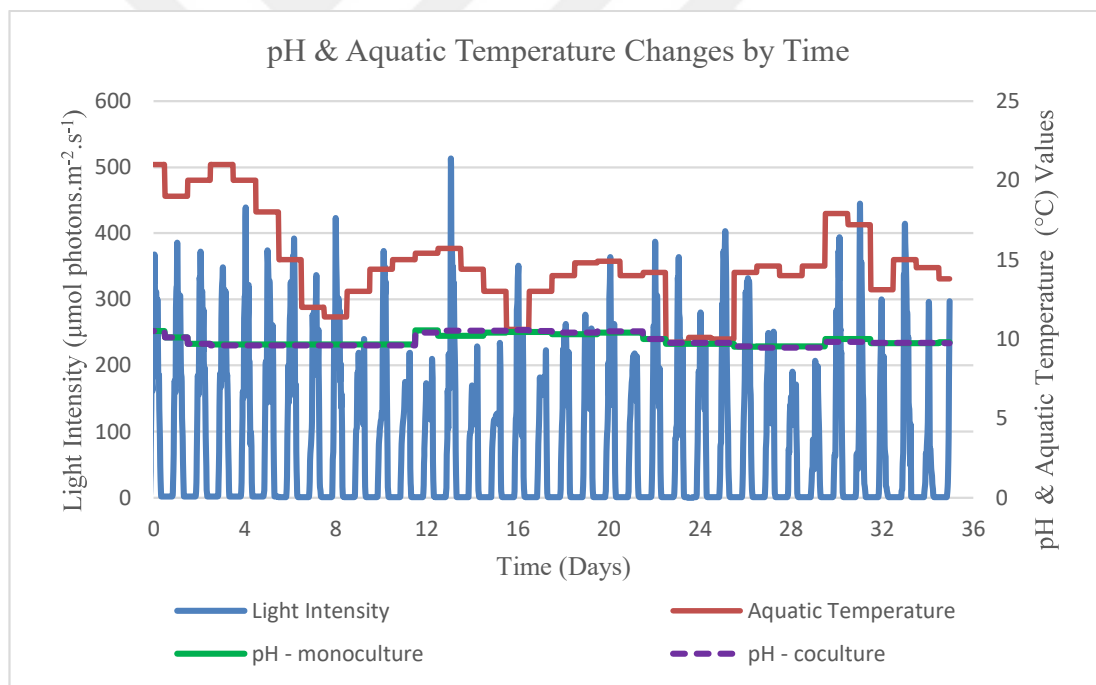


Figure 4.32 : pH and aquatic temperature changes by time.

As the season was autumn, aquatic temperature was measured around 20°C degrees only once. The average temperature was 14.8 °C degrees. Date of light intensity, pH and aquatic temperature are given in Figure 4.32.

For OD measurements, due to an error in calculating the volume of monoculture media, its OD_{600} was started from 0.532 while the coculture media's density was

correct as 0.296. the densities of the media were equalized in 12th day and then moved together mostly. In 22nd day, there was CaCl_2 addition to medias to stimulate chemical reaction and precipitate CaCO_3 . Coculture's optical density remained same roughly while the monoculture's optical density increased rapidly. Then both media equalized again in 4 days.

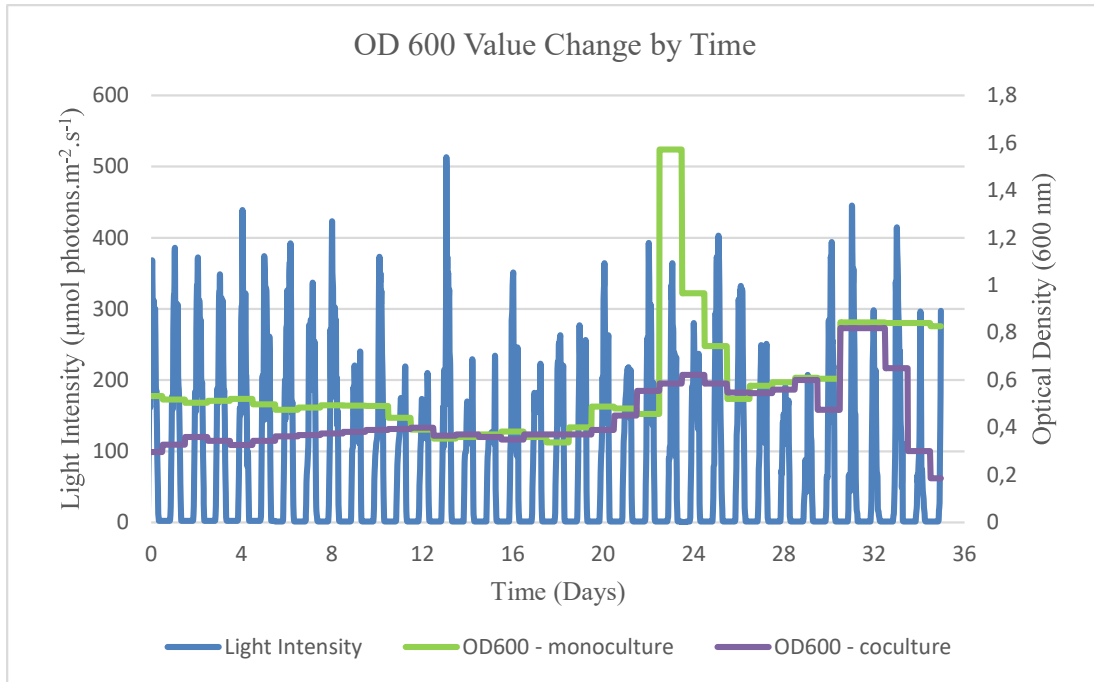


Figure 4.33 : OD₆₀₀ value change by time.

After 32nd day of incubation, coculture pond was inhibited somehow. Although its pH and temperature values remained the same, OD value started to decrease dramatically. At the last day, this situation resulted in the color change in the last day of experiment, given in Figure 4.34.



Figure 4.34 : Last day of the 35-day cultivation experiment. Coculture and monoculture, respectively.

4.5.2 Total chlorophyll and carotenoid

Total chlorophyll and the carotenoid pigments were measured by the samples that were obtained on 6th, 13th, 22nd, 27th and 31st days. By measuring the different day's pigment content, it can be managed to monitor the pigment concentration change by time. Total chlorophyll and carotenoid concentration changes are given in Figure 4.35 and Figure 4.36, respectively.

The crucial point is that the *Spirulina* monoculture had already been growth in one of those raceways and the coculture pond was fed by it. This is the reason why initial pigment content is the highest at the beginning and then it decrease. Furthermore, coculture's pigment levels could manage to beat monoculture levels after the half of the cultivation period. Yang et al. also claims that chlorophyll-a, chlorophyll-b and carotenoid contents can be increased between 5th and 8th days of incubation. Thus, in the early phases it was measured as expected (2024).

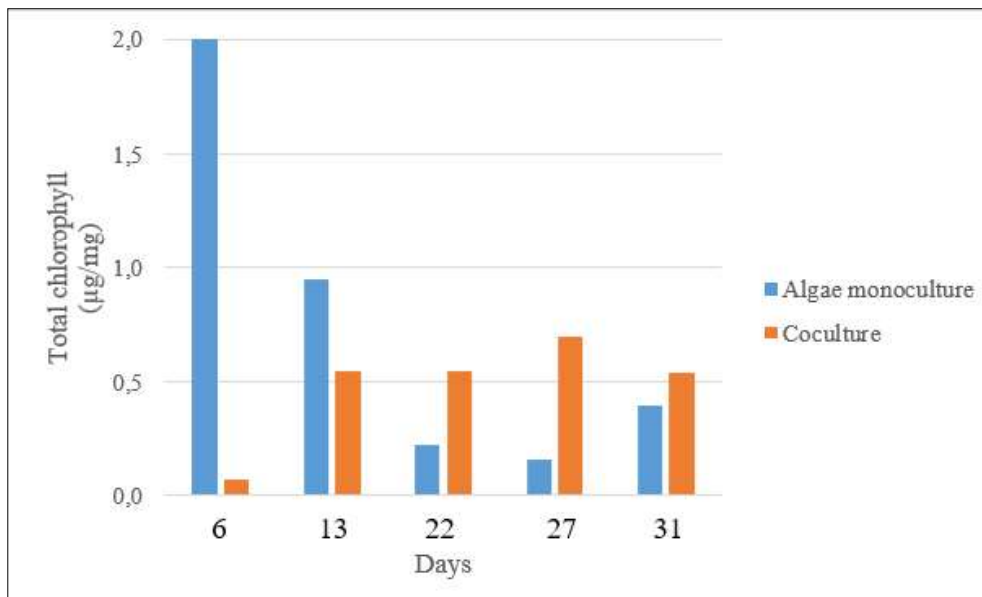


Figure 4.35 : Total chlorophyll concentration change in raceway by time.

However, in previous coculture experiments, carotenoid values were measured as lower than total chlorophyll value of same sample, in this experiment results are changed by the time passed. It was stated that the carotenoid and chlorophyll extractions from *A. platensis* by using acetone, ethanol and different ionic liquids resulted with the much higher carotenoid pigment concentrations rather than total chlorophyll measurements (Fernandes et al., 2024).

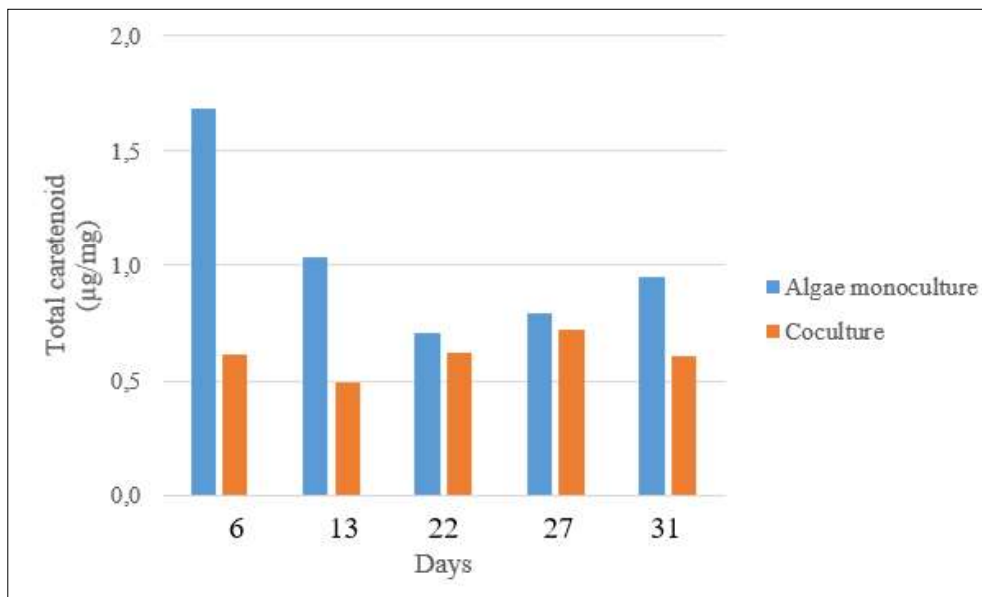


Figure 4.36 : Total carotenoid concentration change in raceway by time.

4.5.3 Suspended solids and volatile suspended solids

The monoculture media's values are greater than coculture which supports optical density values at initial point. However suspended solids were increasing in time, after 24th day, a slight decrease was observed. The situation was related to decay phase of algae, especially in coculture raceway. Contrary, monoculture's suspended solids rates were still tending to increase which lead us to calcification still continues.

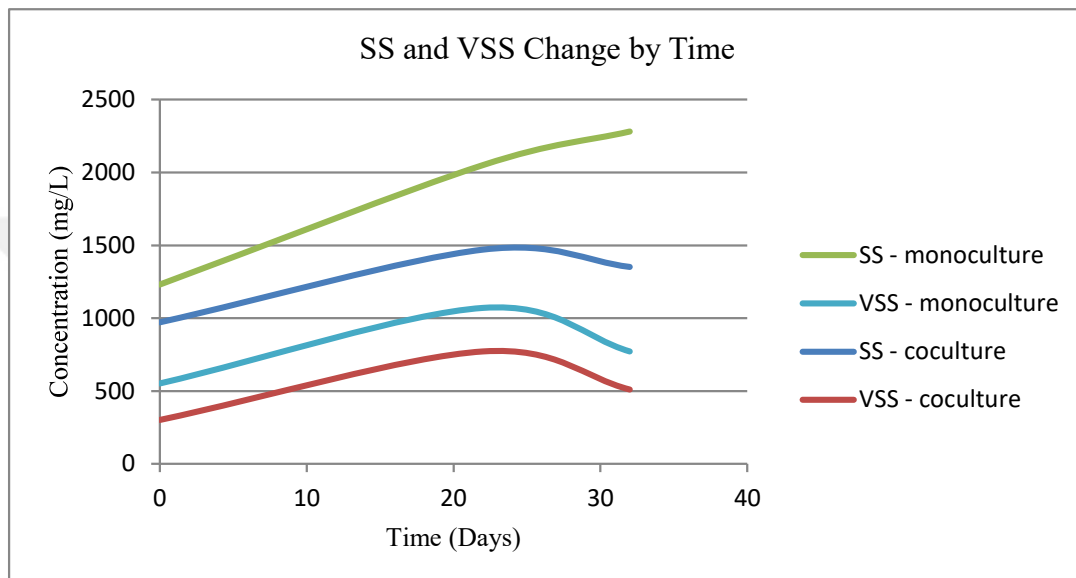


Figure 4.37 : TSS and VSS change of both monoculture and coculture experiments.

Initial concentration of monoculture is nearly 2 times greater than the coculture concentration. However, there was a disadvantage at starting point, coculture's VSS increased 1.7 times according to its starting point while monoculture's increasing was 1.4. Coculturing with bacteria resulted in great biomass yield. On the other hand, monoculture's VSS value reached 1.07 g/L, lower than the lab scale coculture experiments due to cold water temperature basically. It is mentioned that the Spirulina's biomass can reach up to 0,62 g/L.d if the optimum growing conditions can be presented (Chaiklahan et al., 2021).

4.5.4 CaCO₃ mass balance

To produce CaCO₃, CaCl₂ was added to the system after 22 days of cultivation period. 882.1 g CaCl₂ was needed to obtain 60 mM Ca²⁺ concentration in each media. On the other hand, the initial idea was to maximize CaCO₃ sedimentation

yield, 1.5 times more gram of CaCl_2 was added to monoculture. Despite the extra addition, the excess amount was participated directly as CaCl_2 salt. In conclusion, calcium source amount calculation according to achieve 60mM Ca^{2+} was approved by the experiment set. Mass balance equations are given in Table 4.6 and Table 4.7.

Table 4.6 : Mass balance in raceway pond - Spirulina monoculture.

Monoculture - <i>Spirulina</i>	Just Before CaCl_2 Addition (g)	End of Cultivation (g)
$\text{CaCl}_2 \cdot 2\text{H}_2\text{O}$ solved part (Ca mass)	241,73	-
$\text{CaCl}_2 \cdot 2\text{H}_2\text{O}$ unsolved part (CaCl_2 mass)	174,50	-
Sediment Harvest (dry weight)	-	654,70
Fixed solids	98,00	151,00
VSS	107,00	77,00
CO_2 capture (CO_3 equivalent)	262,64	
Balance	883,35	883,87

Due to narrow spaces and hard to reach points approximately 85% of the sedimentation could be collected by hand. So, 553.22 g weighted by scale, however it counted as 654.7 g in mass balance. Whole sediments were dried by oven which was set to 50°C degrees for 10 days. Because sediment doesn't include only the calcite precipitation in monoculture, but also the massive amount of CaCl_2 , by extracting unsolved CaCl_2 from harvested sediment amount lead us to figure out the calcite production. Fixed solids was found by extracting VSS values from TSS values, thus their values are exact thanks to quantitative measurement by scale. CO_2 capture rate was assumed as 1.8 times from 1 g biomass.

Table 4.7 : Mass balance in raceway pond - Coculture.

Coculture	Just Before CaCl_2 Addition (g)	End of Cultivation (g)
$\text{CaCl}_2 \cdot 2\text{H}_2\text{O}$ fully solved (Ca mass)	240,53	-
Sediment Harvest (dry weight)	-	252,21
Fixed solids	70,00	84,00
VSS	77,00	51,00
CO_2 capture (CO_3 equivalent)	66,00	
Balance	387,53	387,21

Unlike monoculture pond, in the coculture pond CaCl_2 addition was mixed well, hence all the sediment amount was counted as calcite production. In this pond, there was less amount of sediment, so it didn't accumulate in hard-to-reach points. As a result, approximately 90% of the sediment could be collected by hand. CO_2 capture rate was assumed as 0,6 times from 1 g biomass.

4.5.5 CA enzyme activity

Samples from 5 different days were picked according to sample availability and their green color. Not only for the last day's enzyme activity, but the developments of the activity in different days could be measured by this method. Because the calibration of the standard solution was considered for 348 λ , whole measurements were carried out with 348 λ wavelength.

For *Spirulina* monoculture, CA activity was steady between 0,4 and 0,6 mU/mg until the CaCl_2 addition. After calcium addition there was a dramatic decrease in the enzyme activity.

On the other hand, for coculture enzyme activity was steady between 0,2 and 0,35 mU/mg. In contrast, enzyme activity boosted after calcium addition to above 1 mU/mg. This value corresponded to the value in IVR determination experiments. The rest values are relatively lower than IVR determination experiment results because of the negative correlation between enzyme activity and temperature between 15-25°C degrees. It was also stated that the carbonic anhydrase enzyme activity was measured around 0,3 mU/mg at 15°C degrees (Zheng&Qian, 2019).

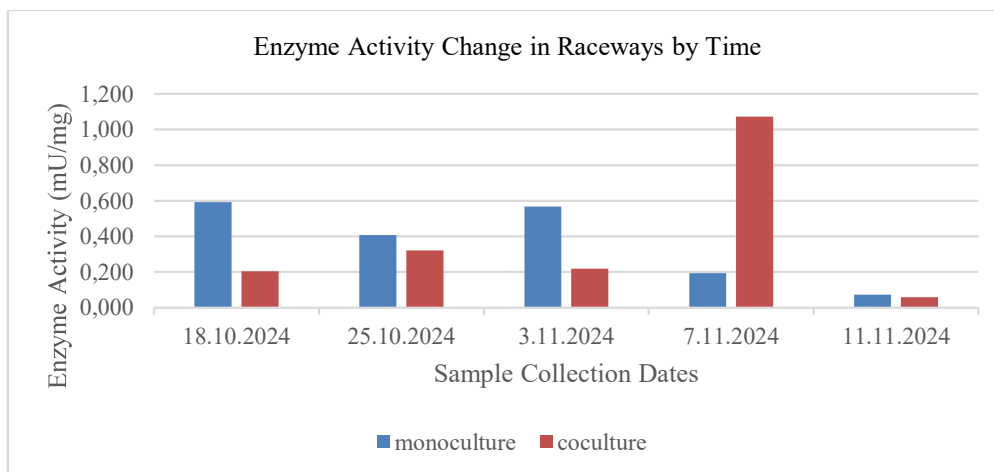


Figure 4.38 : Enzyme activity change in raceways by time.

4.5.6 EPS analysis

In lab scale experiments, total EPS for Spirulina monoculture was measured as 0.79 mg/L at the end of 15 days of incubation while it is measured as 0.46 maximum in raceway pond. In addition, coculture IVR 3:1 was measured as 0.92 mg/L, but it was 0.43 in raceway pond. This dramatic decrease is mainly based on the temperature change and as a result loosely bounded EPS concentration couldn't increase. The concentration changes of monoculture and coculture are given in Figure 4.39 and Figure 4.40, respectively.

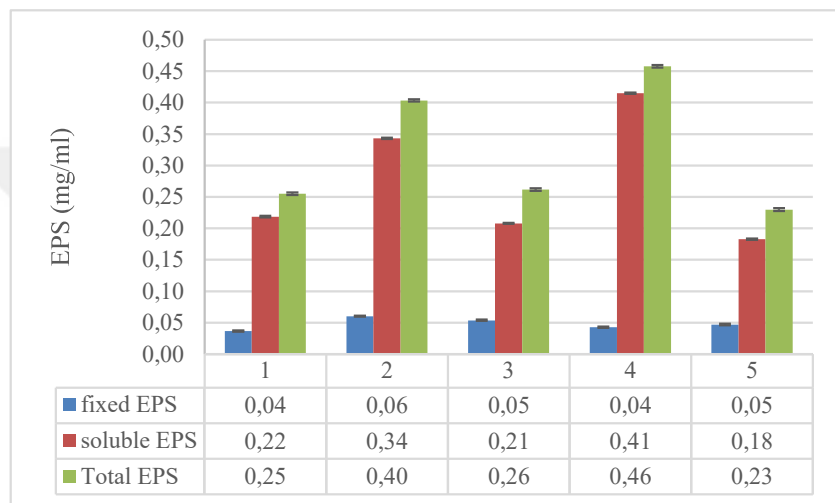


Figure 4.39 : EPS concentration in algae monoculture raceway pond (1) 18.10.2024, (2) 25.10.2024, (3) 03.11.2024, (4) 07.11.2024, (5) 11.11.2024.

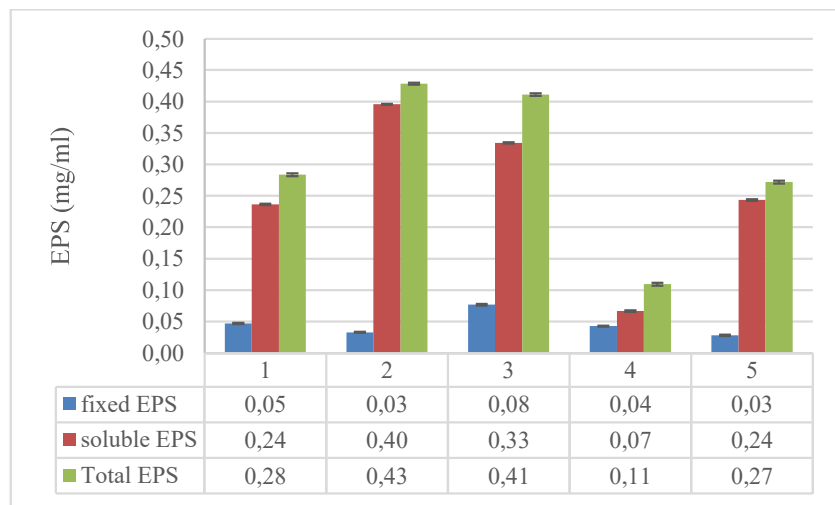


Figure 4.40 : EPS concentration in coculture raceway pond (1) 18.10.2024, (2) 25.10.2024, (3) 03.11.2024, (4) 07.11.2024, (5) 11.11.2024.

4.5.7 Carbonate and bicarbonate ions content

According to a similar experiment conducted by Zheng & Qian, bicarbonate ion concentration was inclined from 0 to around 45 mM and carbonate ion concentration was inclined from 0 to around 2 mM (2019). The concentrations were increased because of the enzyme activity triggers the hydration process of carbon dioxide. Thus, bicarbonate and carbonate ion concentration increase in time. However, the main difference between that experiment and ours is the aquatic temperature. That experiment was carried out on a lab scale and conducted at 30°C degrees, however our experiment was pilot scale and conducted in October and November months which can be considered as cold session obviously. Low enzyme activity resulted in decreasing trend of carbonate and bicarbonate ions. In Table 4.30, the measurement started from Day 0 which was the date of CaCl_2 addition (03.11.2024), until the end of the cultivation period (16.11.2024).

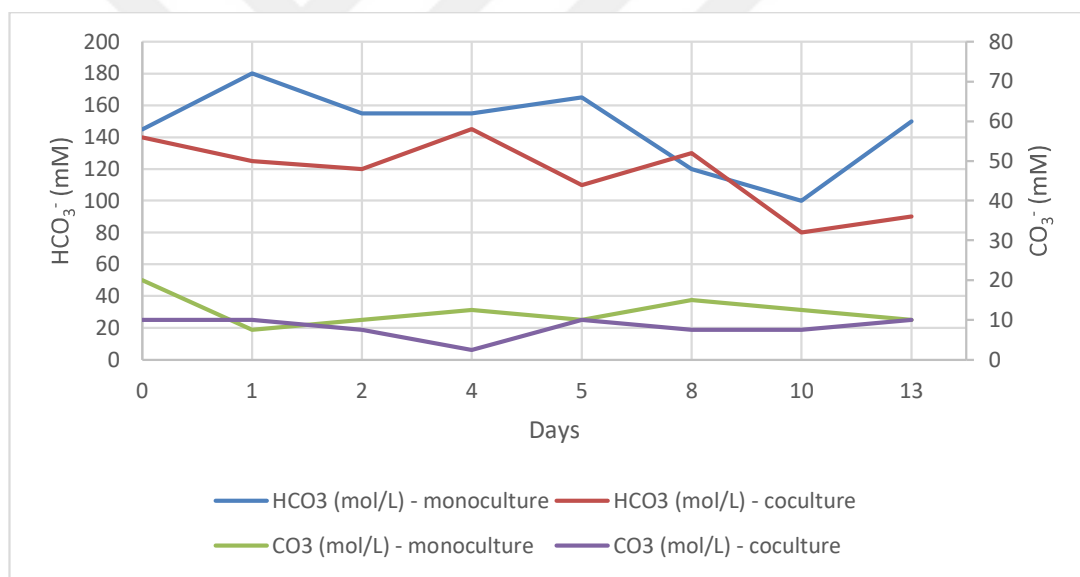


Figure 4.41 : Carbonate and bicarbonate ion concentrations change in time.

In monoculture, carbonate ion concentration started from 20 mM and ended at 10 mM while it was 145 to 150 mM for bicarbonate. For coculture, carbonate ion concentration ended as same as its starting point as 10 mM while bicarbonate ion concentration decreased to 90 from 140 mM.

4.6 Closed Photobioreactor Outcomes

4.6.1 Growth, suspended solids and volatile suspended solids

Spirulina monoculture could grow more than 10 times in only 4 days, hence CaCl_2 addition was made as no significant growth was expected. On the other hand, coculture grew exponentially for the first 6 days but couldn't reach the monoculture growth rates yet. On the 8th day, data was obtained and the culture seemed like it was passing to stationary phase due to very low increase in last 2 days. Then its CaCl_2 was added. CaCl_2 contact periods were the same as 4 days for both experiments.

Total suspended solids and volatile suspended solids concentrations are given in Figure 4.42.

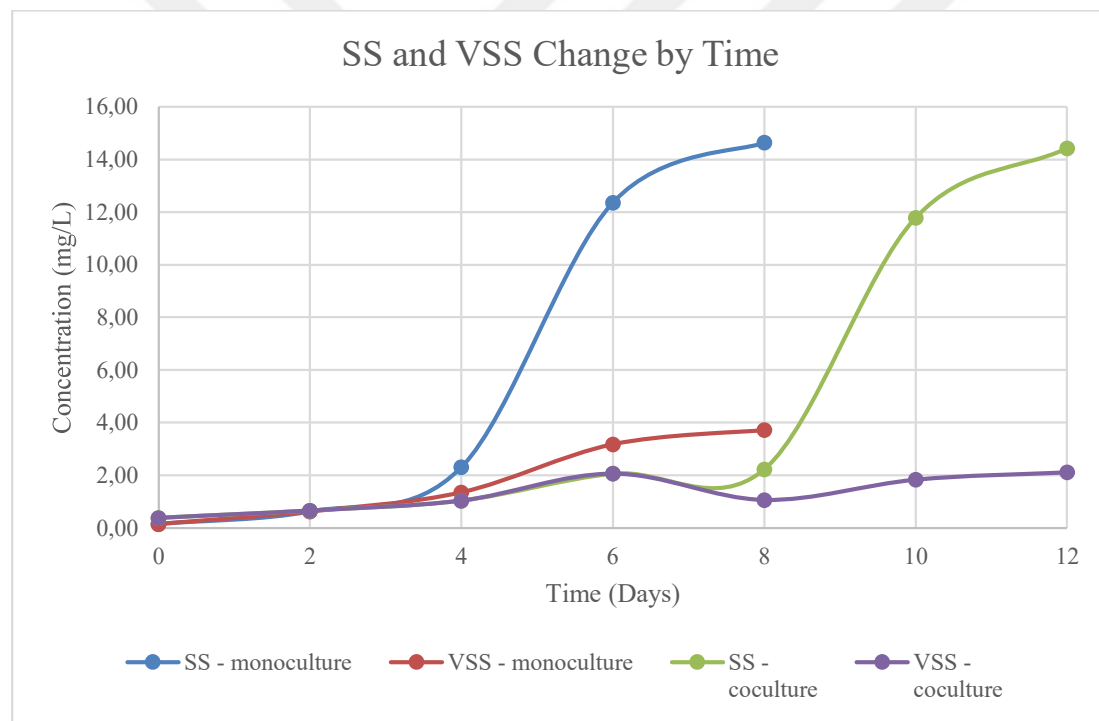


Figure 4.42 : SS and VSS Change by Time for Entire Cultivation.

4.6.2 Total chlorophyll and carotenoid

Pigment analysis values were well developed just before the CaCl_2 addition. Coculture's pigment levels were lower than monoculture as expected because of the existence of bacteria. During the calcification process while monoculture's pigment values decreased smoothly, coculture's pigment values decreased dramatically. Also,

the color of the PBR turned grayish color. OD levels were getting to stationary phase on 8th day of experiment, so it could be said that if the algae's growth rate decreased, bacterium was become an abundant microorganism in the media. It could be said that there is a competition to grow in the media and bacteria fed on the algae.

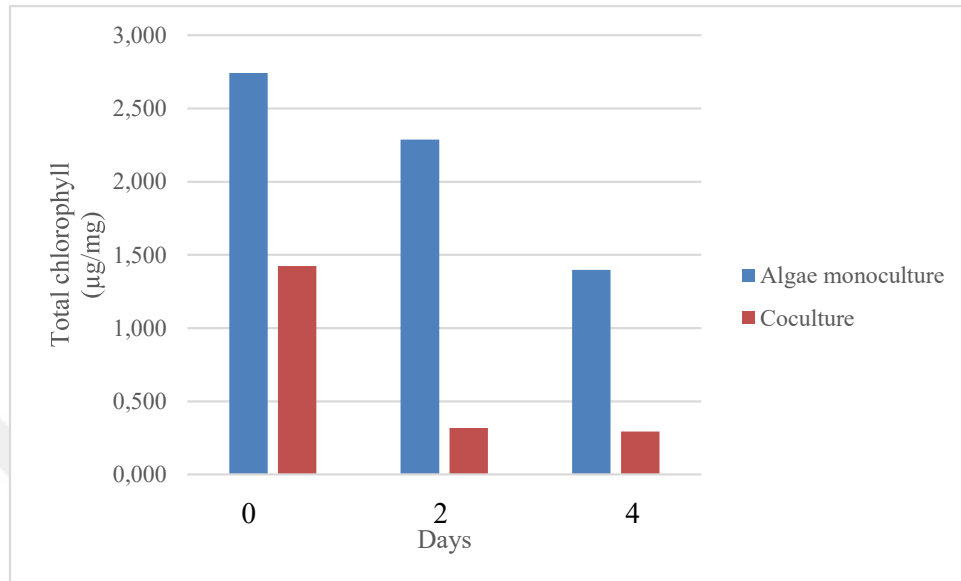


Figure 4.43 : Total chlorophyll content of PBR experiments.

Carotenoid pigment concentration was higher just before the CaCl₂ addition in coculture than the monoculture set unlike all other measurements. Total chlorophyll and carotenoid concentration changes by 2 days interval are provided in Figure 4.43 and Figure 4.44, respectively.

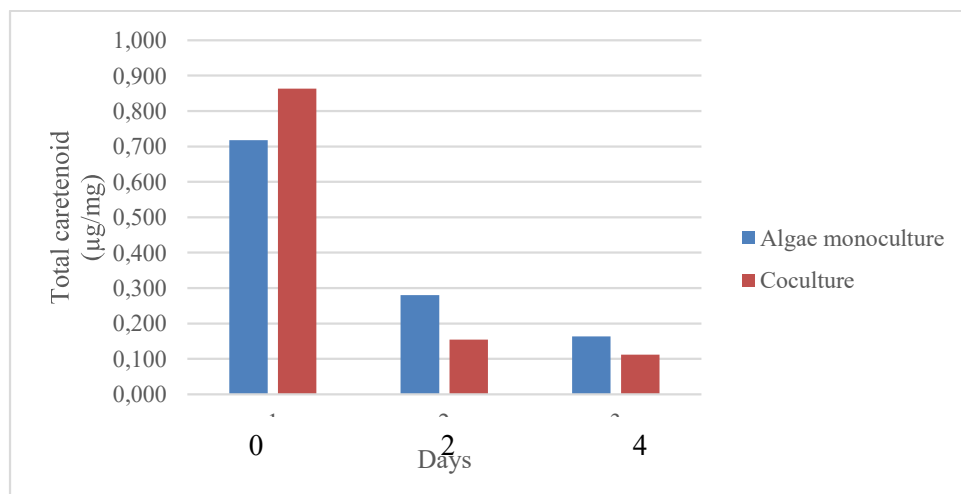


Figure 4.44 : Total carotenoid content of PBR experiments.

4.6.3 Suspended solids and volatile suspended solids

After 4th day, 100 ml sample was taken from the PBR and the total volume decreased to 1.9 L. Also 50 ml samples were obtained from the PBR on 6th and 8th days. At the end of the experiment, there was 1.8 L of media collected and all of the calculations are based on this volume.

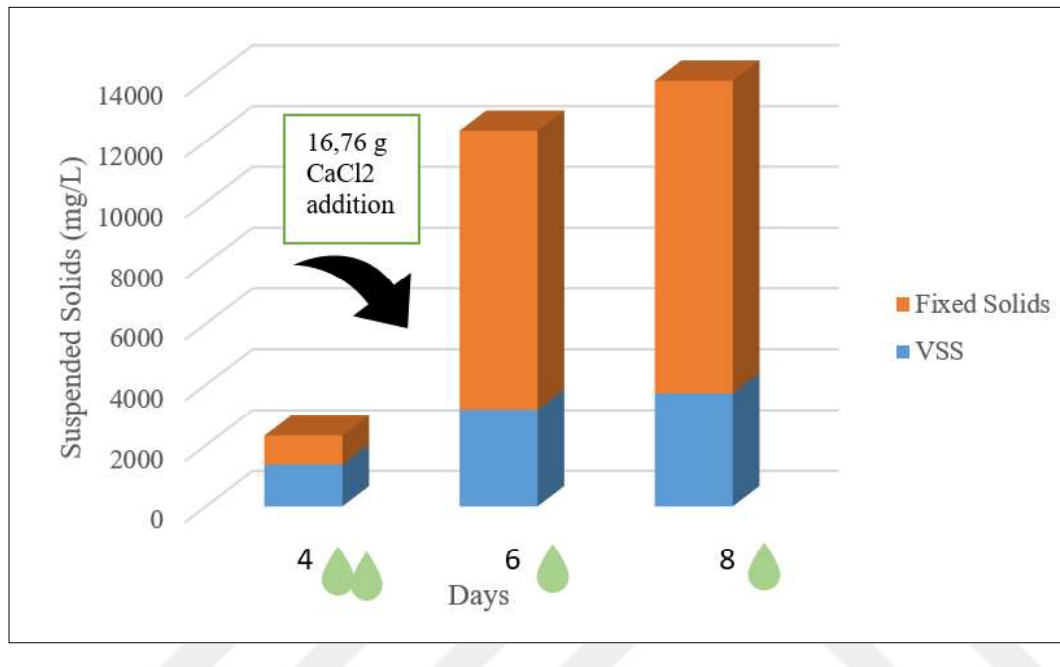


Figure 4.45 : VSS and mineral content in algae monoculture bubble type photobioreactor for calcification period.

The initial suspended solid amounts were differentiated due to different starting IVR. But their total suspended solid amounts became almost similar just before CaCl_2 addition. Also, total suspended solid increased proportionally together and came to same level on 4th day of calcification. The major difference between monoculture and coculture is the calcite yield. In coculture fixed solids concentration is 1.2 times greater than monoculture. However, there was lower biomass amount, approximately 0.6 times of monoculture, coculture achieved to produce calcite more efficiently. Biomass to calcite transformation ratio for monoculture and coculture are measured as 2.9 and 5.8 by weight, respectively.

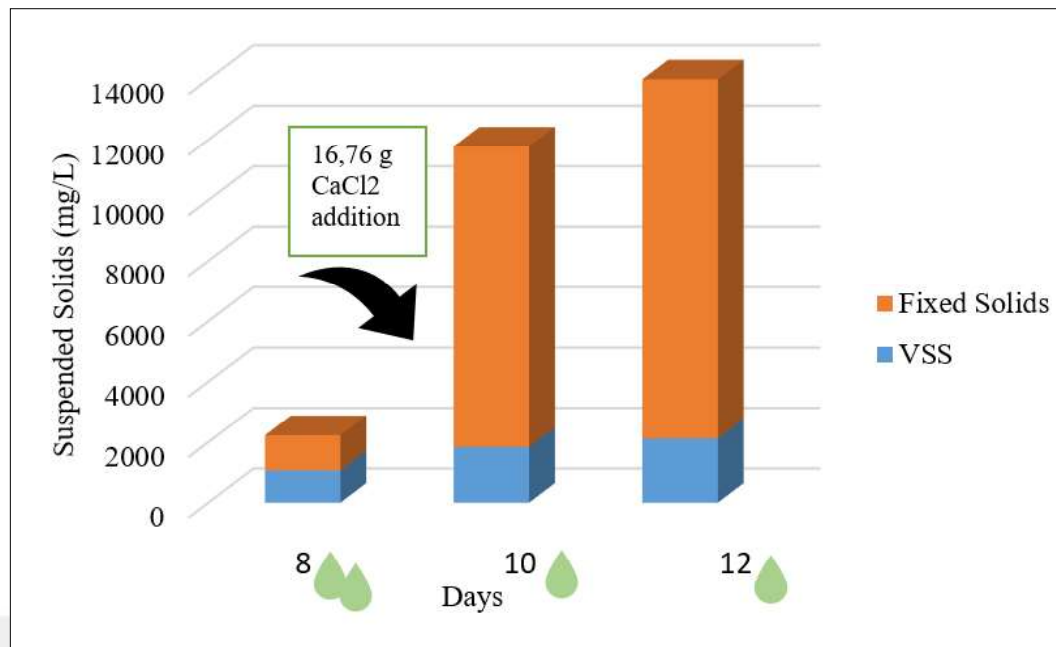


Figure 4.46 : VSS and mineral content in coculture bubble type photobioreactor for calcification period.

4.6.4 CaCO₃ mass balance

After adding the calcium mass, initial fixed solids and the initial VSS each other, result was equal to 8.98 g. On the other hand last measured fixed solids and VSS amount's addition was equal to 27.82 g which was far higher than the measured solids in the system. However, air compressor was also working during the experiment and due to enzymatic activities carbon dioxide was reduced to CO₃ which can explain the gap between input and output. CO₂ capture rate was assumed as 1.8 times from 1 g biomass. Monoculture's mass balance is given in Table 4.8.

Table 4.8 : Mass balance in BPR - Monoculture.

Monoculture	Just Before CaCl ₂ Addition (g)	End of Cultivation (g)
CaCl ₂ ·2H ₂ O fully solved (Ca mass)	4,57	-
Fixed solids	1,82	20,75
VSS	2,58	7,07
Semi Total	8,98	27,82
CO ₃ from CO ₂ reduction	17,35	
CaCl ₂ ·2H ₂ O unsolved part (CaCl ₂ mass)	1,49	-
Balance	27,82	27,82

Despite the calcification rate of coculture was greater than the monoculture, their total suspended solid increased parallel to each other. CO_2 capture rate was calculated as 3.1 times from 1 g biomass in coculture media. Mass balance belong to coculture experiment set is given in Table 4.9.

Table 4.9 : Mass balance in BPR - Coculture.

Coculture	Just Before CaCl_2 Addition (g)	End of Cultivation (g)
$\text{CaCl}_2 \cdot 2\text{H}_2\text{O}$ fully solved (Ca mass)	4,57	-
Fixed solids	2,21	23,37
VSS	2,02	4,03
Semi Total	8,81	27,40
CO_3 from CO_2 reduction	17,10	
$\text{CaCl}_2 \cdot 2\text{H}_2\text{O}$ unsolved part (CaCl ₂ mass)	1,49	-
Balance	27,40	27,40

4.6.5 CA enzyme activity

Enzyme activity was changed between 0.05-0.2 mU/mg during the calcification process which indicates very low activity results. During the IVR determination experiments, temperature was at $30 \pm 0.2^\circ\text{C}$ degrees, on the other hand this experiment was run at $23 \pm 0.2^\circ\text{C}$ degrees. The difference in the temperature explains relatively low activity results.

Enzyme activity in coculture media was higher than monoculture just before CaCl_2 addition as expected. However, coculture's enzyme activity decreased during the calcification while there was an incline in monoculture. The change can be seen in Figure 4.47.

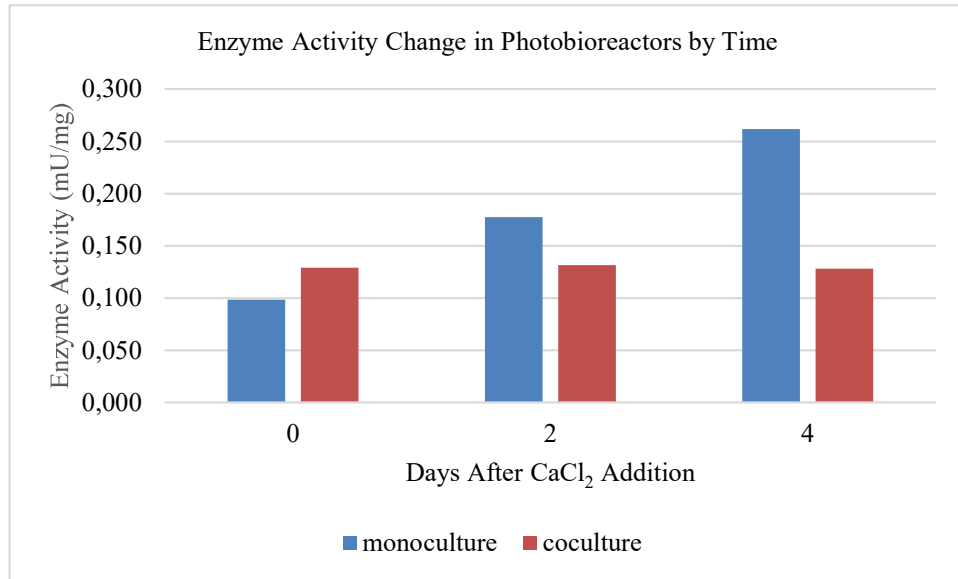


Figure 4.47 : Enzyme activity change in PBR by time.

4.6.6 EPS analysis

Unlike raceway pond experiments, EPS concentration was increased again when the aquatic temperature increased to 25°C degrees. Total EPS concentration was more than 1 mg/L and steady during calcification process. EPS concentration change in algae monoculture is given in Figure 4.48.

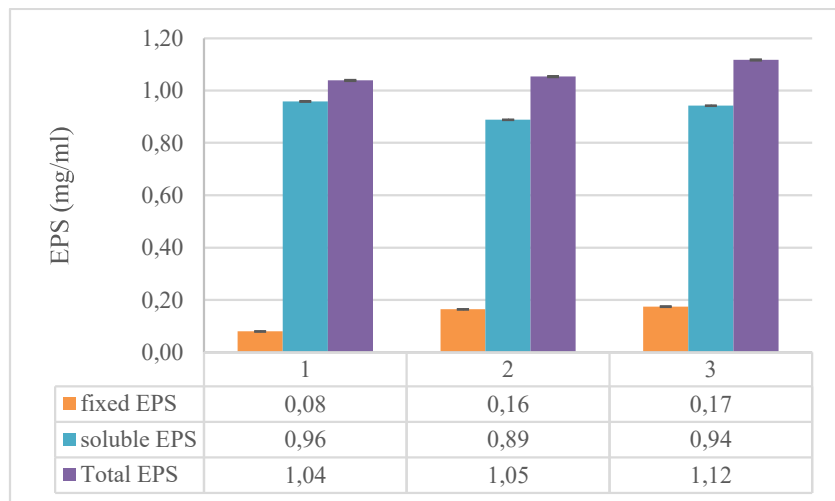


Figure 4.48 : EPS concentration in algae monoculture PBR (1) before calcium addition, (2) after 2 days of calcium addition, (3) after 4 days of calcium addition.

On the other hand, coculture EPS concentration was similar to raceway pond value at the beginning of calcification process. Surprisingly, EPS concentration was increased

during the calcification and the highest concentration rate could be obtained via PBR. EPS concentration change in coculture is given in Figure 4.49.

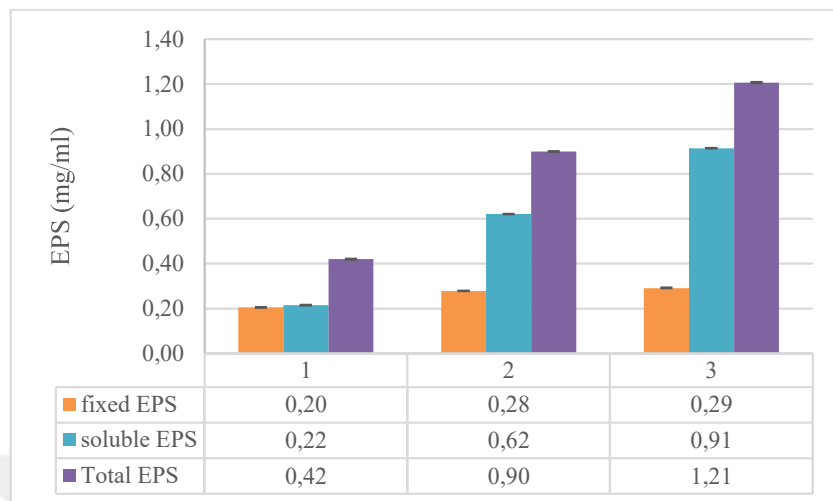


Figure 4.49 : EPS concentration in coculture PBR (1) before calcium addition, (2) after 2 days of calcium addition, (3) after 4 days of calcium addition.

4.6.7 Carbonate and bicarbonate ions content

Due to low enzyme activity, bicarbonate and carbonate ion formations couldn't be done successfully. Except for the slight increase in bicarbonate ions in monoculture, all the values decreased. In order to prevent such a decrease, increasing the temperature will provide more enzyme activity and more carbonate and bicarbonate ions in the media.

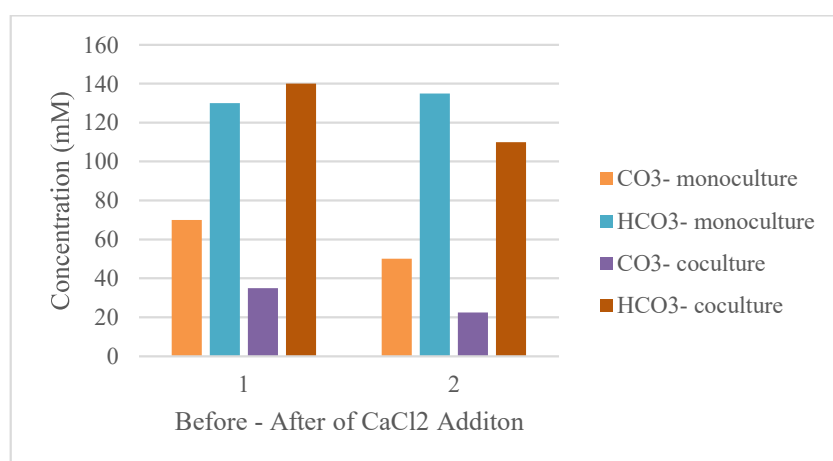


Figure 4.50 : Carbonate and bicarbonate ion changes in PBR.

5. CONCLUSIONS AND RECOMMENDATIONS

In conclusion, the comprehensive analyses and experiments conducted in this study have explained the versatility potential of microalgae, specifically *Spirulina* sp., in diverse biotechnological applications. From the initial characterization of CaCO_3 to the enzyme activity of CA and EPS analysis, our findings provide critical insights into optimizing conditions for enhanced biomass productivity and efficient CO_2 utilization.

The outcomes derived from the closed photobioreactor experiments further substantiate the advantages of regulating environmental parameters to maximize algal growth and productivity. Notably, the evaluation of suspended solids and volatile suspended solids has yielded critical data on the overall efficiency and sustainability of the cultivation processes.

Our investigation into the structural and compositional attributes of CaCO_3 has revealed essential information pertinent to its application in various industrial processes. The enzyme activity studies have highlighted the pivotal role of CA in facilitating CO_2 capture and conversion, thereby underscoring its potential in mitigating greenhouse gas emissions. The EPS analysis has illuminated the complex nature of the extracellular matrix, offering avenues for further research into its implications for biofilm formation and stability.

These findings are supported by a robust body of literature. The effects of pH, light and temperature were examined in detail throughout the study. Furthermore, biochemical structures, enzyme activities and at the end developing the mass balances were the crucial milestones of this experiment series. Collectively, these studies underscore the pivotal role of microalgae in addressing global challenges such as sustainable energy production and environmental management (Anwar et al., 2020).

Although lab-scale and pilot scale experiments were conducted within this scope, there are still concerns regarding industrial scale applications of algae and coculture with bacteria. Comparing carbon capture via algae with conventional CCS

technologies such as physical absorption, chemical absorption and adsorption-based processes for factories that have multiple combustion units, there are advantages and disadvantages that arise. Despite carbon dioxide capture via algae and coculture providing plenty of benefits, there are still hardnesses with scaling it up in energy intensive sectors. On the other hand, absorption and adsorption are widely regarded as the most economical and advanced methods for capturing substantial quantities of carbon dioxide (Chang et al., 2024).

To introduce a more realistic comparison, the AHP method is applied to this clause. Thus, it could be claimed that the most logical and feasible technology for industrial scale-up is after scoring all the criteria. The efficiency of unit amount of the system is vital, and it can be named as carbon capture capacity. Total cost, operational difficulties, scalability & flexibility and space & infrastructure requirement are determined as other parameters. Total cost consists of both capital and operational expenditures. Furthermore, turnaround frequency, energy requirement and competent personnel need are sub-criteria of operational difficulties. Hierarchy is given in Figure 5.1.

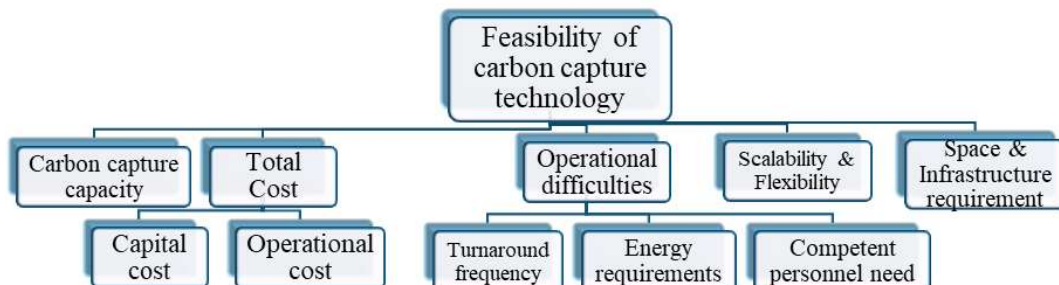


Figure 5.1 : Hierarchy for feasibility of carbon capture technologies.

While the efficiency and cost factors are based on the article of Chang et al. (2024), algal bioreactor factors are gathered from Acien et al. (2012) and the values are proportioned each other based on CO₂ load. The economic costs are a significant challenge for microalgae cultivating projects. Current algae-based capture and CO₂ mitigation technologies range from 702,00 USD to 1.585,00 USD per ton of CO₂ captured. On the other hand, the average global cost of existing conventional CCS technologies to be between 15,00 USD and 340,00 USD per ton, depending on the emission source, technology, and approach. Given that the carbon mitigation efficiency of novel algae-based CCS technology is between 51% and 73%, there is

considerable potential for further development in this area (Environmental, 2023). In addition to the cost factor, space requirement is one of the major hardships to apply PBR technologies on site.

Table 5.1 : Selection of the most feasible CCS technology for industrial applications using the AHP method.

FACTOR	Algae & Coculture PBR	Physical Absorption with Dimethyl ether	Chemical Absorption with MEA	Adsorption with silica gel	Importance Score Multiplier
CO₂ Capture Capacity	6,50	9,50	9,00	9,20	0,118
Capital Cost	2,00	3,13	8,62	3,90	0,116
Operation Cost	1,33	4,20	8,93	8,51	0,175
Replacements/ Turnaround Frequency	6,00	7,50	7,00	7,00	0,027
Corrosion Risk	9,00	5,00	5,00	8,00	0,040
Competent Personnel Need	5,00	9,00	7,00	7,00	0,080
Scalability and Flexibility	9,00	9,00	5,00	7,00	0,162
Space and Infrastructure Requirement	4,00	10,00	6,00	6,00	0,282
TOTAL SCORE	4,74	7,62	7,07	6,92	

AHP study also supports that the carbon capture via microalgae needs more research and development to be more desirable by industries. Unless there is a legal imposition for using microorganisms to mitigate emitted carbon, there will be less chance to take place on an industrial scale.

To sum up, this research stresses the transformative potential of microalgae in biotechnological applications both in lab scale and pilot scale. By harnessing the unique properties of these microorganisms, innovative solutions to some of the most pressing environmental and energy challenges of our time can be achieved. Continued research and collaboration will advance the field of microalgal biotechnology, fostering sustainable development.



REFERENCES

- Acién, F. G., Fernández, J. M., Magán, J. J., & Molina, E.** (2012). Production cost of a real microalgae production plant and strategies to reduce it. *Biotechnology Advances*, 30(6), 1344–1353. <https://doi.org/10.1016/j.biotechadv.2012.02.005>.
- Adam, B.S., Abubakar, B.M., Garba, L.L., & Hassan, I.A.** (2022). Effect of Growth Media and pH on Microalgal Biomass of Chlorella vulgaris for Biodiesel Production. *Bioremediation Science and Technology Research*.
- Akca, M. S., Ceylan-Perver, G., Duranay, A., Kinaci, O. K., & Inanc, B.** (2023). Application of Vortex Induced Vibration Systems to Improve Vertical Mixing and Create Light/Dark Cycles for Enhanced Algal Biomass Productivity in Raceway Ponds. *Journal of Marine Science and Engineering*, 11(2), 245. <https://doi.org/10.3390/jmse11020245>.
- Alami, A. H., Alasad, S., Ali, M., & Alshamsi, M.** (2021). Investigating algae for CO₂ capture and accumulation and simultaneous production of biomass for biodiesel production. *Science of the Total Environment*, 759, 143529. <https://doi.org/10.1016/j.scitotenv.2020.143529>.
- Alkhamis, Y. A., Mathew, R. T., Nagarajan, G., Rahman, S. M., & Rahman, Md. M.** (2022). pH induced stress enhances lipid accumulation in microalgae grown under mixotrophic and autotrophic condition. *Frontiers in Energy Research*, 10. <https://doi.org/10.3389/fenrg.2022.1033068>.
- Andreeva, A.P., Budenkova, E., Babich, O.O., Sukhikh, S., Ulrikh, E., Ivanova, S., Prosekov, A.Y., & Dolganyuk, V.F.** (2021). Production, Purification, and Study of the Amino Acid Composition of Microalgae Proteins. *Molecules*, 26.
- Angelaaliney, M., Senthilkumar, N., Karpagam, R., Kumar, G. G., Ashokkumar, B., & Varalakshmi, P.** (2017). Enhanced Extracellular Polysaccharide Production and Self-Sustainable Electricity Generation for PAMFCs by *Scenedesmus* sp. SB1. *ACS Omega*, 2(7), 3754–3765. <https://doi.org/10.1021/acsomega.7b00326>.
- Anwar, M. N., Fayyaz, A., Sohail, N. F., Khokhar, M. F., Baqar, M., Yasar, A., Rasool, K., Nazir, A., Raja, M. U. F., Rehan, M., Aghbashlo, M., Tabatabaei, M., & Nizami, A. S.** (2020). CO₂ utilization: Turning greenhouse gas into fuels and valuable products. *Journal of Environmental Management*, 260, 110059. <https://doi.org/10.1016/j.jenvman.2019.110059>.
- Balci, N., Gunes, Y., Kaiser, J., On, S. A., Eris, K., Garczynski, B., & Horgan, B. H. N.** (2020). Biotic and Abiotic Imprints on Mg-Rich Stromatolites: Lessons from Lake Salda, SW Turkey. *Geomicrobiology Journal*, 37(5), 401–425. <https://doi.org/10.1080/01490451.2019.1710784>.

- Bartošová, A., Blinová, L., & Gerulová, K.** (2015). Characterisation Of Polysacharides and Lipids from Selected Green Algae Species By FTIR-ATR Spectroscopy. *Research Papers Faculty of Materials Science and Technology Slovak University of Technology*, 23(36), 97–102. <https://doi.org/doi:10.1515/rput-2015-0011>.
- Carbon Border Adjustment Mechanism.** (n.d.). Taxation and Customs Union. Retrieved May 28, 2023, from https://taxation-customs.ec.europa.eu/carbon-border-adjustment-mechanism_en.
- Chaiklahan, R., Chirasawan, N., Srinorasing, T., Attasat, S., Nopharatana, A., & Bunnag, B.** (2022). Enhanced biomass and phycocyanin production of *Arthrospira (Spirulina) platensis* by a cultivation management strategy: Light intensity and cell concentration. *Bioresource Technology*, 343, 126077. <https://doi.org/10.1016/j.biortech.2021.126077>.
- Chang, S.F., Chiu, H.H., Jao, H.S., Shang, J., Lin, Y.J., & Yu, B.Y.** (2024). Comprehensive Evaluation of Various CO₂ capture Technologies through Rigorous simulation: Economic, Equipment Footprint, and Environmental Analysis. *Carbon Capture Science & Technology*, 100342. <https://doi.org/10.1016/j.ccst.2024.100342>.
- Cheah, C., Cheow, Y. L., & Ting, A. S. Y.** (2022). Comparative Analysis on Metal Removal Potential of Exopolymeric Substances with Live and Dead Cells of Bacteria. *International Journal of Environmental Research*, 16(1), 12. <https://doi.org/10.1007/s41742-021-00386-2>.
- Chen, C., Kao, P., Tan, C.H., Show, P.L., Cheah, W.Y., Lee, W., Ling, T.C., & Chang, J.** (2016). Using an innovative pH-stat CO₂ feeding strategy to enhance cell growth and C-phycocyanin production from *Spirulina platensis*. *Biochemical Engineering Journal*, 112, 78-85.
- Chen, J., Wei, D., & Pohnert, G.** (2017). Rapid Estimation of Astaxanthin and the Carotenoid-to-Chlorophyll Ratio in the Green Microalga *Chromochloris zofingiensis* Using Flow Cytometry. *Marine Drugs*, 15.
- Cheng, C., Lo, Y.C., Huang, K.L., Nagarajan, D., Chen, C., Lee, D., & Chang, J.** (2022). Effect of pH on biomass production and carbohydrate accumulation of *Chlorella vulgaris* JSC-6 under autotrophic, mixotrophic, and photoheterotrophic cultivation. *Bioresource technology*, 127021.
- Choi, O. K., Hendren, Z., Kim, G. D., Dong, D., & Lee, J. W.** (2020). Influence of activated sludge derived-extracellular polymeric substance (ASD-EPS) as bio-flocculation of microalgae for biofuel recovery. *Algal Research*, 45, 101736. <https://doi.org/https://doi.org/10.1016/j.algal.2019.101736>.
- Choi, Y. Y., Patel, A. K., Hong, M. E., Chang, W. S., & Sim, S. J.** (2019). Microalgae Bioenergy with Carbon Capture and Storage (BECCS): An emerging sustainable bioprocess for reduced CO₂ emission and biofuel production. *Bioresource Technology Reports*, 7. <https://doi.org/10.1016/j.biteb.2019.100270>

- Conde, T.A., Neves, B., Couto, D., Melo, T., Neves, B.M., Costa, M., Silva, J.L., Domingues, P., & Domingues, M.R.** (2021). Microalgae as Sustainable Bio-Factories of Healthy Lipids: Evaluating Fatty Acid Content and Antioxidant Activity. *Marine Drugs*, 19.
- Corliss, J.O., Sneath, P.H., & Sokal, R.R.** (1973). Numerical Taxonomy: The Principles and Practice of Numerical Classification.
- Correia, A.S., & Vale, N.** (2022). Tryptophan Metabolism in Depression: A Narrative Review with a Focus on Serotonin and Kynurenone Pathways. *International Journal of Molecular Sciences*, 23.
- Croft, M. T., Lawrence, A. D., Raux-Deery, E., Warren, M. J., & Smith, A. G.** (2005). Algae acquire vitamin B12 through a symbiotic relationship with bacteria. *Nature*, 438(7064), 90–93. <https://doi.org/10.1038/nature04056>.
- de Oliveira Maciel, A., Christakopoulos, P., Rova, U., & Antonopoulou, I.** (2022). Carbonic anhydrase to boost CO₂ sequestration: Improving carbon capture utilization and storage (CCUS). *Chemosphere*, 299, 134419. <https://doi.org/10.1016/j.chemosphere.2022.134419>.
- Destanoğlu, O.** (2022). Discrimination and authentication of geographical origin of Turkish Taşköprü garlic by investigating volatile organosulfur compound profiles and multivariate analyses. *Turkish Journal of Chemistry*, 46(4), 1152–1163. <https://doi.org/10.55730/1300-0527.3423>.
- Dizge, N., Koseoglu-Imer, D. Y., Karagunduz, A., Keskinler, B.** (2011). Effects of cationic polyelectrolyte on filterability and fouling reduction of submerged membrane bioreactor (MBR). *Journal of Membrane Science*, 377(1), 175–181. <https://doi.org/10.1016/j.memsci.2011.04.048>.
- Ellerbrock, R. H., Ahmed, M. A., & Gerke, H. H.** (2019). Spectroscopic characterization of mucilage (Chia seed) and polygalacturonic acid. *Journal of Plant Nutrition and Soil Science*, 182(6), 888–895. [https://doi.org/https://doi.org/10.1002/jpln.201800554](https://doi.org/10.1002/jpln.201800554).
- Ennaji, H., Bourhia, M., Taouam, I., Falaq, A., Bellahcen, T.O., Salamatullah, A.M., Alzahrani, A.A., Alyahya, H.K., Ullah, R., Ibenmoussa, S., Khilil, N., & Cherki, M.** (2021). Physicochemical Evaluation of Edible Cyanobacterium *Arthrospira platensis* Collected from the South Atlantic Coast of Morocco: A Promising Source of Dietary Supplements. *Evidence-based Complementary and Alternative Medicine : eCAM*, 2021.
- Environmental Protection Agency.** (n.d.). EPA. Retrieved February 5, 2023, from <https://www.epa.gov/ghgemissions/global-greenhouse-gas-emissions-data>.
- Environmental, N. R.** (2023). *Liquid Trees: Carbon Capture and Sequestration Via Mass Algae Farming and Marine Spatial Planning - Joseph Gabris*. Law.lclark.edu. <https://law.lclark.edu/live/blogs/253-liquid-trees-carbon-capture-and-sequestration-via>.
- European Commission.** (2023). The EU Emissions Trading System (EU ETS). Retrieved on December 16, 2024, from <https://ec.europa.eu>.

- Fernandes, A. S., Caetano, P. A., Jacob-Lopes, E., Leila Queiroz Zepka, & Vera.** (2024). Alternative green solvents associated with ultrasound-assisted extraction: A green chemistry approach for the extraction of carotenoids and chlorophylls from microalgae. *Food Chemistry*, 455, 139939–139939. <https://doi.org/10.1016/j.foodchem.2024.139939>.
- Frantz, C. M., Petryshyn, V. A., & Corsetti, F. A.** (2015). Grain trapping by filamentous cyanobacterial and algal mats: implications for stromatolite microfabrics through time. *Geobiology*, 13(5), 409–423. <https://doi.org/10.1111/gbi.12145>.
- Gao, K., Mu, C., Farzi, A., & Zhu, W.** (2019). Tryptophan Metabolism: A Link Between the Gut Microbiota and Brain. *Advances in nutrition*.
- Gauthier, M., Senhorinho, G.N., & Scott, J.A.** (2020). Microalgae under environmental stress as a source of antioxidants. *Algal Research-Biomass Biofuels and Bioproducts*, 52, 102104.
- Gerotto, C., Norici, A., & Giordano, M.** (2020). Toward Enhanced Fixation of CO₂ in Aquatic Biomass: Focus on Microalgae. *Frontiers in Energy Research*.
- Han, J., Zhang, L., Wang, S., Yang, G., Zhao, L., & Pan, K.** (2016). Co-culturing bacteria and microalgae in organic carbon containing medium. *Journal of Biological Research-Thessaloniki*, 23(1). <https://doi.org/10.1186/s40709-016-0047-6>.
- Hawrot-Paw, M., Ratomski, P., Koniuszy, A., Golimowski, W., Teleszko, M., & Grygier, A.** (2021). Fatty Acid Profile of Microalgal Oils as a Criterion for Selection of the Best Feedstock for Biodiesel Production. *Energies*.
- Higgins, B. T., Gennity, I., Samra, S., Kind, T., Fiehn, O., & Vandergheynst, J. S.** (2016). Cofactor symbiosis for enhanced algal growth, biofuel production, and wastewater treatment. *Algal Research*, 17, 308–315. <https://doi.org/10.1016/j.algal.2016.05.024>.
- Ingrisano, R., Tosato, E., Trost, P., Gurrieri, L., & Sparla, F.** (2023). Proline, Cysteine and Branched-Chain Amino Acids in Abiotic Stress Response of Land Plants and Microalgae. *Plants*, 12.
- Jana, B. B.** (2019). CO₂ Mitigation Potentials of Microalgae: Its Expansion to a New Dimension for Closing the Loop of Carbon Between Source and Acquisition Through Food Chain of Phytophagous Fish in Open Ponds. *Advances in Biotechnology & Microbiology*, 12(1). <https://doi.org/10.19080/aibm.2019.12.555827>.
- Jansson C, Northen T.** (2010) Calcifying cyanobacteria—the potential of biominerization for carbon capture and storage. *Current Opinion in Biotechnology*. 21. 365-371. [10.1016/j.copbio.2010.03.017](https://doi.org/10.1016/j.copbio.2010.03.017).
- Katırcıoğlu Sinmaz, G., Erden, B., & Şengil, I.A.** (2022). Cultivation of Chlorella vulgaris in alkaline condition for biodiesel feedstock after biological treatment of poultry slaughterhouse wastewater. *International Journal of Environmental Science and Technology*, 20, 3237-3246.

- Khaligh, S. S., Polat, E., & Altinbas, M.** (2022). Optimization of Lipid Accumulation by *Yarrowia lipolytica* Growing on Fermented Food Waste in Two-Stage Batch Strategy. *Waste and Biomass Valorization*, 14(6), 2037–2059. <https://doi.org/10.1007/s12649-022-02009-z>.
- Kim, P., Otim, O.** (2019). Optimizing a Municipal Wastewater-based Chlorella vulgaris Photobioreactor for Sequestering Atmospheric CO₂. *Southern California Academy of Sciences*, 42–57. Bull. Southern California Acad. Sci. 118(1), 2019, pp. 42–57.
- Koller, M.** (2015). Design of Closed Photobioreactors for Algal Cultivation. In: Prokop, A., Bajpai, R., Zappi, M. (eds) *Algal Biorefineries*. Springer, Cham. https://doi.org/10.1007/978-3-319-20200-6_4.
- Lee, C. S., Lee, S.-A., Ko, S.-R., Oh, H.-M., & Ahn, C.-Y.** (2015). Effects of photoperiod on nutrient removal, biomass production, and algal-bacterial population dynamics in lab-scale photobioreactors treating municipal wastewater. *Water Research*, 68, 680–691. <https://doi.org/10.1016/j.watres.2014.10.029>.
- Lee, T. H., Lee, C. H., Azmi, N. A., Liew, R. K., Hamdan, N., Wong, S. L., & Ong, P. Y.** (2022). Amino acid determination by HPLC combined with multivariate approach for geographical classification of Malaysian Edible Bird's Nest. *Journal of Food Composition and Analysis*, 107, 104399. <https://doi.org/10.1016/j.jfca.2022.104399>.
- León-Vaz, A., Giráldez, I., Moreno-Garrido, I., Varela, J.C., Vigara, J., Léon, R., & Cañavate, J.P.** (2023). Amino acids profile of 56 species of microalgae reveals that free amino acids allow to distinguish between phylogenetic groups. *Algal Research*.
- Lin, W., Lai, Y., Sung, P., Tan, S., Chang, C., Chen, C., Chang, J., & Ng, I.** (2018). Enhancing carbon capture and lipid accumulation by genetic carbonic anhydrase in microalgae. *Journal of the Taiwan Institute of Chemical Engineers*.
- Lindblad, P., Fuente, D., Borbe, F., Cicchi, B., Conejero, J. A., Couto, N., Čelešnik, H., Diano, M. M., Dolinar, M., Esposito, S., Evans, C., Ferreira, E. A., Keller, J., Khanna, N., Kind, G., Landels, A., Lemus, L., Noirel, J., Ocklenburg, S., & Oliveira, P.** (2019). CyanoFactory, a European consortium to develop technologies needed to advance cyanobacteria as chassis for production of chemicals and fuels. *Algal Research*, 41, 101510. <https://doi.org/10.1016/j.algal.2019.101510>.
- Lordan, S., Ross, R. P., & Stanton, C.** (2011). Marine bioactives as functional food ingredients: potential to reduce the incidence of chronic diseases. *Marine Drugs*, 9(6), 1056–1100.
- Lowry, O. H., Rosebrough, N. J., Farr, A. L., & Randall, R. J.** (1951). Protein measurement with the Folin phenol reagent. *Journal of Biological Chemistry*, 193(1), 265–275. [https://doi.org/10.1016/s0021-9258\(19\)52451-6](https://doi.org/10.1016/s0021-9258(19)52451-6).

- Ludwig, T. G., & Goldberg, H. J. V.** (1956). The Anthrone Method for the Determination of Carbohydrates in Foods and in Oral Rinsing. *Journal of Dental Research*, 35(1), 90–94. <https://doi.org/10.1177/00220345560350012301>.
- Mahata, C., Dhar, S., Ray, S., & Das, D.** (2021). Flocculation characteristics of anaerobic sludge driven-extracellular polymeric substance (EPS) extracted by different methods on microalgae harvesting for lipid utilization. *Biochemical Engineering Journal*, 167, 107898. <https://doi.org/https://doi.org/10.1016/j.bej.2020.107898>.
- Mecozzi, M., Pietroletti, M., Scarpiniti, M., Acquistucci, R., & Conti, M. E.** (2012). Monitoring of marine mucilage formation in Italian seas investigated by infrared spectroscopy and independent component analysis. *Environmental Monitoring and Assessment*, 184(10), 6025–6036. <https://doi.org/10.1007/s10661-011-2400-4>.
- Michelon, W., da Silva, M.L., Matthiensen, A., de Andrade, C.J., de Andrade, L.M., & Soares, H.M.** (2021). Amino acids, fatty acids, and peptides in microalgae biomass harvested from phycoremediation of swine wastewaters. *Biomass Conversion and Biorefinery*, 12, 869-880.
- Mufidatun, A., Koerniawan, M.D., Siregar, U.J., Suwanti, L.T., Budiman, A.S., & Suyono, E.A.** (2023). The Effect of pH on Contamination Reduction and Metabolite Contents in Mass Cultures of Spirulina (Arthospira platensis Gomont). *International Journal on Advanced Science, Engineering and Information Technology*.
- Ores, J. da C., Amarante, M. C. A. de, & Kalil, S. J.** (2016). Co-production of carbonic anhydrase and phycobiliproteins by Spirulina sp. and Synechococcus nidulans. *Bioresource Technology*, 219, 219–227. <https://doi.org/10.1016/j.biortech.2016.07.133>.
- Östbring, K., Tullberg, C., Burri, S., Malmqvist, E., & Rayner, M.** (2019). Protein Recovery from Rapeseed Press Cake: Varietal and Processing Condition Effects on Yield, Emulsifying Capacity and Antioxidant Activity of the Protein Rich Extract. *Foods*, 8(12), 627. <https://doi.org/10.3390/foods8120627>.
- Pinhati, R. R., Hudson Caetano Polonini, Antônio, M., Rezende, N., Corchs, F., & Wagner Farid Gattaz.** (2012). Quantification of tryptophan in plasma by high performance liquid chromatography. *Química Nova*, 35(3), 623–626. <https://doi.org/10.1590/s0100-40422012000300032>.
- Polat, E., Yüksel, E., & Altınbaş, M.** (2020). Effect of different iron sources on sustainable microalgae-based biodiesel production using Auxenochlorella protothecoides. *Renewable Energy*, 162, 1970–1978. <https://doi.org/10.1016/j.renene.2020.09.030>.
- Polat, E., Yüksel, E., & Altınbaş, M.** (2020). Mutual effect of sodium and magnesium on the cultivation of microalgae Auxenochlorella protothecoides. *Biomass & Bioenergy*, 132, 105441.

- Qin, L., Alam, M.A., & Wang, Z.** (2019). Open Pond Culture Systems and Photobioreactors for Microalgal Biofuel Production. *Microalgae Biotechnology for Development of Biofuel and Wastewater Treatment*.
- Rai, A., Chen, T., & Moroney, J. V.** (2021). Mitochondrial carbonic anhydrases are needed for optimal photosynthesis at low CO₂ levels in Chlamydomonas. *Plant Physiology*, 187(3), 1387–1398. <https://doi.org/10.1093/plphys/kiab351>.
- Ritchie, R. J.** (2006). Consistent Sets of Spectrophotometric Chlorophyll Equations for Acetone, Methanol and Ethanol Solvents. *Photosynthesis Research*, 89(1), 27–41. <https://doi.org/10.1007/s11120-006-9065-9>.
- Rugnini, L., Rossi, C., Antonaroli, S., Rakaj, A., & Bruno, L.** (2020). The Influence of Light and Nutrient Starvation on Morphology, Biomass and Lipid Content in Seven Strains of Green Microalgae as a Source of Biodiesel. *Microorganisms*, 8(8), 1254. <https://doi.org/10.3390/microorganisms8081254>.
- Sanchez-Machado, D.I., Lopez-Cervantes, J., Lopez-Hernandez, H., Paseiro-Losada, P., Simal-Lozano, J.** (2003). High-Performance Liquid Chromatographic Analysis of Amino Acids in Edible Seaweeds after Derivatization with Phenyl Isothiocyanate. *Chromatographia*, 58(3-4), 159–163. <https://doi.org/10.1365/s10337-003-0031-9>.
- Shaw, R., Mukherjee, S.** (2022). The development of carbon capture and storage (CCS) in India: A critical review. *Carbon Capture Science & Technology*, 2, 100036. <https://doi.org/10.1016/j.ccst.2022.100036>.
- Shi, T., Wang, L., Zhang, Z., Sun, X., & Huang, H.** (2020). Stresses as First-Line Tools for Enhancing Lipid and Carotenoid Production in Microalgae. *Frontiers in Bioengineering and Biotechnology*, 8.
- Sigma-Aldrich.** (n.d.). Carbonic Anhydrase Activity Assay Kit (Colorimetric), <https://www.sigmaaldrich.com/deepweb/assets/sigmaaldrich/product/documents/329/277/mak404bul-mk.pdf>.
- Silva, D. A., Cardoso, L. G., de Jesus Silva, J. S., de Souza, C. O., Lemos, P. V. F., de Almeida, P. F., Ferreira, E. de S., Lombardi, A. T., & Druzian, J. I.** (2022). Strategy for the cultivation of Chlorella vulgaris with high biomass production and biofuel potential in wastewater from the oil industry. *Environmental Technology & Innovation*, 25, 102204. <https://doi.org/10.1016/j.eti.2021.102204>.
- Sharma, A., Chiang, R., Manginell, M., I.R. de Nardi, Coker, E. N., Vanegas, J. M., Rempe, S., & Bachand, G. D.** (2023). Carbonic Anhydrase Robustness for Use in Nanoscale CO₂ Capture Technologies. *ACS Omega*, 8(41), 37830–37841. <https://doi.org/10.1021/acsomega.3c02630>.
- Sornchai, P., Iamtham, S.** (2013). Effects of Different Initial pH of Modified Zarrok Medium on Large-scale Spirulina Maxima Culture. *Journal of medical and bioengineering*, 2, 266-269.

- Steger, F., Reich, J., Fuchs, W., Rittmann, S. K. -M. R., Gübitz, G. M., Ribitsch, D., & Bochmann, G.** (2022). Comparison of Carbonic Anhydrases for CO₂ Sequestration. *International Journal of Molecular Sciences*, 23(2), 957. <https://doi.org/10.3390/ijms23020957>.
- Sudhakar, K., Suresh, S., Premalatha, M.** (2011). AN OVERVIEW OF CO₂ MITIGATION USING ALGAE CULTIVATION TECHNOLOGY. *International Journal of Chemical Research*, 3(3), 110–117. <https://doi.org/10.9735/0975-3699.3.3.110-117>.
- Sun, X., Ren, L., Zhao, Q., Ji, X., & Huang, H.** (2018). Microalgae for the production of lipid and carotenoids: a review with focus on stress regulation and adaptation. *Biotechnology for Biofuels*, 11.
- Theepharaksapan, S., Lerkmahalikit, Y., Namyuang, C., & Ittisupornrat, S.** (2023). Performance of membrane photobioreactor for integrated Spirulina strain cultivation and nutrient removal of membrane bioreactor effluent. *Journal of Environmental Chemical Engineering*, 11(5), 110579. <https://doi.org/10.1016/j.jece.2023.110579>.
- Trading Economics** (2024), EU Carbon Permits, Retrieved on December 20, 2024, <https://tradingeconomics.com/commodity/carbon>.
- Torzillo, G., Chini Zittelli, G.** (2015). Tubular Photobioreactors. In: Prokop, A., Bajpai, R., Zappi, M. (eds) *Algal Biorefineries*. Springer, Cham. https://doi.org/10.1007/978-3-319-20200-6_5.
- Udayan, A., Pandey, A.K., Sirohi, R., Sreekumar, N., Sang, B., Sim, S.J., Kim, S.H., & Pandey, A.** (2022). Production of microalgae with high lipid content and their potential as sources of nutraceuticals. *Phytochemistry Reviews*, 1 - 28.
- Unfccc.int.** (n.d.). Retrieved February 5, 2023, from <https://unfccc.int/process-and-meetings/the-paris-agreement/the-paris-agreement>.
- Varela, J.C., Pereira, H., Vila, M., & Léon, R.** (2015). Production of carotenoids by microalgae: achievements and challenges. *Photosynthesis Research*, 125, 423-436.
- Visentin, T. G., Guimarães, B. M., & Bastos, R. G.** (2023). Effects of temperature, pH, and C/N ratio of sugarcane wastewater processing (vinasse) on Phormidium autumnale heterotrophic cultivation. *Algal Research*, 77, 103349. <https://doi.org/10.1016/j.algal.2023.103349>.
- Weinstein, J.D., & Castelfranco, P.A.** (1977). Protoporphyrin IX biosynthesis from glutamate in isolated greening chloroplasts. *Archives of biochemistry and biophysics*, 178 2, 671-3.
- Xia, L., Yang, H., He, Q., & Hu, C.** (2015). Physiological responses of freshwater oleaginous microalgae *Desmodesmus* sp. NMX451 under nitrogen deficiency and alkaline pH-induced lipid accumulation. *Journal of Applied Phycology*, 27, 649-659.

- Xu, P., Fan, H., Leng, L., Fan, L., Liu, S., Chen, P., & Zhou, W.** (2020). Feasibility of microbially induced carbonate precipitation through a Chlorella-Sporosarcina co-culture system. *Algal Research-Biomass Biofuels and Bioproducts*, 47, 101831. <https://doi.org/10.1016/j.algal.2020.101831>.
- Yang, Y., Li, R., Zhao, J., Qiu, Y., Song, M., Yin, D., & Chen, X.** (2024). Stable isotope tracer IAA-induced cultivation of microalgae with contaminated carbon sources in multiple medias: Carbon fixation and biomass conversion. *Chemical Engineering Journal*, 499, 156287. <https://doi.org/10.1016/j.cej.2024.156287>.
- Yao, D., Wu, L., Tan, D., Yu, Y., Jiang, Q., Wu, Y., Wang, H., & Liu, Y.** (2024). Enhancing CO₂ fixation by microalgae in a Photobioreactor: Molecular mechanisms with exogenous carbonic anhydrase. *Bioresource Technology*, 131176–131176. <https://doi.org/10.1016/j.biortech.2024.131176>.
- Yoong Kit Leong, Chang, J.S., & Lee, D.J.** (2023). Types of photobioreactors. Elsevier EBooks, 33–58. <https://doi.org/10.1016/b978-0-323-99911-3.00007-5>.
- Zarrouk, C.** (1966). Contribution à l'étude d'une cyanophycée. Influence de divers facteurs physiques et chimiques sur la croissance et la photosynthèse de *Spirulina maxima* (Setch. et gardner) Geitler. Ph. D. Thesis, University of Paris, France
- Zhang, P., Sun, Q., Dong, Y., & Lian, S.** (2023). Effects of different bicarbonate on spirulina in CO₂ absorption and microalgae conversion hybrid system. *Frontiers in Bioengineering and Biotechnology*, 10. <https://doi.org/10.3389/fbioe.2022.1119111>.
- Zhang, Q., Wang, T., & Hong, Y.** (2014). Investigation of initial pH effects on growth of an oleaginous microalgae Chlorella sp. HQ for lipid production and nutrient uptake. *Water science and technology : a journal of the International Association on Water Pollution Research*, 70 4, 712-9.
- Zheng, S., Zou, S., Wang, H., Feng, T., Sun, S., Chen, H., & Wang, Q.** (2022). Reducing culture medium nitrogen supply coupled with replenishing carbon nutrient simultaneously enhances the biomass and lipid production of *Chlamydomonas reinhardtii*. *Frontiers in Microbiology*, 13, 1019806. <https://doi.org/10.3389/fmicb.2022.1019806>.
- Zheng, T.** (2021). Bacteria-induced facile biotic calcium carbonate precipitation. *Journal of Crystal Growth*, 563. <https://doi.org/10.1016/j.jcrysgro.2021.126096>.
- Zheng, T., & Qian, C.** (2019). Influencing factors and formation mechanism of CaCO₃ precipitation induced by microbial carbonic anhydrase. *Process Biochemistry*. <https://doi.org/10.1016/j.procbio.2019.12.018>.
- Zhu, Z., Cao, H., Li, X., Rong, J., Cao, X., & Tian, J.** (2021). A Carbon Fixation Enhanced *Chlamydomonas reinhardtii* Strain for Achieving the Double-Win Between Growth and Biofuel Production Under Non-stressed Conditions. *Frontiers in Bioengineering and Biotechnology*, 8.



APPENDICES

APPENDIX A: XRD results of entire sample set.



APPENDIX A : XRD results of entire sample set.

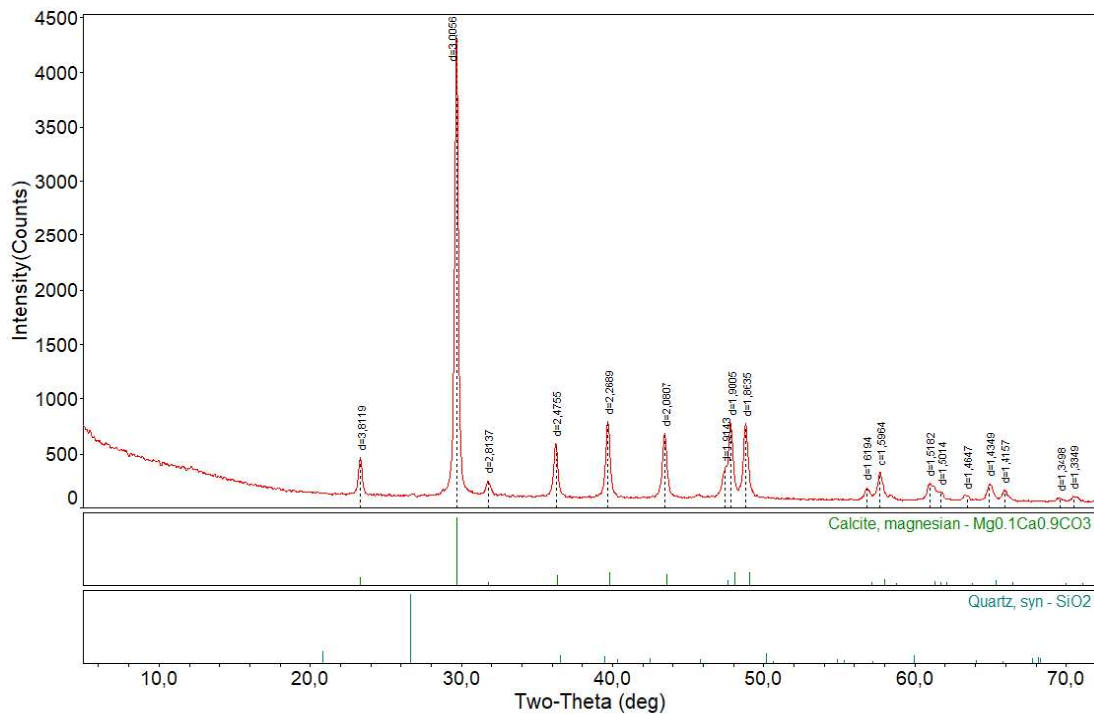


Figure A.1 : Control sample (Zarrouk media only).

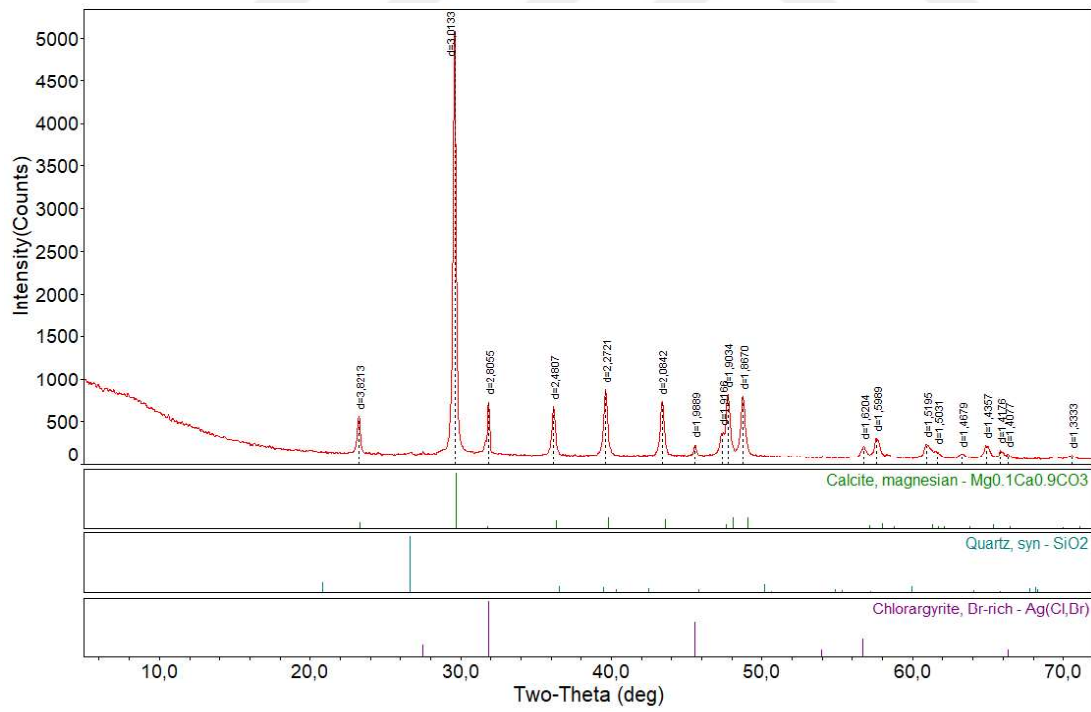


Figure A.2 : IVR:1/1 sample.

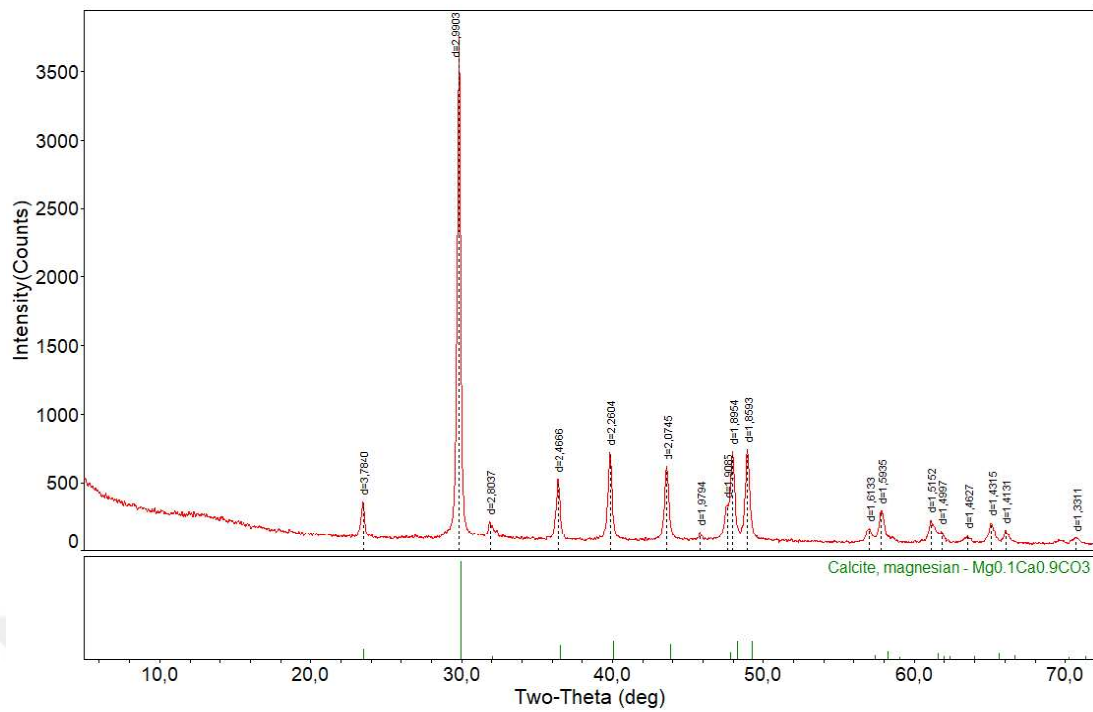


Figure A.3 : *Spirulina* monoculture sample.

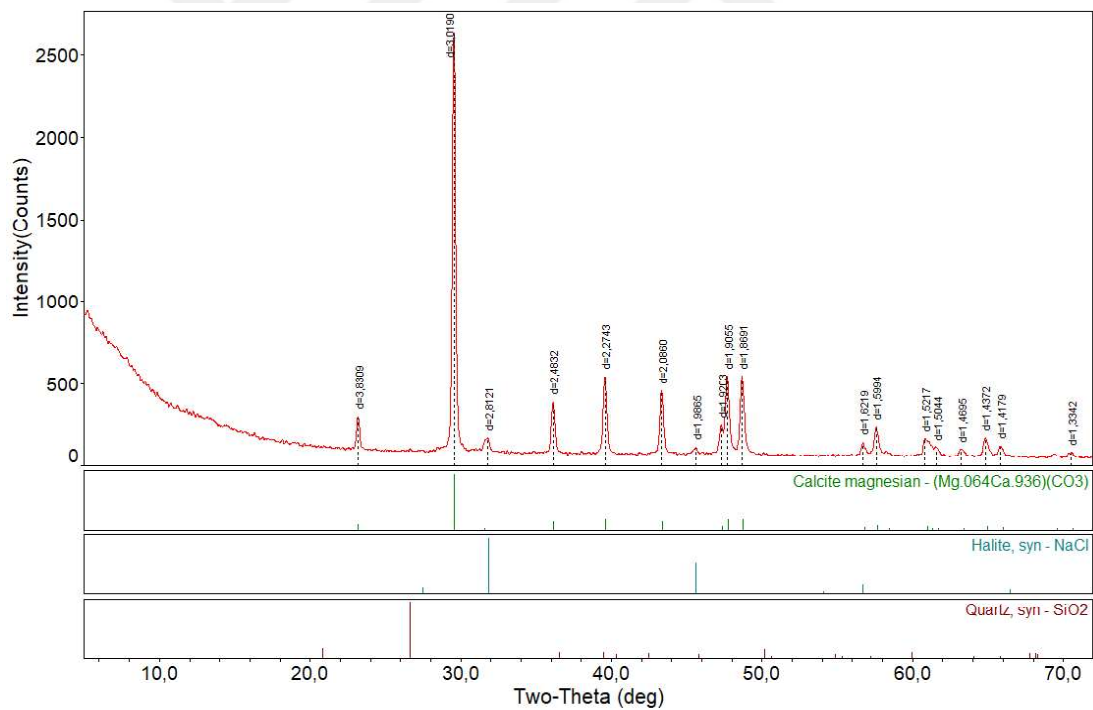


Figure A.4 : *Bacillus* monoculture sample.

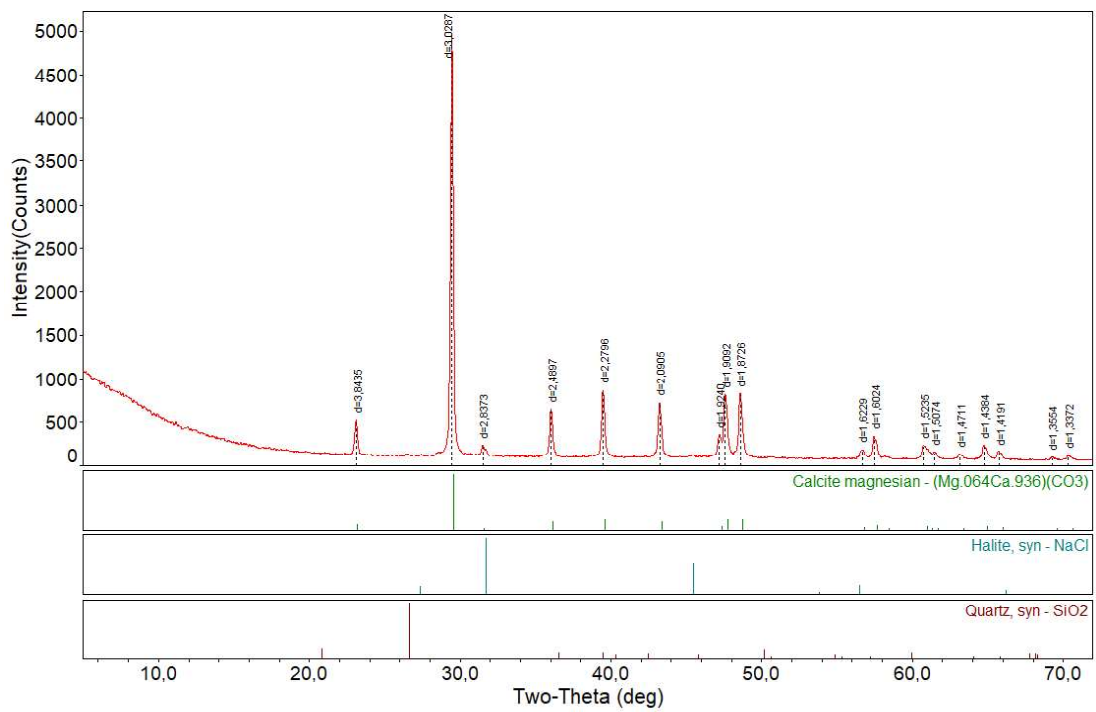


Figure A.5 : IVR: 1/3 sample.

CURRICULUM VITAE

Name Surname : Mert KOLUKISAOĞLU

EDUCATION:

- **B.Sc.** : 2015, Istanbul Technical University, Faculty of Civil Engineering, Environmental Engineering Department
- **M.Sc.** : 2017, Istanbul Technical University, Graduate School of Science Engineering and Technology, Environmental Engineering Department, Environmental Science, Engineering and Management Program

PROFESSIONAL EXPERIENCE AND REWARDS:

- TUPRAS, 2015-*still*, Sourcing & Procurement Manager.

PUBLICATIONS, PRESENTATIONS AND PATENTS ON THE THESIS:

- **Kolukisaoglu, M., Polat, E., Balcı, N. Ç., & Altınbaş, M.** (2024). Carbonic anhydrase activity and metabolite variation of different microalgae species at alkaline pHs. *Algal Research*, 84, 103778.